

1-1-1996

## Two-dimensional finite element model for heat transfer in residential attic using an attic barrier system

Neezar Taher Alsaiegh  
*University of Nevada, Las Vegas*

Follow this and additional works at: <https://digitalscholarship.unlv.edu/rtds>

---

### Repository Citation

Alsaiegh, Neezar Taher, "Two-dimensional finite element model for heat transfer in residential attic using an attic barrier system" (1996). *UNLV Retrospective Theses & Dissertations*. 821.  
<http://dx.doi.org/10.25669/oiy1-k5uk>

This Thesis is protected by copyright and/or related rights. It has been brought to you by Digital Scholarship@UNLV with permission from the rights-holder(s). You are free to use this Thesis in any way that is permitted by the copyright and related rights legislation that applies to your use. For other uses you need to obtain permission from the rights-holder(s) directly, unless additional rights are indicated by a Creative Commons license in the record and/or on the work itself.

This Thesis has been accepted for inclusion in UNLV Retrospective Theses & Dissertations by an authorized administrator of Digital Scholarship@UNLV. For more information, please contact [digitalscholarship@unlv.edu](mailto:digitalscholarship@unlv.edu).

## INFORMATION TO USERS

This manuscript has been reproduced from the microfilm master. UMI films the text directly from the original or copy submitted. Thus, some thesis and dissertation copies are in typewriter face, while others may be from any type of computer printer.

**The quality of this reproduction is dependent upon the quality of the copy submitted.** Broken or indistinct print, colored or poor quality illustrations and photographs, print bleedthrough, substandard margins, and improper alignment can adversely affect reproduction.

In the unlikely event that the author did not send UMI a complete manuscript and there are missing pages, these will be noted. Also, if unauthorized copyright material had to be removed, a note will indicate the deletion.

Oversize materials (e.g., maps, drawings, charts) are reproduced by sectioning the original, beginning at the upper left-hand corner and continuing from left to right in equal sections with small overlaps. Each original is also photographed in one exposure and is included in reduced form at the back of the book.

Photographs included in the original manuscript have been reproduced xerographically in this copy. Higher quality 6" x 9" black and white photographic prints are available for any photographs or illustrations appearing in this copy for an additional charge. Contact UMI directly to order.

# UMI

A Bell & Howell Information Company  
300 North Zeeb Road, Ann Arbor MI 48106-1346 USA  
313/761-4700 800/521-0600



## **NOTE TO USERS**

**The original manuscript received by UMI contains pages with slanted print. Pages were microfilmed as received.**

**This reproduction is the best copy available**

**UMI**



**2-D FINITE ELEMENT MODEL FOR HEAT TRANSFER  
IN RESIDENTIAL ATTIC USING AN  
ATTIC BARRIER SYSTEM**

by

**Neezar Taher Alsaiegh**

**Associate in Applied Science  
Wentworth Institute of Technology  
1976**

**Bachelor of Science  
Northeastern University  
1980**

**A thesis submitted in partial fulfillment  
of requirement for the degree of**

**Master of Science**

**In**

**Mechanical Engineering**

**Department of Mechanical Engineering  
University of Nevada, Las Vegas  
May 1998**

**UMI Number: 1390624**

**Copyright 1999 by  
Alsaiegh, Neezar Taher**

**All rights reserved.**

---

**UMI Microform 1390624  
Copyright 1998, by UMI Company. All rights reserved.**

**This microform edition is protected against unauthorized  
copying under Title 17, United States Code.**

---

**UMI**  
**300 North Zeeb Road**  
**Ann Arbor, MI 48103**

## Thesis Approval

The Graduate College  
University of Nevada, Las Vegas

JANUARY 16, 19 98

The Thesis prepared by

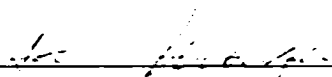
NEEZAR T. ALSAIEGH

### Entitled

2-D ELEMENT MODEL FOR HEAT TRANSFER IN RESIDENTIAL ATTIC USING AN  
ATTIC BARRIER SYSTEM

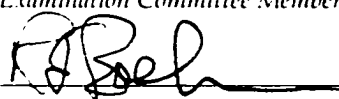
is approved in partial fulfillment of the requirements for the degree of

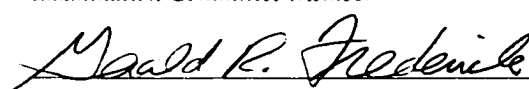
MASTER OF SCIENCE IN MECHANICAL ENGINEERING

  
Examination Committee Chair

  
Dean of the Graduate College

  
Examination Committee Member

  
Examination Committee Member

  
Graduate College Faculty Representative



## **ABSTRACT**

### **2-D Finite Element Model for Heat Transfer in Residential Attic Using an Attic Barrier System**

by

**Neezar Taher Alsaiegh**

**Dr. Samir Moujaes, Examination Committee Chair  
Professor of Mechanical Engineering  
University of Nevada, Las Vegas**

A two- dimensional finite element model is developed to simulate the thermal performance of a residential attic. The attic is ventilated using an evaporative cooler for the occupied space which vents its exhaust air into the attic. The attic is also ventilated by outside air introduced at the perimeter(soffit) of the attic ceiling and is exhausted at the ridge of the roof.

The thermal effects of an installed Attic Radiant Barrier System (ARBS) on the underside of the roof are also investigated. The model is steady state in nature using different solar insolation fluxes and ambient temperatures as driving functions at several discrete hourly values during the day. Due to the expected turbulent Reynolds numbers and Rayleigh numbers that exist at the inlets and the outlets and at the inclined surfaces, a  $(k- \epsilon)$  turbulent model has been used to describe velocity and thermal distributions in the attic. The temperature imposed on the underside of the insulation at each of the discrete times is obtained from a previously developed one-dimensional model. The air temperature which is vented from the

evaporative cooler is assumed to be at constant temperature of 300 K. Several recirculation zones have been observed in the attic which seem to affect the surface temperature close by and seem to suggest the existences of convective cells. Also the effect of lowering the emissivity on the underside of the roof was investigated. This emissivity reduction seems to raise the temperature on the underside of the roof and increase the average bulk temperature of the air leaving the attic while reducing the net heat flux passing through the ceiling insulation. It is also suggested that the more simple one dimensional assumption is only applicable on parts of the surface areas. Variations of temperatures have been shown to exist at the edges of the inclined surfaces and insulation especially at the locations of inlet and outlet vents of the attic. Finally, the model will give some correlations, and be compared with the existing correlations, of the length averaged convective heat transfer coefficients on the underside of the inclined surfaces of the roof due to the combined forced and natural flow over these surfaces.

## TABLE OF CONTENTS

ABSTRACT.....	iii
LIST OF FIGURES.....	vii
LIST OF TABLES.....	ix
NOMENCLATURE.....	x
ACKNOWLEDGMENTS.....	xi
CHAPTER 1 INTRODUCTION.....	1
CHAPTER 2 PHYSICAL AND NUMERICAL MODEL DESCRIPTION.....	4
2.1 Physical Model.....	4
2.2 Numerical Model.....	9
2.2.1 The Governing Equations.....	9
2.2.2 FIDAP Solution.....	12
2.2.3 Turbulence Modeling.....	18
2.2.4 Radiation Exchange.....	21
CHAPTER 3 RESULTS AND DISCUSSIONS.....	23
3.1 Velocity Profile and Velocity Contour of Air With Emissivity of 0.9.....	23
3.2 Temperature Profile in Air With Emissivity of 0.9.....	36
3.3 Temperature Profile Along the Inclined surfaces.....	42
3.4 Velocity Profile and Velocity Contour of Air With Emissivity of 0.05.....	45
3.5 Temperature Profile in Air With Emissivity of 0.05.....	49
3.6 Temperature Profile Along The Inclined Surfaces With Emissivity of 0.9.....	53
3.7 Calculation of Energy Balance for the Entire Attic.....	56
3.8 Calculation of Length Average Heat Transfer Coefficient.....	60
3.9 Comparison for Inclined Surface Temperatures, Outlet Air Temperatures and Air Outlet Velocities for the Two Cases of Emissivity.....	64

<b>CHAPTER 4 CONCLUSION AND RECOMMENDATION.....</b>	<b>67</b>
4.1 Conclusions.....	67
4.2 Recommendations.....	68
<b>APPENDIX A INPUT FILE.....</b>	<b>69</b>
<b>APPENDIX B PROCEDURES AND COMMANDS FOR                   OPERATING FIDAP.....</b>	<b>90</b>
<b>REFERENCES.....</b>	<b>96</b>
<b>VITA.....</b>	<b>98</b>

## LIST OF FIGURES

Figure 2-1	Physical Model Geometric Layout.....	5
Figure 2-2	Ambient Temperature Versus Time of the Day.....	8
Figure 2-3	Sample Mesh Plot for Paving and Mapping.....	14
Figure 2-4	Variation of Temperature at the Outlet of the Attic.....	15
	Due to Different Mesh Sizes.	
Figure 2-5	Selected Nodes for Tolerance Comparison.....	17
Figure 2-6	View Factor Calculation.....	22
Figure 3-1	Overall Attic's Velocity Profile.....	24
Figure 3-2	Selected Nodes for Rayleigh Number Calculation.....	26
Figure 3-3	Velocity Profile for Section "D" and "E" of the Attic.....	27
Figure 3-4	Velocity Profile for Section "C" ( Right Inner Inlet) of the Attic.....	28
Figure 3-5	Velocity Contour Plot in Y- Direction at 12:00 PM with Emissivity = 0.9.....	30
Figure 3-6	Velocity Contour Plot in X- Direction with Emissivity = 0.9.....	31
Figure 3-7	Velocity Profile for Section "A" (The Outlet) of the Attic.....	32
Figure 3-8	Velocity Profile in Y- Direction at the Top of the Attic at 12:00 PM with Emissivity = 0.9.....	33
Figure 3-9	Velocity Profile in X- Direction at the Top of the Attic (L.Outlet) and (R.Outlet) at 12:00 PM with Emissivity = 0.9.....	34
Figure 3-10	Velocity Profile in X- Direction at the Bottom of the Attic (L.Outer Inlet) at 12:00 PM with Emissivity =0.9.....	35
Figure 3-11	Temperature Contour Plot for the Attic at 12:00 PM with.....	37
	Emissivity = 0.9.	
Figure 3-12	Air Temperature Profile at the Top of the Attic (L. Outlet) at 12:00 PM with Emissivity = 0.9.....	38
Figure 3-13	Temperature Distribution Layout within the Thermal B.L.....	39
Figure 3-14	Temperature Profile at the Center Bottom Inner Surface at 12:00 PM with Emissivity = 0.9.....	40
Figure 3-15	Temperature Profile at the Left Bottom Inner Surface at 12:00 PM with Emissivity = 0.9.....	41
Figure 3-16	Temperature Profile for the Left Inclined (Inner and Outer) Surfaces at 12:00 PM with Emissivity = 0.9 .....	42
Figure 3-17	Recalculation Zones at the Right Air Inlets and the Outlet of the Attic.....	43

Figure 3-18	Streamline Contour Plot Inside the Attic at 12:00 PM with Emissivity = 0.9.....	44
Figure 3-19	Velocity Contour Plot in Y- Direction at 12:00 PM with Emissivity = 0.05.....	45
Figure 3-20	Velocity Contour Plot in X- Direction at 12:00 PM with Emissivity = 0.05.....	46
Figure 3-21	Velocity Profile in Y- Direction at the Top of the Attic (R. Outlet) at 12:00 PM with Emissivity = 0.05.....	47
Figure 3-22	Velocity Profile in X- Direction at the Top of the Attic (L.Outlet and R.Outlet) at 12:00 PM with Emissivity = 0.05.....	48
Figure 3-23	Temperature Contour Plot for the Attic at 12:00 PM with Emissivity = 0.05.....	49
Figure 3-24	Temperature Profile at the Top of the Attic (L.Outlet) at 12:00 PM with Emissivity = 0.05.....	50
Figure 3-25	Temperature Profile at the Center Bottom Inner Surface at 12:00 PM with Emissivity = 0.05.....	51
Figure 3-26	Temperature profile at the Left Bottom Inner Surface at 12:00 PM with Emissivity = 0.05.....	52
Figure 3-27	Temperature Profile at the Left Inclined (Inner and Outer) Surface at 12:00 PM with Emissivity = 0.05.....	53
Figure 3-28	Air Velocity Contour Plot for the Entire Attic at 12:00 PM with Emissivity = 0.05.....	54
Figure 3-29	Streamline Contour Plot Inside the Attic at 12:00 PM with Emissivity = 0.05.....	55
Figure 3-30	Temperature and Velocity Distribution at 12:00 PM with Emissivity = 0.9 at the Left Outlet for Energy Balance Calculations.....	58
Figure 3-31	Temperature and Velocity Distribution at 12:00 PM with Emissivity = 0.05 at the Left Outlet for Energy Balance Calculations.....	59
Figure 3-32	Schematic Diagram for Long Tilted Plate.....	60
Figure 3-33	Connective Heat Transfer Coefficient for the InnerInclined Surface at 12:00 PM with Emissivity = 0.9.....	62
Figure 3-34	Connective Heat Transfer Coefficient for the InnerInclined Surface at 12:00 PM with Emissivity = 0.9.....	63
Figure 3-35	Inclined Surface Temperature Distribution at 12:00 PM for Both Emissivity (Curve A = 0.9 and Curve B = 0.05).....	64
Figure 3-36	Left Outlet Temperature Distribution at 12:00 PM for Both Emissivity (Curve A = 0.9 and Curve B = 0.05).....	65
Figure 3-37	Left Outlet Velocity Profile in Y- Direction at 12:00 PM for Both Emissivity (Curve A = 0.9 and Curve B = 0.05).....	66

## LIST OF TABLES

Table 2-1 Properties of the Materials.....	6
Table 2-2 Boundary Conditions for All the Surfaces and the Inlet of the Attic at Various Hours.....	7
Table 2-3 Variable Values for Selected Nodes with Tolerance of $10^{-4}$ .....	16
Table 2-4 Variable Values for Selected Nodes with Tolerance of $10^{-7}$ .....	16
Table 3-1 Rayleigh Number for Selected Nodes on Both Inclined Surfaces.....	25

## NOMENCLATURE

<b>T</b>	<b>temperature, K</b>
<b>t</b>	<b>time, hour</b>
<b>U</b>	<b>velocity, m/sec</b>
<b>u</b>	<b>velocity, m/sec</b>
<b>P</b>	<b>pressure, N/m<sup>2</sup></b>
<b>e</b>	<b>emissivity</b>
<b>g</b>	<b>gravitational acceleration, m/sec<sup>2</sup></b>
<b>c<sub>p</sub></b>	<b>specific heat, J/Kg K</b>
<b>D</b>	<b>characteristic length ( slot width), m</b>
<b>Re</b>	<b>Reynolds number</b>
<b>Ra</b>	<b>Rayleigh number</b>
<b>L</b>	<b>characteristic length ( length of the inclined surface), m</b>
<b>Pr</b>	<b>Prandtl number</b>
<b>k</b>	<b>turbulent kinetic energy</b>
<b>l</b>	<b>length scale, m</b>
<b>u<sub>t</sub></b>	<b>turbulent eddy velocity, m/sec</b>
<b>A</b>	<b>surface area, m<sup>2</sup></b>
<b>F</b>	<b>radiation shape factor</b>
<b>r</b>	<b>distance between elements, m</b>
<b>H</b>	<b>enthalpy, J/kg</b>
<b>K</b>	<b>thermal conductivity, W/m K</b>
<b>h</b>	<b>convective heat transfer coefficient, W/m<sup>2</sup> K</b>
<b>β</b>	<b>volumetric thermal expansion coefficient, K<sup>-1</sup></b>
<b>ε</b>	<b>turbulent viscous dissipation</b>
<b>ρ</b>	<b>density, Kg/m<sup>3</sup></b>
<b>μ</b>	<b>dynamic viscosity, N.sec/m<sup>2</sup></b>
<b>ρ<sub>0</sub></b>	<b>reference density, Kg/m<sup>3</sup></b>
<b>ν</b>	<b>kinematic viscosity, m<sup>2</sup>/sec</b>
<b>ε</b>	<b>emissivity</b>
<b>Φ</b>	<b>viscous dissipation</b>



## **ACKNOWLEDGMENTS**

**I would like to express my profound gratitude to my advisor and committee chairman Dr. Samir Moujaes for his guidance and contribution to this thesis. I would also like to thank Dr. Samaan Ladkany for his support and encouragement to finish this study, also thanks to Dr. Mohamed Trabia for his support throughout the master's program. I would like to thank Dr. Darrell Pepper, Dr. Robert Boehm and Dr. Gerald Frederick for serving as members of my thesis committee. I sincerely thank the Department of Mechanical Engineering for giving me the chance to study in this great institution.**

## CHAPTER 1

### INTRODUCTION

Proper attic ventilation is an important part of healthy homes for both the structure and its occupants. Moisture and build up of heat are two principal reasons for designing vents in an attic. There are a wide variety of sources of moisture in a home from the building materials themselves to normal every day activities such as cooking, bathing and washing clothes which all release varying amounts of water vapor into the air. Water vapor condensation can be a problem inside the average home because the vapor concentrations can be smaller inside the house than outside. Hence, a problem is created if the vapor concentration inside the house is less than outside, vapor travels inward and works its way inward towards the living area. As warm moist air cools, the vapor begins to condense into water droplets; if this happens inside an unfinished attic, it can wet the insulation and framing. This process not only reduces the R-value of the insulation, but also can cause mold, mildew and rot to grow near the insulation.

During the summer, when the outside temperature is typically much higher than the inside temperature, attic ventilation serves a different purpose. An unfinished attic builds up a tremendous amount of heat, and if that heated air has no place to escape, it can make the inside of the house much warmer, or cause an air conditioning system to work harder to cool the house. A good attic ventilation system is designed for summer needs and it includes two

types of vents such as intake vents which are placed along the soffit to allow fresh air into the attic, and exhaust vents installed in the upper part of the attic ridge to allow hot attic air to escape. The objective is to create a continuous “wash” of air along the underside of the roof sheathing. The rule of thumb in the summer is to provide enough ventilation to completely change the air every six minutes Al-asmar<sup>1</sup> (1996). Restaurants and meeting rooms are good examples for this kind of ventilation system.

Several works have been completed on attic ventilation modeling. McQuiston<sup>2</sup> et. al (1984) performed experimental and theoretical studies of the thermal performance of a typical residential attics and commercial ceiling spaces. Response factor and transfer function methods were used in the models simulating several attics and it was concluded that the model using response factors represented attic behavior quite well. Cleary<sup>3</sup> (1985) studied the moisture that enters an attic both from the house and from the ventilation air. Results from his experimental study showed that the roof sheathing is in dynamic equilibrium with moisture in the attic air and that several hundred pounds of water can be stored in the attic wood without ill effects. Katipamula<sup>4</sup> et. al (1987) presented an experimental study concerned with different modes of heat transfer in fibrous and cellulose insulating material using an attic simulator to determine the effect of ventilation on attic heat transfer. Yarborough<sup>5</sup> et. al (1988) investigated the effectiveness of thermal insulation in the attic spaces of manufactured homes, and reported experimental measurements of the settling of stabilized cellulosic insulation showing that the attic insulation in manufactured home is significantly affected by the limited space in many floor designs.

A computational fluid dynamics method (CFD) was developed by Baker<sup>6</sup> (1994) to predict room air temperature and motion. The model was also shown to predict very low-level

velocity fields and subtle pressure variations, which cannot be experimentally detected. In other work by Medina<sup>7</sup> et. al (1995) highlighted transient heat and mass transfer modeling. They presented a model to predict hourly ceiling heat gain/loss in a residence with the purpose of estimating reductions in cooling and heating loads produced by radiant barriers. The model accounted for transient conduction, convection and radiation and incorporated moisture and air transport across the attic. Al-asmar<sup>1</sup> et al. (1996) completed an experimental study to evaluate the impact of an Attic Radiant Barrier System (ARBS) on summer cooling loads in residential buildings; it concluded that the soffit to ridge ventilation was more effective in reducing ceiling heat gain than gable-to-gable ventilation. Moujaes<sup>8</sup> (1996) developed a one dimensional transient approximation of various heat transfer processes to investigate the attic insulation and the Attic Radiant Barrier System (ARBS). The work showed a parametric study on the effects of ventilation rates through the attic as well as the effect of not having ARBS or insulation for comparative purposes. His study showed that the existence of ARBS can reduce the ceiling heat gain significantly and also showed the attic ventilation using evaporative cooler exhaust air can be very beneficial up to a certain point.

The objective of this research is to study the air movement inside the attic in more detail than has been performed in the above mentioned studies. A two dimensional finite element model of the heat transfer processes in an attic is developed. The effect of radiant barriers on ceiling load is also investigated, and the convective heat transfer coefficients on the inclined surface are reported and compared with the literature.

## CHAPTER 2

### PHYSICAL AND NUMERICAL MODEL DESCRIPTION

First, the details of the physical model and some of the simplifying assumption will be presented. Secondly, the numerical model to be solved using a commercially available finite element code FIDAP (Fluid Dynamics Analysis Package) will be presented.

#### 2-1 Description of Physical Model

A schematic diagram (Figure 2-1) shows the dimensions of the physical model which is considered as a two dimensional object. The total length of the bottom surface is 8 m, the total length of each inclined wall of the attic is 4.25 m and the height of the enclosure is approximately 1.9 m. This simulates very closely a realistic attic space in a tract house in the Las Vegas area. No trusses have been included in this model. Four slots at the bottom surface introduce the air into the attic. The total width of each slot is 0.1 m, and the total width of the upper slot (outlet) is 0.4 m. The air speed due to wind effects at the outer inlets is 0.3 m / s ( velocity boundary condition ) and the imposed air speed due to evaporative cooler air flow at the inner inlets is 0.33 m / s (velocity boundary condition). Fiber glass insulation is used above the ceiling of the house (0.15m thick) and particle board is used on the inclined side (2.7 cm thick). Average properties of these materials plus that of air are

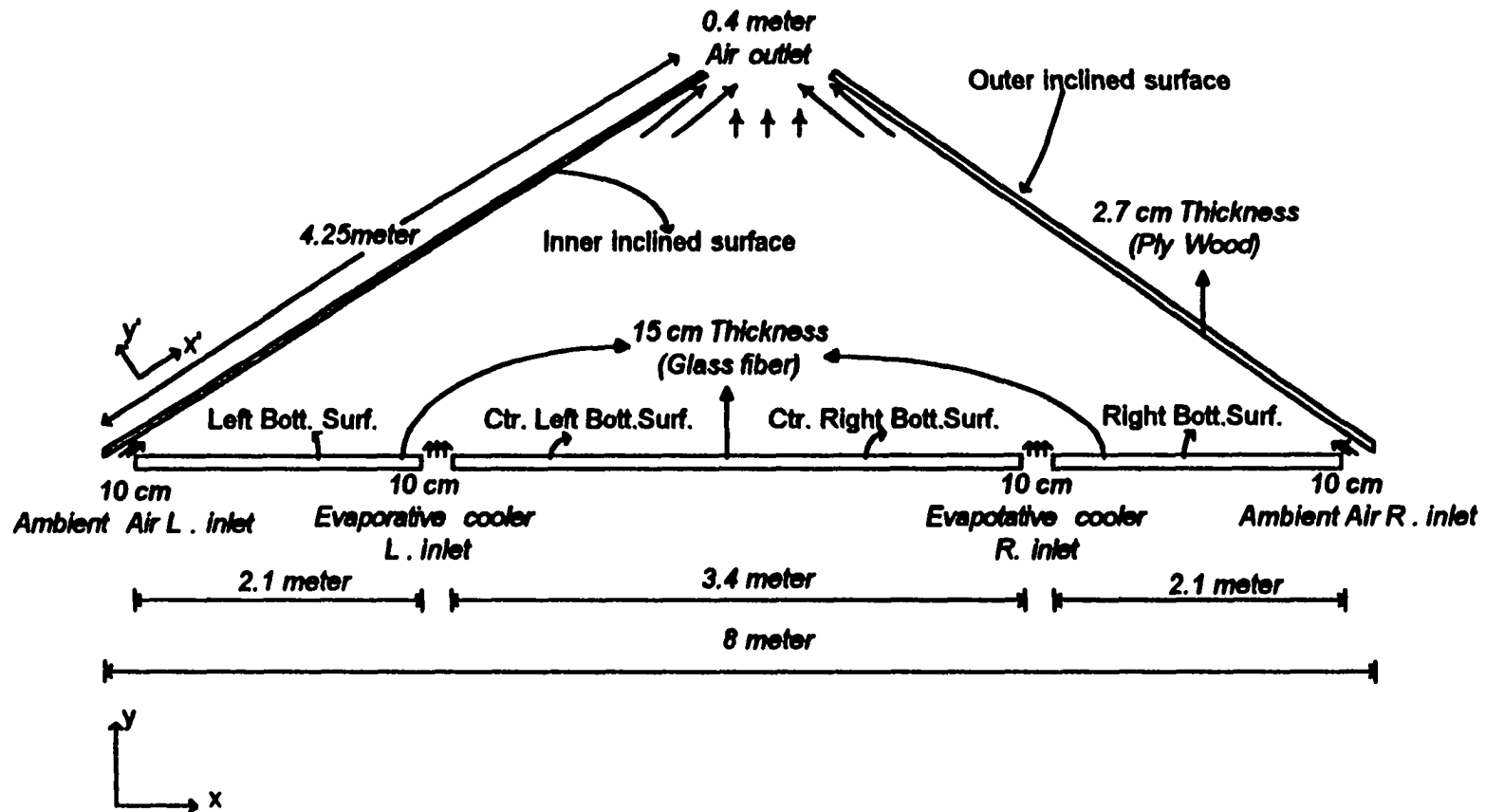


Figure 2-1 Physical Model Geometric Layout.

summarized in Table 2-1. The effect of emissivity for the inner surface of the inclined wall is studied for two values:  $e = 0.05$  (highly reflective) and  $0.9$  (lightly reflective). The emissivity value of  $0.05$  relates to the application of an Attic Radiant Barrier System (ARBS) on the underside of the inclined surfaces, while the  $0.9$  value indicates bare wooden surfaces. The emissivity for the top surface of the insulation of the enclosure is assumed to be at  $0.9$ . A uniform but variable solar flux at discrete hours of the day is imposed on the top side of the inclined surfaces and its values are summarized in Table 2-2.

**Table 2-1 Properties of the Materials**

<b>Properties</b>	<b>Fiberglass For Bottom surfaces</b>	<b>Plywood For Inclined surfaces</b>	<b>Air</b>
Conductivity, $K$ ( $W/m \cdot K$ )	0.035	0.17	0.0265
Density $\rho$ ( $kg/m^3$ )	220	700	1.174
Specific heat, $C_p$ ( $J/kg \cdot K$ )	N/A	2390	1014
Viscosity, $\mu$ ( $N \cdot s/m^2$ )	N/A	N/A	$20.8 \cdot 10^{-6}$
Acceleration, $g$ ( $m/s$ )	N/A	N/A	9.81
Prandtl number	N/A	N/A	0.71
Coef. of thermal expansion, $\beta$ ( $K^{-1}$ )	N/A	N/A	0.00317

**Table 2-2** Boundary Conditions for all the Surfaces and the Inlets of the Attic at Various Hours.

<b>Time of the Day (Hr)</b>	<b>Heat flux R.Wall (West side) (<math>W/m^2</math>)</b>	<b>Heat flux L.Wall (East side) (<math>W/m^2</math>)</b>	<b>Bot. Wall Temperature (<math>K</math>)</b>	<b>Outer Inlets Temperature (<math>K</math>)</b>
6:00 am	26.13	129.70	300.0	301.27
7:00 am	72.57	212.14	301.0	301.55
8:00 am	116.50	259.00	301.5	302.30
9:00 am	160.13	280.00	302.0	303.70
10:00 am	189.90	273.90	303.0	305.44
11:00 am	209.66	239.90	303.0	307.45
12:00 pm	216.20	216.12	304.0	309.60
1:00 pm	239.90	209.66	305.0	311.70
2:00 pm	273.90	189.90	306.0	313.76
3:00 pm	280.00	160.13	305.5	315.50
4:00 pm	259.00	116.50	305.0	316.81
5:00 pm	212.14	72.57	304.0	317.65
6:00 pm	129.70	26.13	303.0	317.93



The air inlet temperatures is obtained analytically in Table 2-2. The following sinusoidal equation made to fit the minimum and maximum values of ambient temperature for a typical summer day in Las Vegas as follows:

$$T_{ambient} = - 8.33 * ( \sin [ \frac{\pi}{12} t ] ) + 309.6$$

Where  $t$  = time of the day, (hrs). The temperature variation is presented in Figure 2-2.

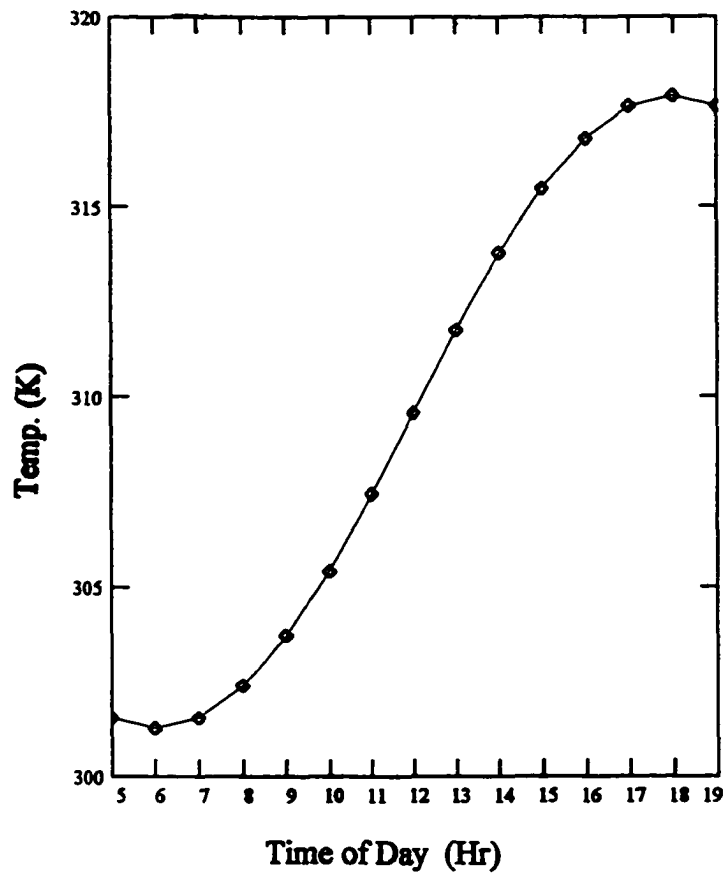


**Figure 2-2 Ambient Temperature vs. Time of Day.**

## 2.2 Numerical Model

### 2.2.1 The governing equations

FIDAP (Fluid Dynamics Analysis Package) is used to solve thermal problems where simultaneous processes of radiation, convection and conduction are taking place at different locations of the solution field. The equations are given as follows:

**Continuity:**

$$u_{i,j} = 0 \quad (2-1)$$

where  $i$  or  $j = x$  or  $y$

$u_i$  = Velocity (mass averaged velocity for single component fluid)

**Linear Momentum:**

$$\rho_0 \left[ \frac{\partial u_i}{\partial t} + u_j u_{i,j} \right] = -P_{,i} + [\mu(u_{i,j} + u_{j,i})]_{,j} - \rho_0 [\beta(T - T_0)] g_i \quad (2-2)$$

**Energy Equation:**

$$\rho_0 C_p \left( \frac{\partial T}{\partial t} + u_i T_{,i} \right) = (K * T_{,j})_{,j} + \mu \Phi \quad (2-3)$$

Natural convection effects are considered in this model to properly model the flow of air in

the attic through the body force in the momentum equation. On the average FIDAP uses a constant density model in the core of solution field, such as:

$$\rho = \rho_0 \quad (2-4)$$

However, close to a solid surface, a Boussinesq approximation models the presence of a buoyancy force caused by density variation resulting from variation in temperature across the fluid normal to the surface. The buoyancy force for air can be written as:

$$(\rho - \rho_0)g_i = -\rho_0[\beta(T - T_0)]g_i \quad (2-5)$$

where  $T_0$  - reference temperature for the problem, K.

$g_i$  - acceleration due to gravity, 9.8 m /s<sup>2</sup>.

$(\beta)$  is the coefficient for thermal expansion for an ideal gas derived as :

$$\beta = \frac{1}{T_0} \quad (2-6)$$

The Reynolds number at the four inlets is defined as :

$$Re = \frac{U_s D \rho}{\mu} \quad (2-7)$$

where  $D$  - slot width.

$U_s$  - average velocity entering the slot, m/s.

$\rho$  - air density, kg / m<sup>3</sup>.

$\mu$  - dynamic viscosity, N.s / m<sup>2</sup>.

The Reynold number is calculated to be about 2200, and is higher than 2000 which the

limiting condition for laminar flow<sup>9</sup>. Hence the flow is turbulent and a turbulent model needs to be used to describe the flow properly.

Also in chapter three the Rayleigh number (Ra) is checked along the inclined surfaces to support the use of the turbulent flow model. The Ra is defined in eq. (2-8) and should be greater than  $10^9$  for turbulent flow to exist.

$$Ra = Gr_L Pr = \left( \frac{g \beta (T_s - T_\infty) L^3}{\nu^2} \right) Pr \quad (2.8)$$

where  $g$  - gravitational acceleration,  $m/s^2$ .

$\beta$  - coefficient of thermal expansion for ideal gas,  $1/K$ .

$T_s$  - surface temperature, K.

$T$  - reference temperature, K.

$L$  - length of the surface, m.

$\nu$  - kinematic viscosity,  $m^2/s$ .

$Pr$  - Prandtl number

### **2.2.2 FIDAP (Fluid Dynamics Analysis Package) Solution:**

An iterative solution technique with a segregated solver as suggested by FIDAP technical consultants, was employed to solve the set of equations sequentially and separately for each active degree of freedom. This method is used because it substantially reduces the disk storage requirement compared to the other solvers used, such as the fully coupled method.

FIDAP (Fluid Dynamics Analysis Package), also used to solved heat conduction through the particle board and insulation by using quadrilateral elements. A total nu of 1996 nodes is used for the conduction problem. A finely graduated spacing of element mesh size was generated near the wall fluid elements to resolve the air flow details(see Figure 2-3).

Two different methods of mesh generation were used in the solution field. The first is “mapping” for the heat conduction part; the second is “paving” for the fluid solution field. A mapped mesh is a regular “ checkerboard” mesh for surface areas that are limited to four-sided regions. The complete finite element mesh for the conduction problem was constructed from a collection of mapped mesh areas. This technique is not automatic as the geometry must be decomposed into regions that are suited to a mapped mesh. The “paving” technique is designed to automatically generate a quadrilateral mesh in arbitrary geometries with qualities similar to those of the mapped mesh technique but without decomposition of the geometry. Also, in order to obtain a symmetrical nodal mesh generator, the fluid field of the problem was divided into two halves along the axis of symmetry of the solution field . The mesh was generated for one half of the solution field by using the paving technique. Then a mirror image command was used to create the other half, hence producing a symmetric meshed model.

### **Parametric Studies:**

In order to test the performance of the mesh sizing regarding its accuracy , a parametric study of the model was performed on three different mesh sizes with three models of different total nodal number of 16000, 22000 and 33000 nodes. A typical nodal arrangement is presented in Figure 2-3 for part of the mesh plot with a total of 16000 nodes. The criterion used to determine this accuracy is obtained by comparing the change of temperature profiles amongst the three that FIDAP predicted at the outlet slot, as shown in Figure 2-4 . Comparing the 33000 nodes model with the 22000 nodes, it was found that the average difference in predicting temperatures between the two models is less than 1.0%. Taking the 33000 node model as a reference, and by comparing the 33000 nodes model with the 16000 nodes, the difference was found to be less than 4.0%. It was decided that the 33000 nodal model is the best choice to use for the numerical solution of the problem. Another parametric run was performed to determine the effect of the velocity convergence tolerance value on the accuracy of the predicted variables. It showed that the 33000 nodal arrangements model reached similar accuracies in predicting the different variables for a tolerance of  $10^{-4}$  . Hence, a  $10^{-7}$  tolerance was kept as the default choice since the total difference of iterations required to reach convergence between the two tolerance is 55 iterations only. Table 2.3 and Table 2.4 shows values for temperature, pressure and velocity using  $10^{-4}$  and  $10^{-7}$  tolerance respectively for selected nodes in the attic as shown in Figure 2-5.

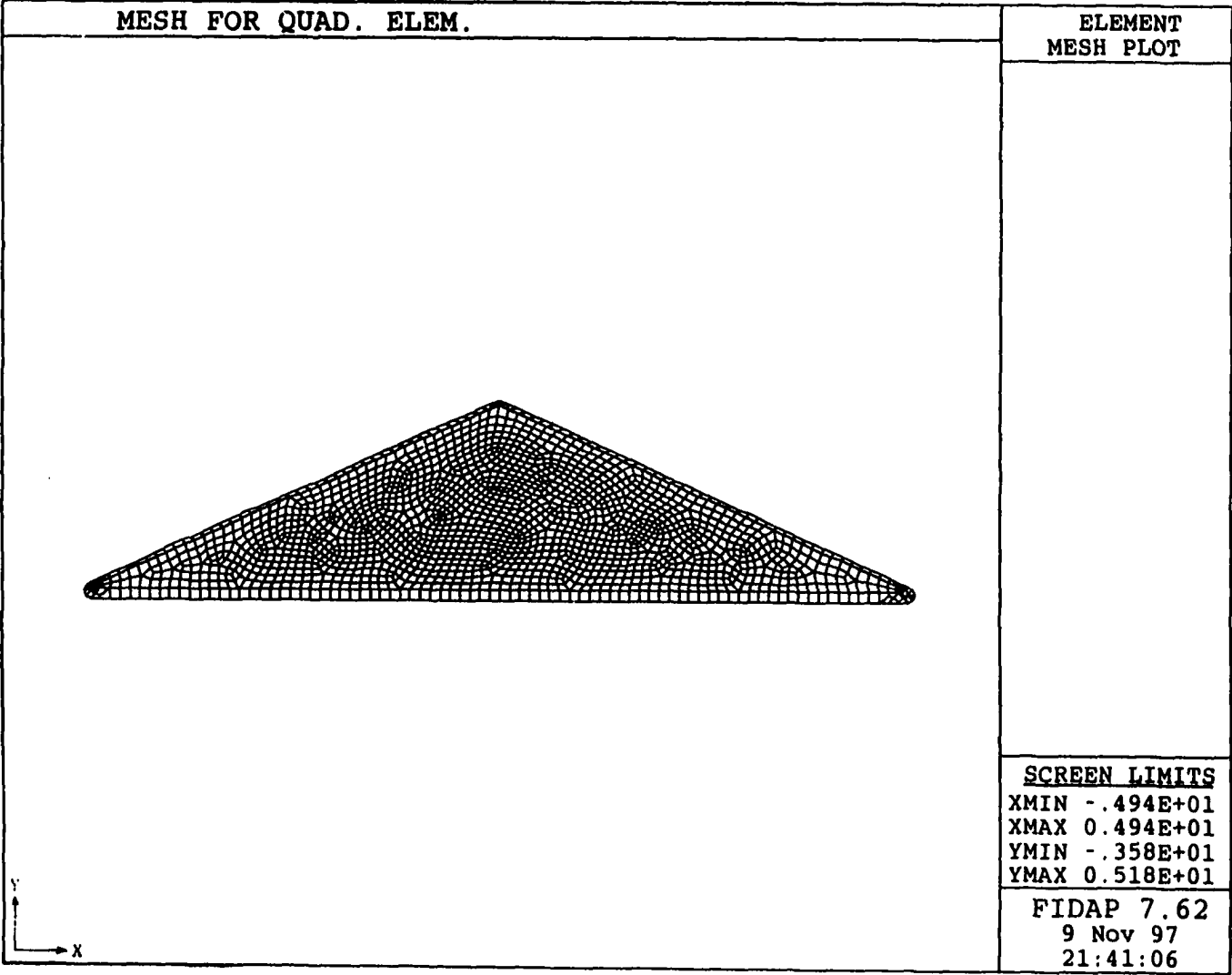


Figure 2-3 Sample Mesh Plot for Paving and Mapping.

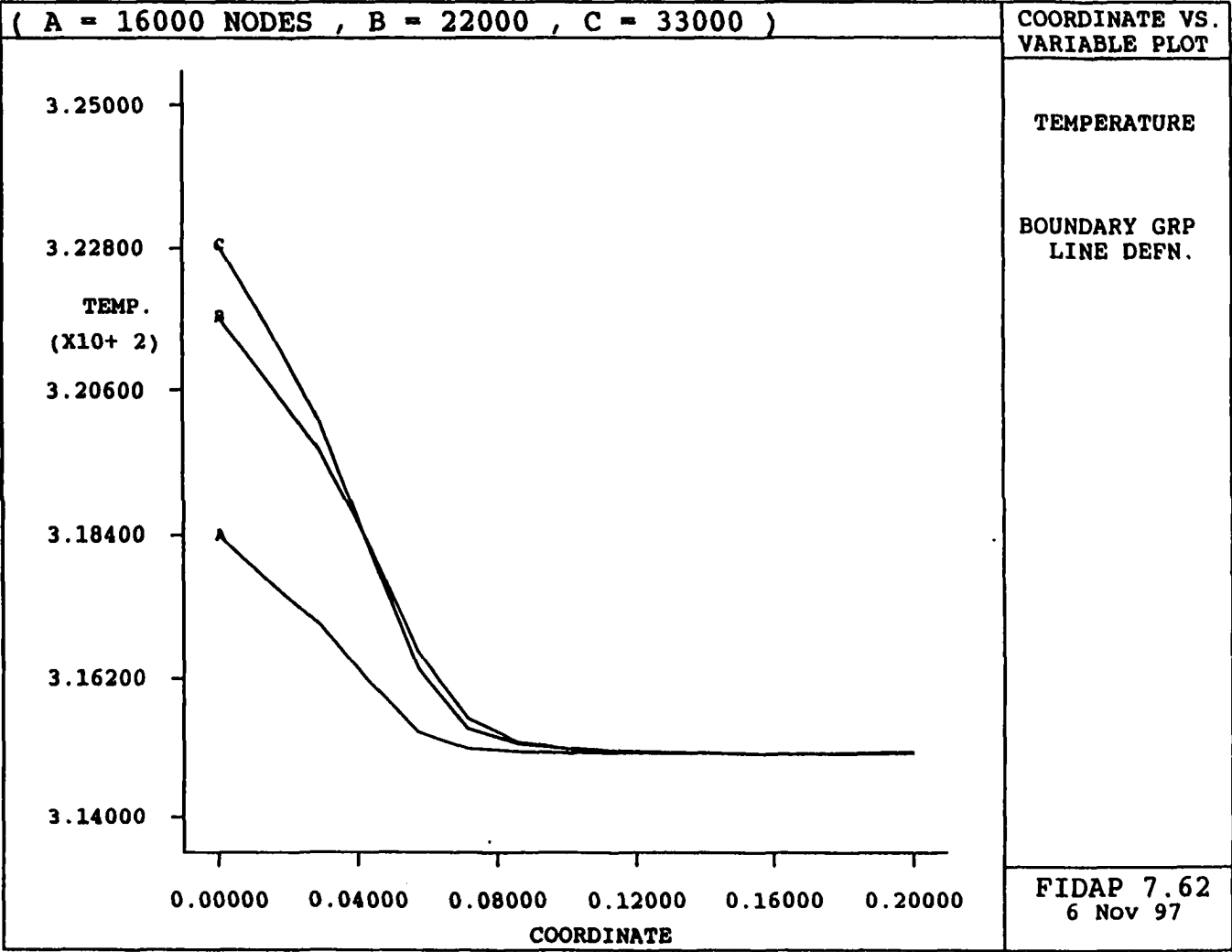


Figure 2-4 Variation of Temperature at the Outlet of the Attic  
Due to Different Mesh Sizes.



**Table 2-3** Variable Values for Selected Nodes with Tolerance of  $10^{-4}$ .

Node No.	Coordinates ( <i>x,y</i> )	Temperature ( <i>K</i> )	Pressure ( <i>bar</i> )	<i>U<sub>x</sub></i> ( <i>m/s</i> )	<i>U<sub>y</sub></i> ( <i>m/s</i> )
5889	-3.2 , 0.062	316.18626	0.026809061	0.0239052	0.0179698
8886	-0.078 , 0.20	316.37034	0.038704471	0.00305242	0.00574496
10795	-2.16 , 0.18	313.51484	0.034842645	0.02001551	0.0166387
18700	-1.11 , 0.81	314.97896	0.043699211	0.00328554	0.0127895
20139	0.015 , 1.82	315.02181	0.029667631	-0.14710501	0.1541601
25946	3.25 , 0.20	313.39926	0.024048039	-0.0387088	-0.0106705
27701	1.6 , 0.270	315.02883	0.041600870	0.00430054	0.0118125
29700	0.88 , 0.120	315.00047	0.044531769	0.00294403	0.0158716

**Table 2-4** Variable Values for Selected Nodes with Tolerance of  $10^{-7}$ .

Node No.	Coordinates ( <i>x,y</i> )	Temperature ( <i>K</i> )	Pressure ( <i>bar</i> )	<i>U<sub>x</sub></i> ( <i>m/s</i> )	<i>U<sub>y</sub></i> ( <i>m/s</i> )
5889	-3.2 , 0.062	316.18867	0.026808673	0.0239154	0.0179698
8886	-0.078 , 0.20	316.37345	0.038704352	0.00305267	0.00574496
10795	-2.16 , 0.18	313.51905	0.034842367	0.02001560	0.0166387
18700	-1.11 , 0.81	314.97598	0.043698233	0.00328560	0.0127895
20139	0.015 , 1.82	315.02505	0.029663301	-0.14710560	0.1541601
25946	3.25 , 0.20	313.39583	0.024048133	-0.0387090	-0.0106702
27701	1.60 , 0.270	315.02976	0.041600988	0.00430079	0.0118145
29700	0.88 , 0.120	315.00147	0.044531677	0.00294405	0.0158783

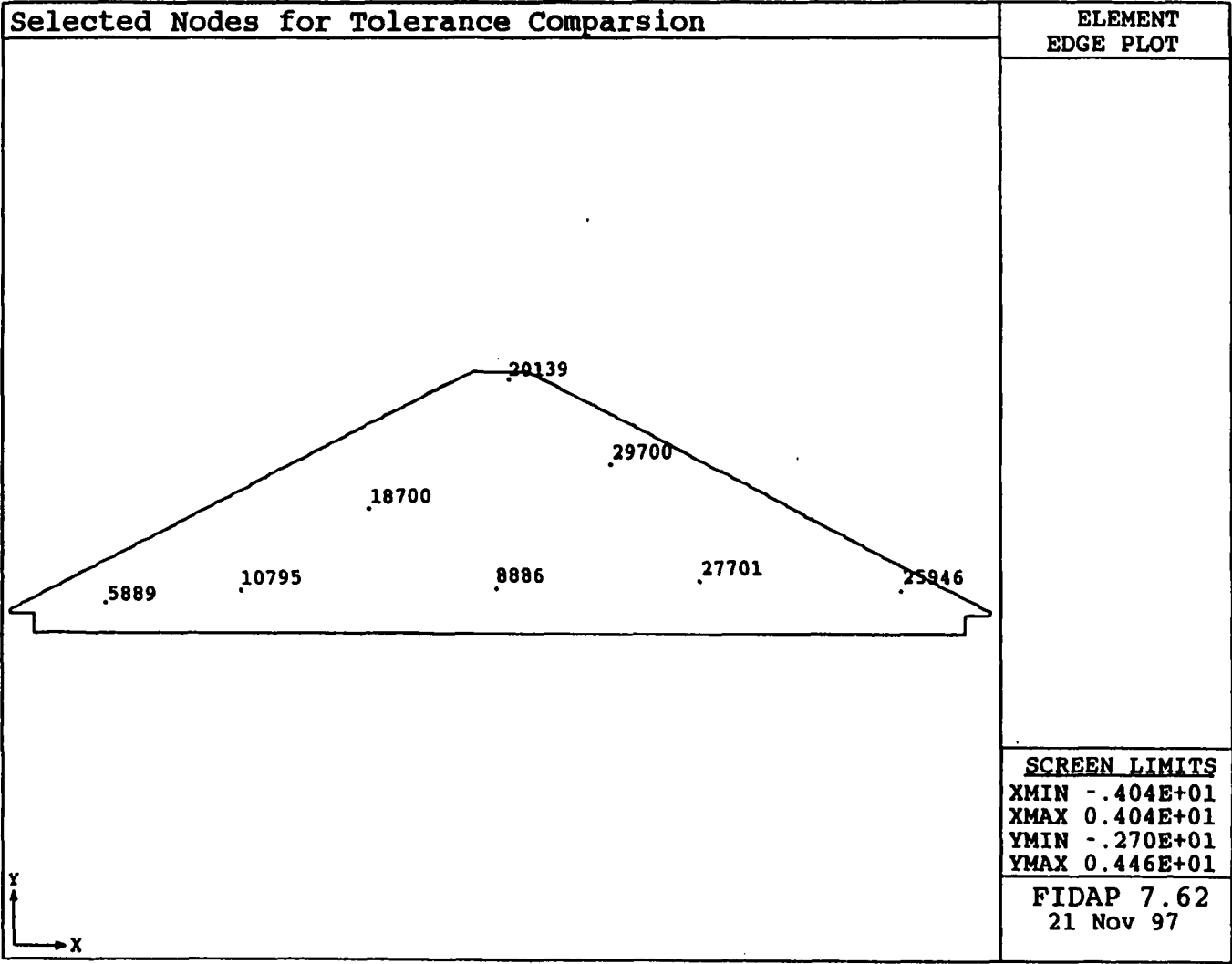


Figure 2-5 Selected Nodes for Tolerance Comparison.

#### 2-2-4 Turbulence Modeling:

Turbulence is one of the more difficult problems to resolve in the area of physical sciences. In many areas of fluid mechanics, flows of practical and industrial relevance are almost always turbulent. This means that the fluid flow is highly random. Even though the solution of the time-dependent governing equations attempt to describe turbulent, today's supercomputers are not fast enough nor do they have the storage capacity to solve these equations directly for the required range of length and time scale.

From a practical point of view, a description of turbulent flow in terms of time averaged quantities rather than instantaneous ones is implemented and incorporated in the conservation of laws of continuity, momentum and energy as described above.

#### The Two-Equation Turbulent Model:

In this problem the two equation model, (  $k$ - $\epsilon$  ) is used to complete the solution comprised of the governing equations mentioned above and the use of two additional equations that describe the transport of  $k$  (turbulent kinetic energy) and  $\epsilon$  (viscous dissipation) as follows:

$$k = \left( \frac{1}{2} \right) \overline{u_i' u_i'} \quad (2-9)$$

where (  $u'$  ) is the fluctuating part of the instantaneous velocity

$$\epsilon = \overline{v u_{i,j} u_{i,j}} = v \frac{1}{\Delta t} \int_t^{t+\Delta t} u_{i,j}' u_{i,j}' dt \quad (2-10)$$

and ( $\varepsilon$ ) the viscous dissipation rate of the kinetic energy.

Transport equations for  $k$  and  $\varepsilon$  can be obtained from the Navier-Stokes equations by a sequence of algebraic manipulations. That transport equations contain a number of unknown correlations. Application of a number of modeling assumptions simplifies these two transport equations for the turbulent kinetic energy and viscous dissipation of the  $k - \varepsilon$  model. Then, the field equations are:

**$k$  - equation**

$$\rho_o \left( \frac{\partial k}{\partial t} + u_j \mu_{t,j} \right) = \left( \mu_o + \frac{\mu_t}{\sigma_k} k_j \right)_j + \mu_t \Phi + \mu_t g_i \left( \frac{\beta_T}{\sigma_t} T_j \right) - \rho_o \varepsilon \quad (2-11)$$

$$\rho_o \left( \frac{\partial \varepsilon}{\partial t} + u_j \varepsilon_j \right) = \left( \mu_o + \frac{\mu_t}{\sigma_\varepsilon} \right)_j + c_1 \frac{\varepsilon}{k} \mu_t \Phi + c_1 (1 - c_3) \frac{\varepsilon}{k} g_i - \rho_o c_2 \frac{\varepsilon^2}{k} \quad (2-12)$$

$$\mu_t = \rho_o c_\mu \frac{k^2}{\varepsilon} \quad (2-13)$$

**$\varepsilon$  - equation** where the turbulent velocity and the length scales (denoted by  $u_t$  and  $l_t$ ) may be characterized as  $k^{1/2}$  and  $k^{1.5} / \varepsilon$ , respectively. This analysis leads to an expression for  $\mu_t$  in terms of the characteristic scales of the turbulent eddies<sup>10</sup>, i.e.,

$$\mu_t \propto \rho_o u'_t \propto \frac{\rho_o k^2}{\varepsilon} \quad (2-14)$$

The equations contain empirical constants. For isothermal flows, it is recommended to use the following set of model constants which FIDAP uses as default values:

$$c_\mu = 0.09, \quad \sigma_k = 1.00, \quad \sigma_\varepsilon = 1.3, \quad c_1 = 1.44, \quad c_2 = 1.92$$

### 2-2-5 Radiation Exchange:

The radiation exchange considered in this model assumes air in the attic as a “non-participating” medium. Hence the radiation exchange is only considered among the interior surfaces of the attic enclosure and the top of the insulation. FIDAP calculates the radiative energy exchange between two surfaces by calculating the view factor between these surfaces.

Figure 2-6 shows a typical representation. Equation

2-15 describes the equation to calculate the view factor. In this equation the surfaces  $A_i$  and  $A_j$  are diffusively emitting and reflecting. The unit vectors  $n_i$  and  $n_j$  are the normals to the elemental surfaces  $dA_i$  and  $dA_j$  respectively, where  $\beta_i$  and  $\beta_j$  are the angles made by  $n_i$  and  $n_j$  respectively with respect to  $r$ .

$$F_{ij} = \frac{1}{A_i} \int_{A_i} \int_{A_j} \frac{\cos\beta_i \cos\beta_j}{\pi r^2} dA_i dA_j \quad (2-15)$$

where

$F_{ij}$  = the radiation shape factor.

$dA_i \cos\beta_i$  = projection of area element  $dA_i$  as seen from  $dA_j$

$dA_j \cos\beta_j$  = projection of area element  $dA_j$  as seen from  $dA_i$

$r$  = distance between elements  $dA_i$  and  $dA_j$

It is also noted that for each surface  $i$  in an enclosure

$$\sum_{j=1}^N F_{ij} = 1 \quad (2-16)$$

should be satisfied, where  $N$  is the number of surfaces that the surface  $i$  sees by radiation.

FIDAP also allows the user to calculate the value of the view factor for further investigation.

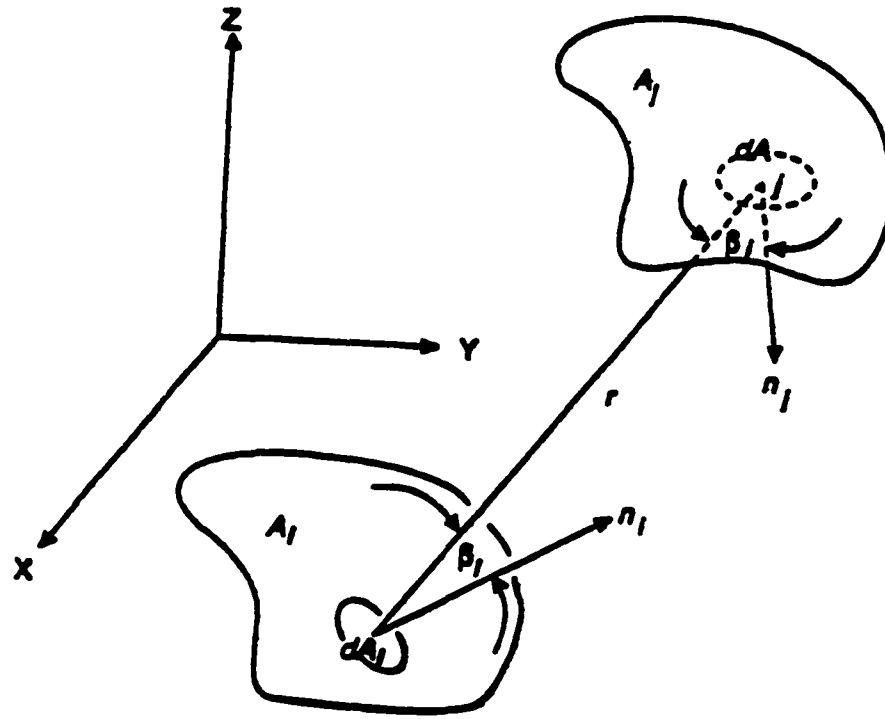


**Figure 2-6 View Factor Calculation**

## CHAPTER 3

### RESULTS AND DISCUSSION

#### 3.1 Velocity Profile and Velocity Contour of Air With Emissivity = 0.9

A reasonable wind velocity of 0.3 m/s was chosen for the outside inlets (B and E) as shown in Figure 3-1 and a velocity of 0.33 m/s was chosen for the inner ones (C and D), to take into consideration the typical airflow rate discharged from an evaporative cooler used for this size residence.

Turbulent flow was expected inside the enclosure due to the fact that Reynold number at the inner and the outer inlets was found to be higher than 2000 for longitudinal infinite slots<sup>9</sup>. It was also found that the Rayleigh number ( $Ra$ ) at the inner side of the inclined surfaces was between  $10^{10}$  and  $10^{13}$ , thus the flow is turbulent<sup>9</sup> since  $Ra > 10^9$ . Figure 3-2 showed values of  $Ra$  for randomly selected points on the inner inclined surfaces where the Rayleigh number exceeds  $10^9$  for each selected point as shown in table 3-1.

The solution showed some recirculation zones near all the inlets as shown in Figure 3-3 and Figure 3-4. To explain this phenomena, it is noticed that the air generated by the evaporative cooler and ambient air that enters the attic have a low temperature. The air automatically dips because of its high density and low temperature, then after it picks up some heat from the surrounding surfaces, it starts to develop some lift. This fact is



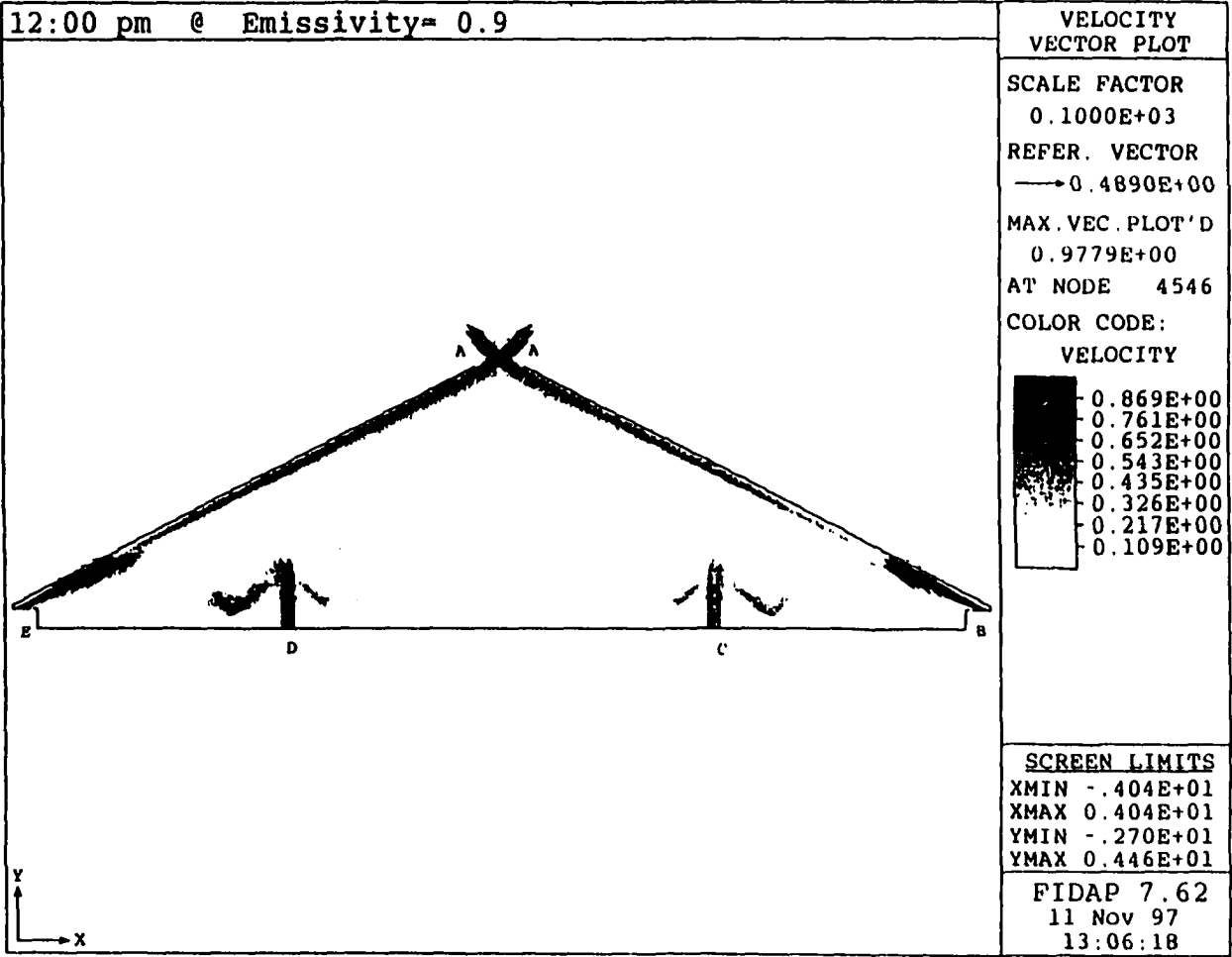


Figure 3-1 Overall Attic's Velocity Profile.

**Table 3-1 Rayleigh Number for Selected Nodes on Both Inclined Surfaces.**

Node Number	Rayleigh Number
4600	$1.00 \times 10^{10}$
4630	$1.15 \times 10^{10}$
4776	$1.06 \times 10^{11}$
4783	$1.01 \times 10^{13}$
20081	$1.04 \times 10^{13}$
20017	$1.20 \times 10^{11}$
20000	$1.01 \times 10^{10}$
19920	$1.18 \times 10^{10}$

incorporated correctly by the Boussinesq approximation<sup>11</sup> and used in the momentum equation.

$$\beta = -\frac{1}{\rho} \frac{\partial \rho}{\partial T} \approx \frac{\rho_{\infty} - \rho}{\rho(T - T_{\infty})} \quad (3-1)$$

where  $\beta$  is the coefficient of thermal expansion,  $T_{\infty}$  is the reference temperature,  $\rho_{\infty}$  is the reference density,  $T$  and  $\rho$  are the temperature and the density, respectively, at any chosen point. Also, there are air movement and recirculation zones along the inclined surface of the attic. This is due to the geometry of the model since some of the air coming from the evaporative cooler gets lifted upward then mixes with the air that is coming from the ambient (i.e outer inlets) and traveling along the side of the inclined surface creating these eddies. Looking at Figure 3-5 the velocity contour plot for the air in the y-direction ( $U_y$ ) with

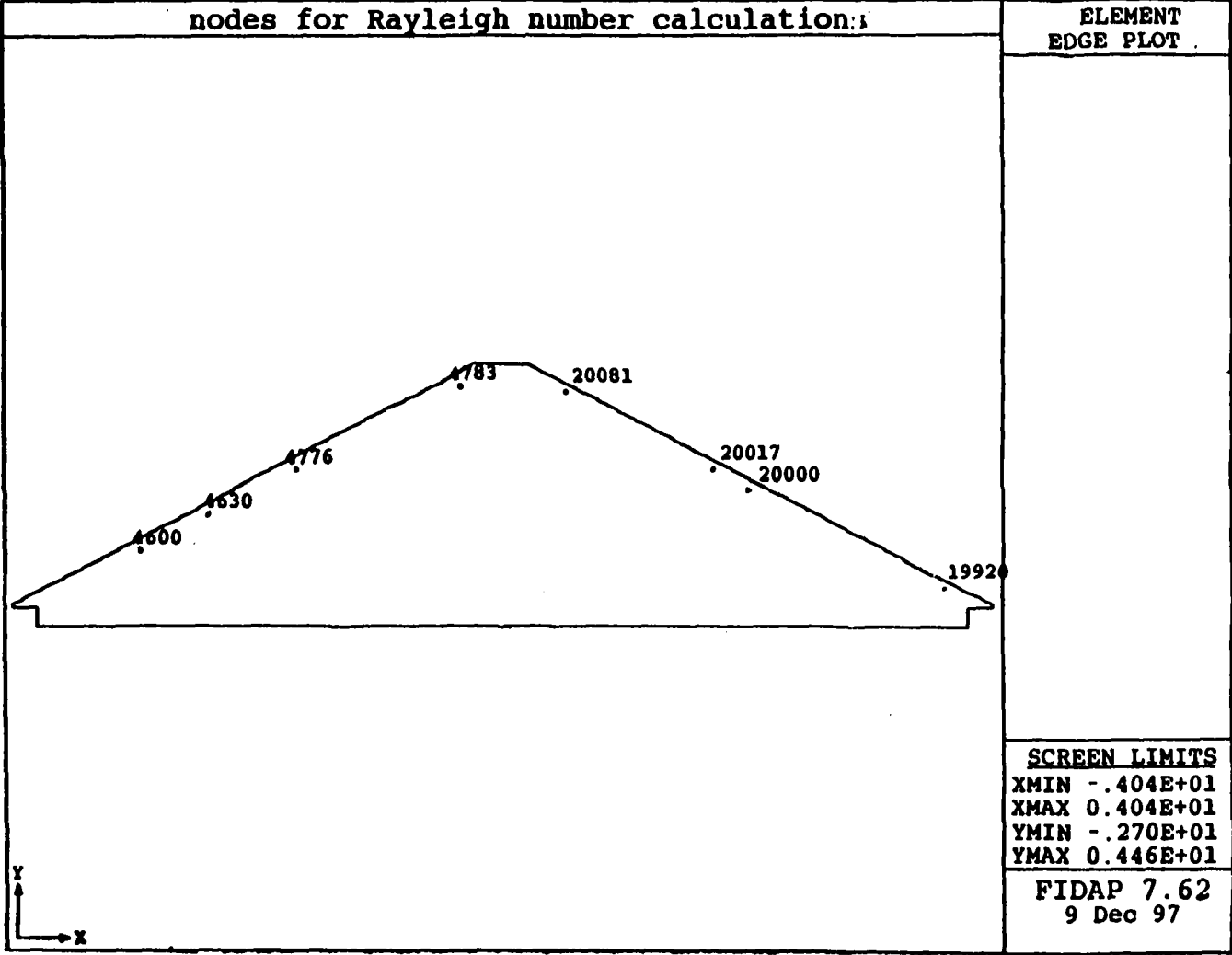


Figure 3-2 Selected Nodes for Rayleigh Number Calculation.

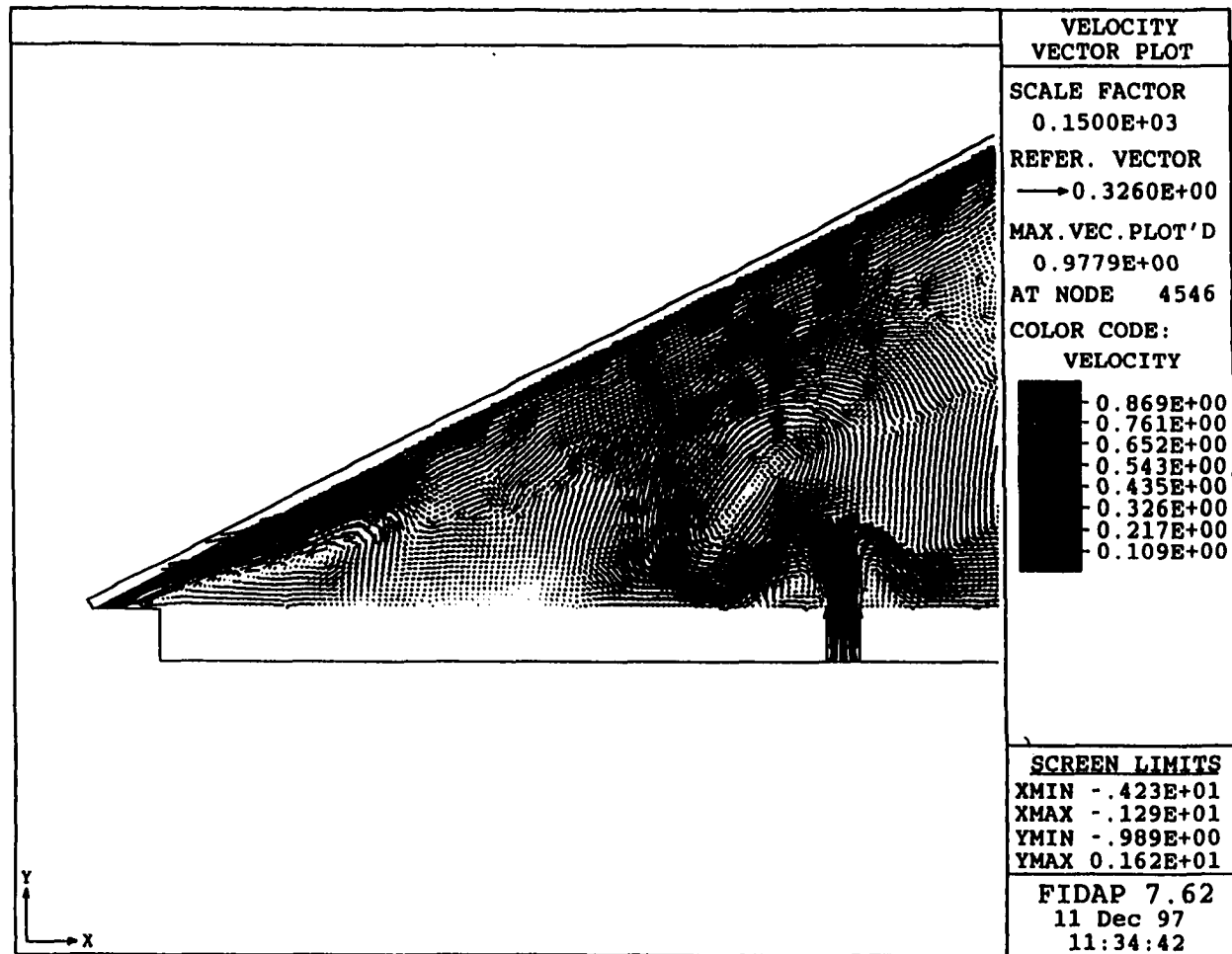
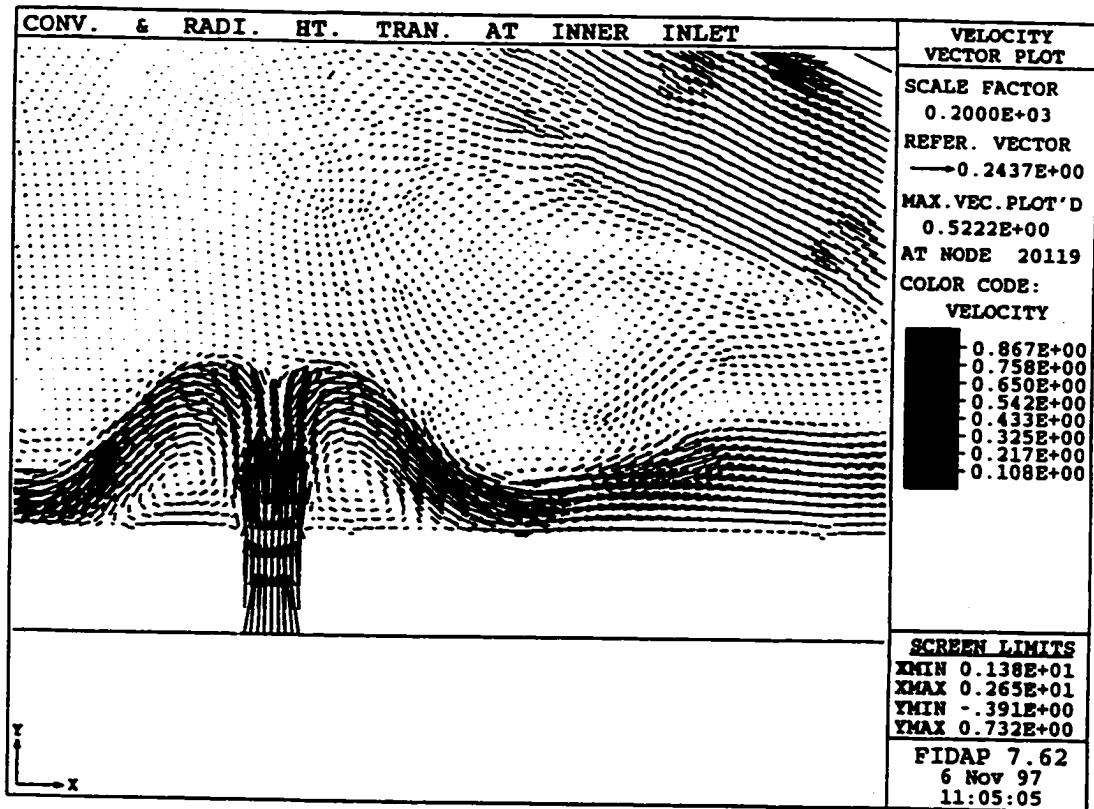
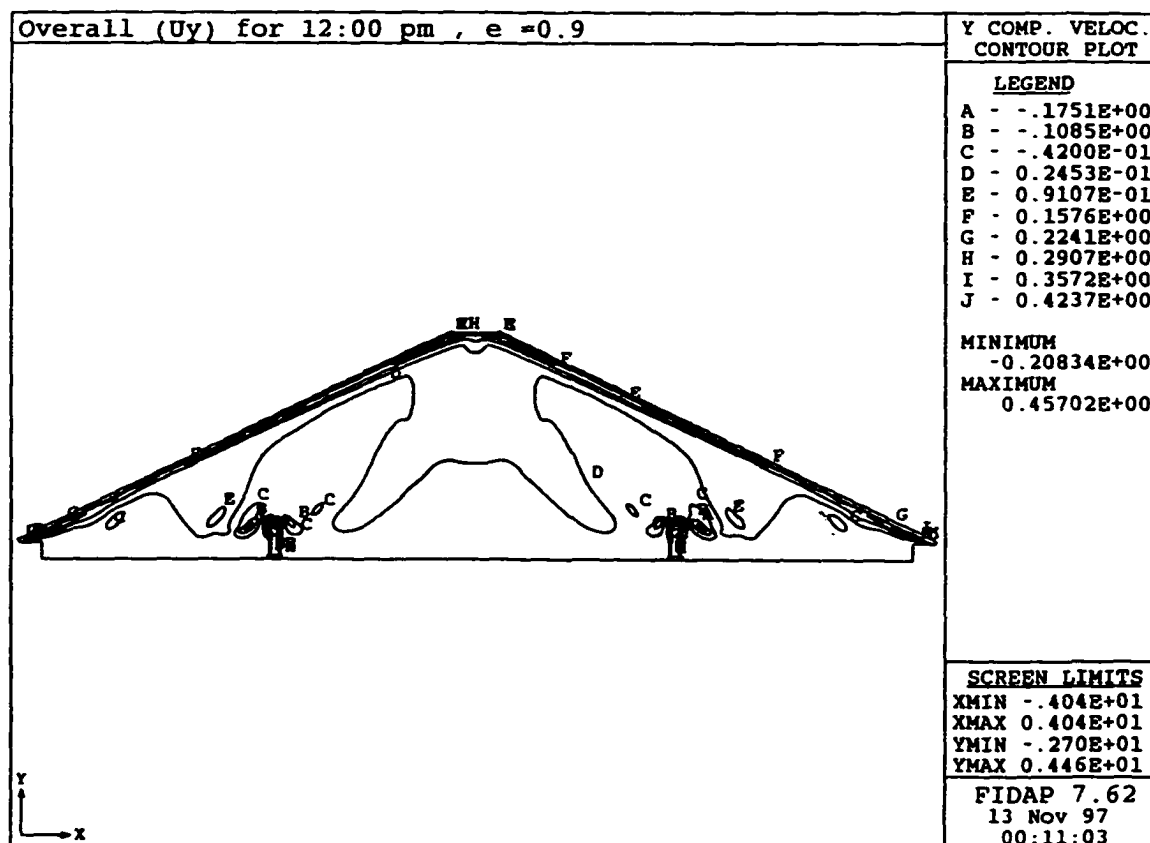


Figure 3-3 Velocity Profile for Section "D" and "E" of the Attic.



**Figure 3-4 Velocity Profile for Section "C" ( Right Inner Inlet) of the Attic.**

emissivity of 0.9, the velocity along the inclined surface has a value between 0.2907 and 0.4237 m/s . The velocity for most of the space at the mid region of the enclosure remains almost constant at 0.02453 m/s. Figure 3-6 (velocity contour plot) shows that the maximum value of the velocity in the x- direction ( $U_x$ ) occurred near the inclined surfaces, where the solar flux had been applied. At the outlet A as shown in Figure 3-7, the solution showed that the air movement has no recirculation zones. As the air gets accelerated by the convective heat generated inside the attic, it was found that the maximum velocity ( $U_y$ ) at 12:00 pm is 0.407 m/s it occurs about 4cm away from the inclined surface as shown in Figure 3-8. It was also shown that the velocity ( $U_z$ ) at the outlet has maximum value of 0.5 m/s as shown in Figure 3-9.



**Figure 3-5 Velocity Contour Plot in Y- Direction at 12:00 PM with Emissivity = 0.9.**

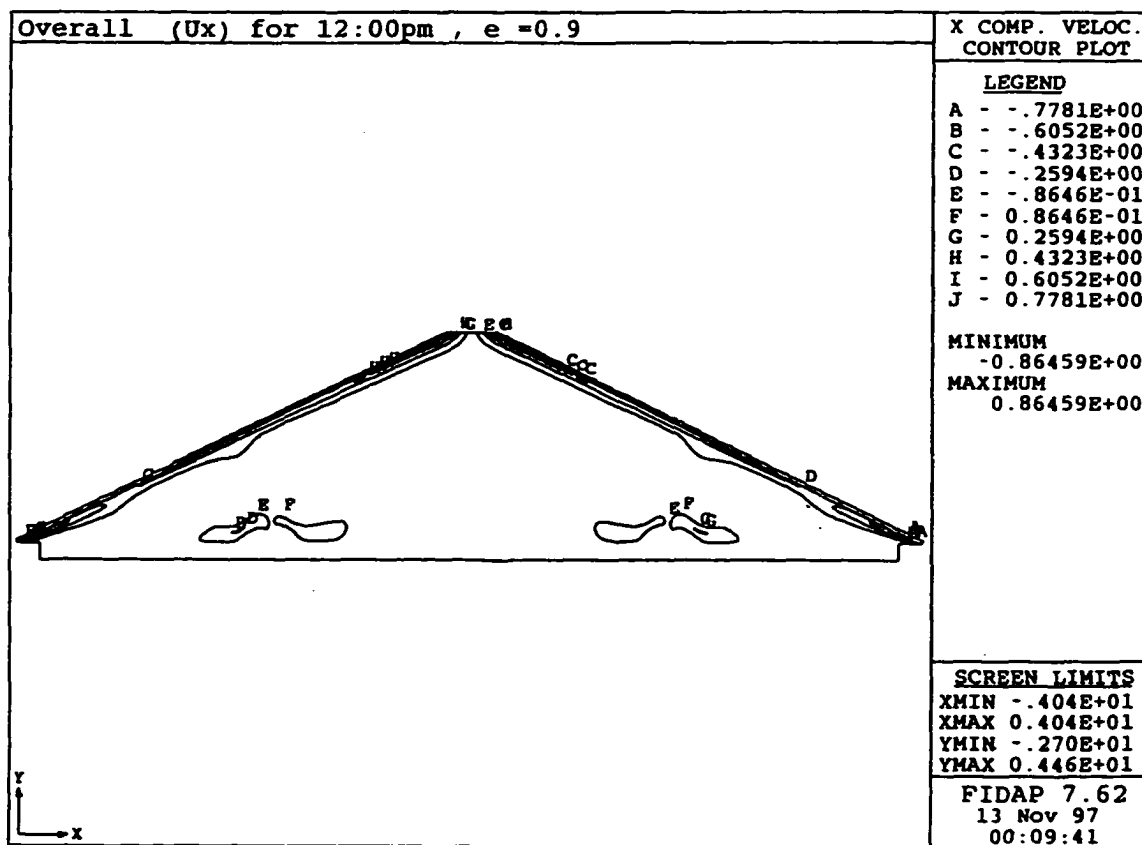


**Figure 3-6** Velocity Contour Plot in X- Direction with Emissivity = 0.9.



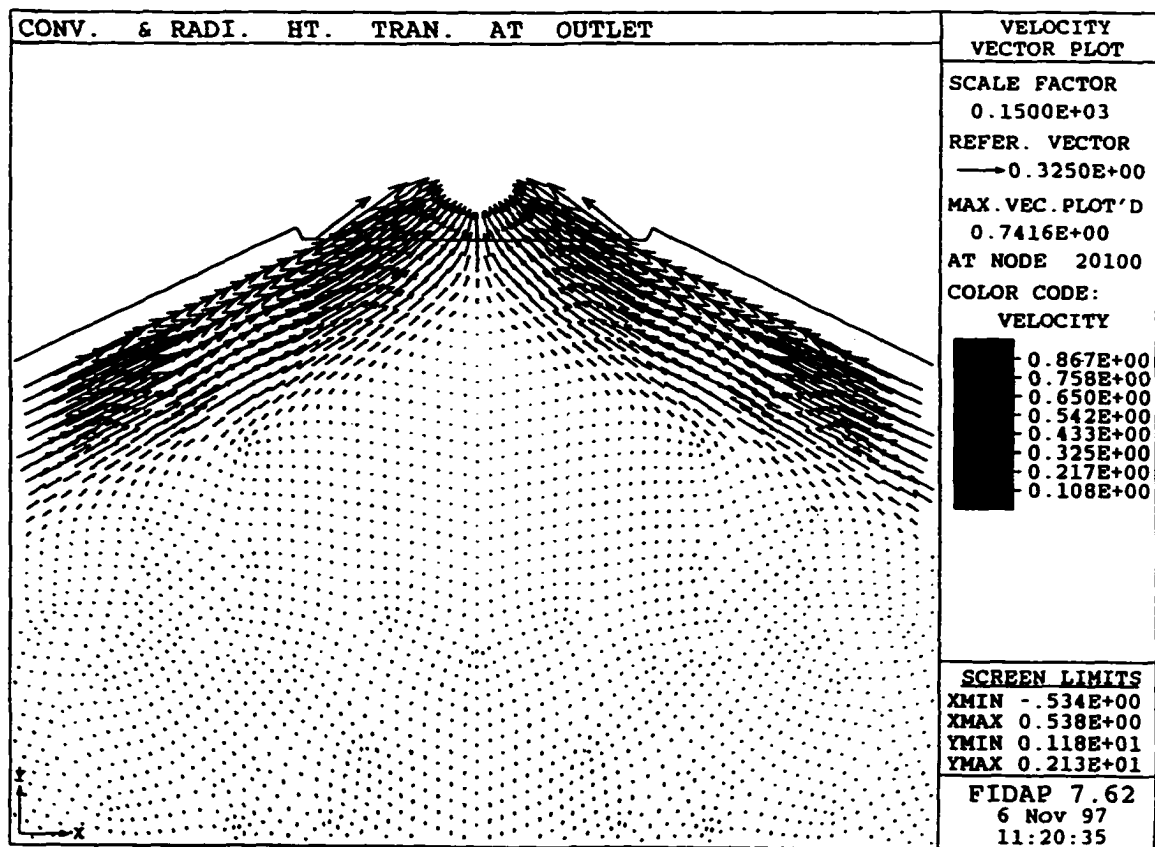


**Figure 3-7 Velocity Profile for Section "A" (The Outlet) of the Attic.**

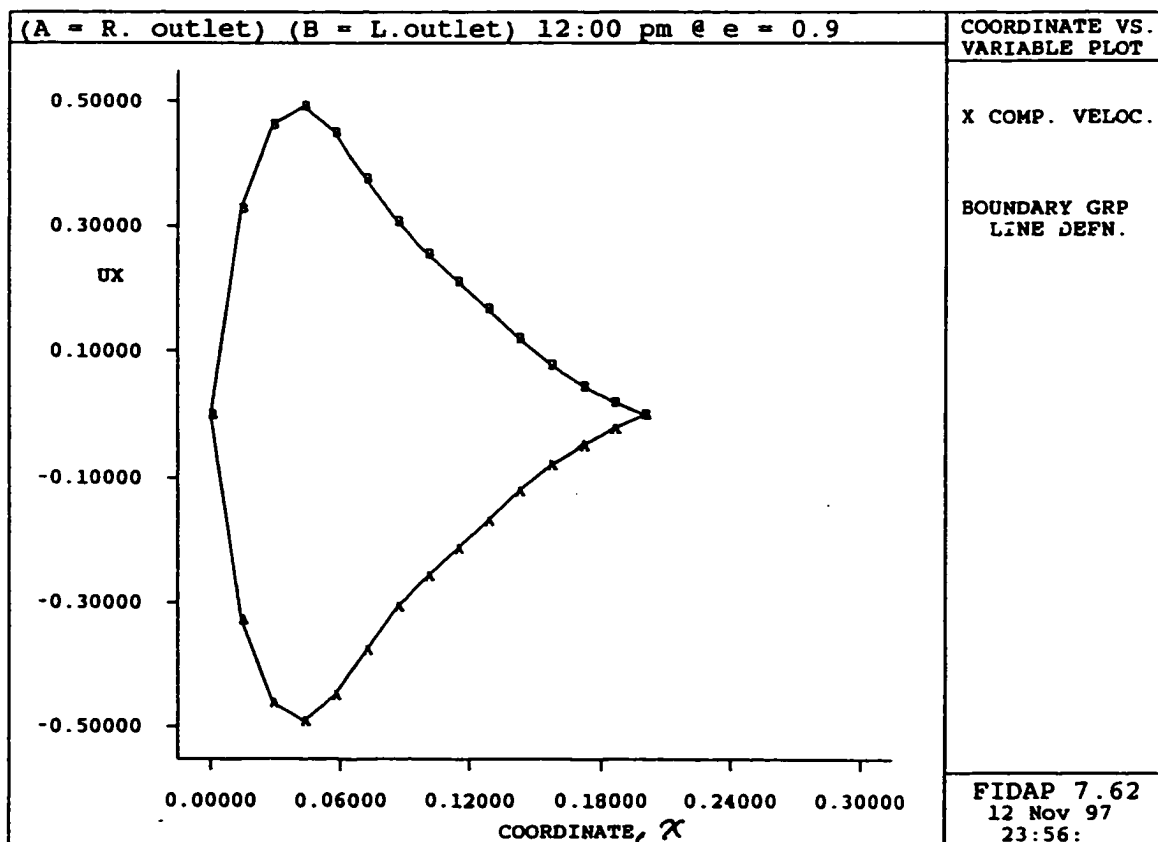


**Figure 3-9 Velocity Profile in X- Direction at the Top of the Attic (L.Outlet) and (R.Outlet) at 12:00 PM with Emissivity = 0.9**

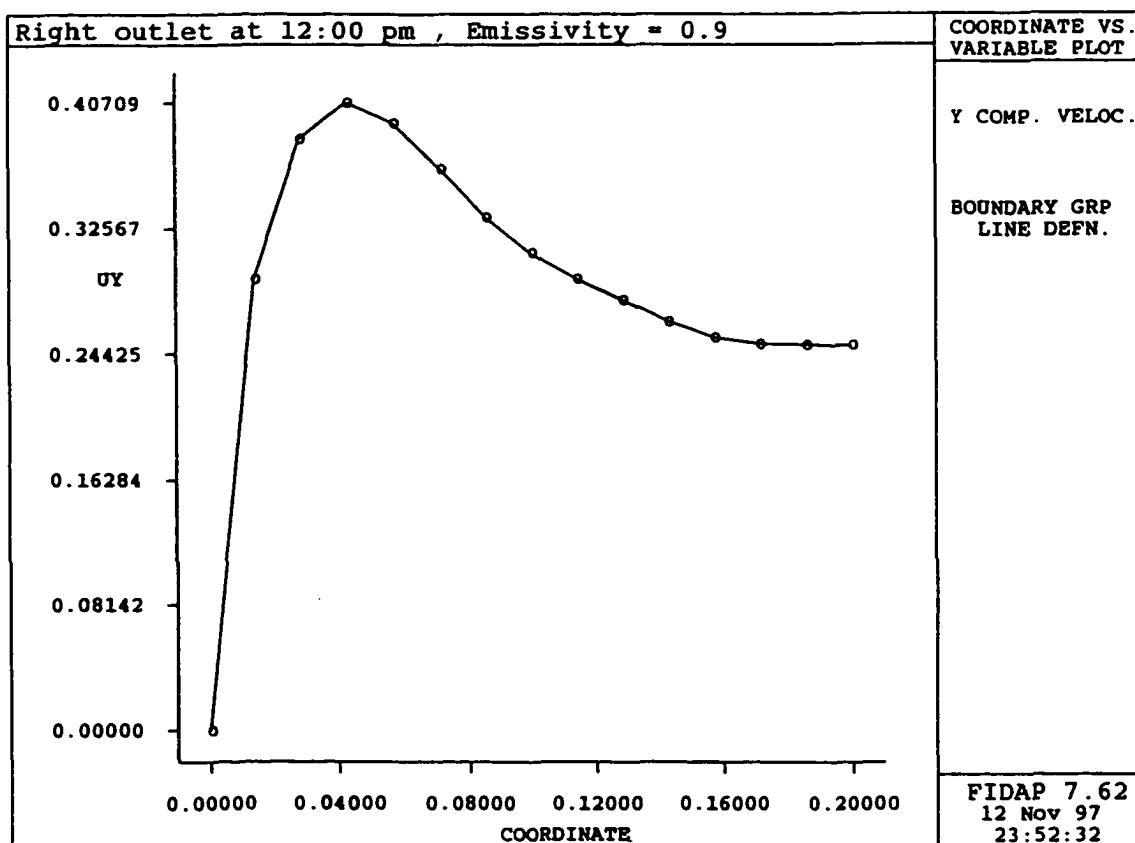


**Figure 3-8** Velocity Profile in Y- Direction at the Top of the Attic  
at 12:00 PM with Emissivity = 0.9.

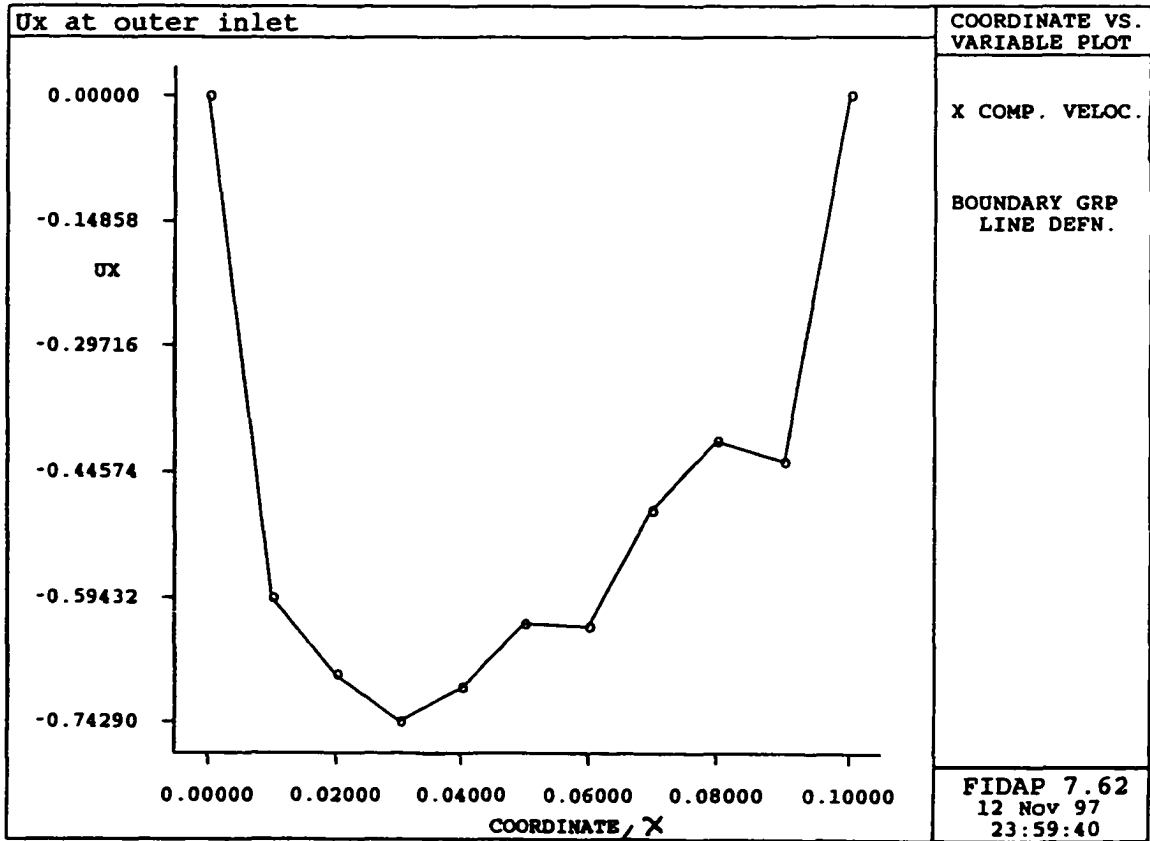


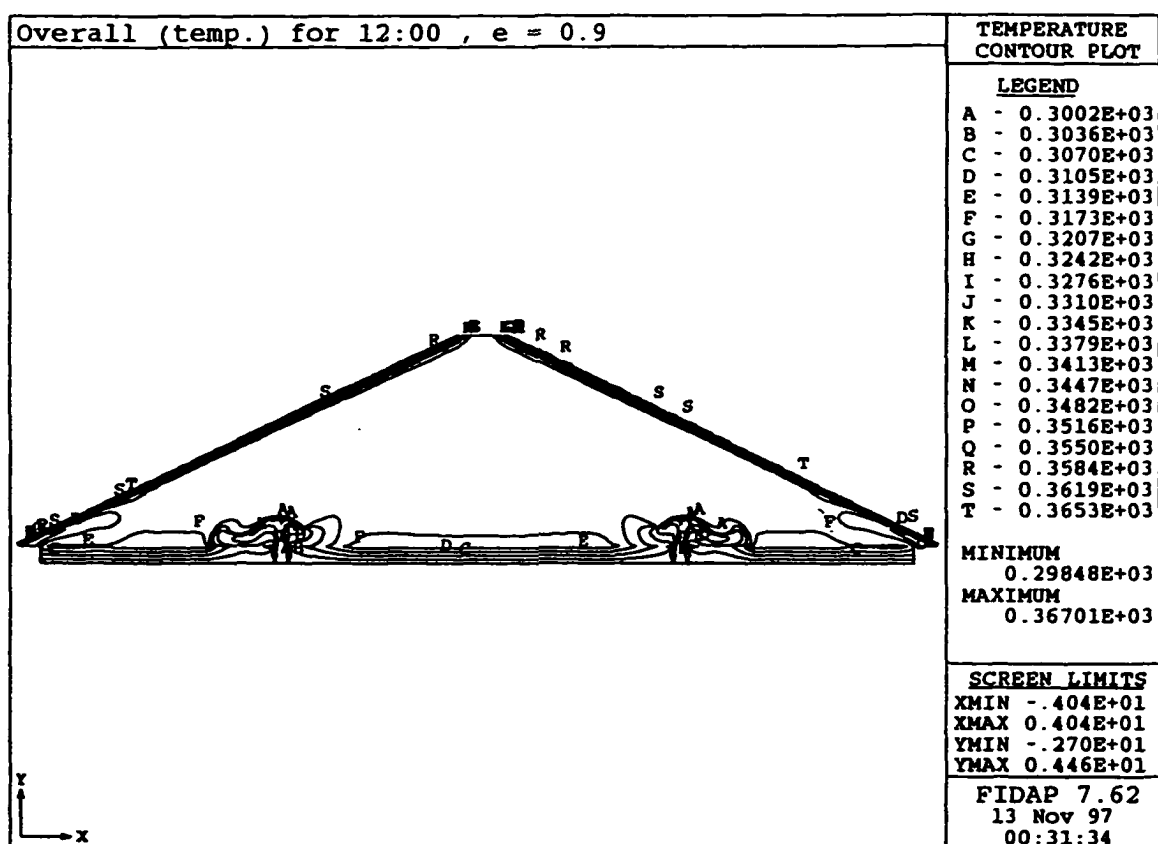
**Figure 3-10** Velocity Profile in X- Direction at the Bottom of the Attic  
(L. Outer Inlet) at 12:00 PM with Emissivity =0.9.

### 3-2 Temperature Profile in Air With Surface Emissivity of 0.9

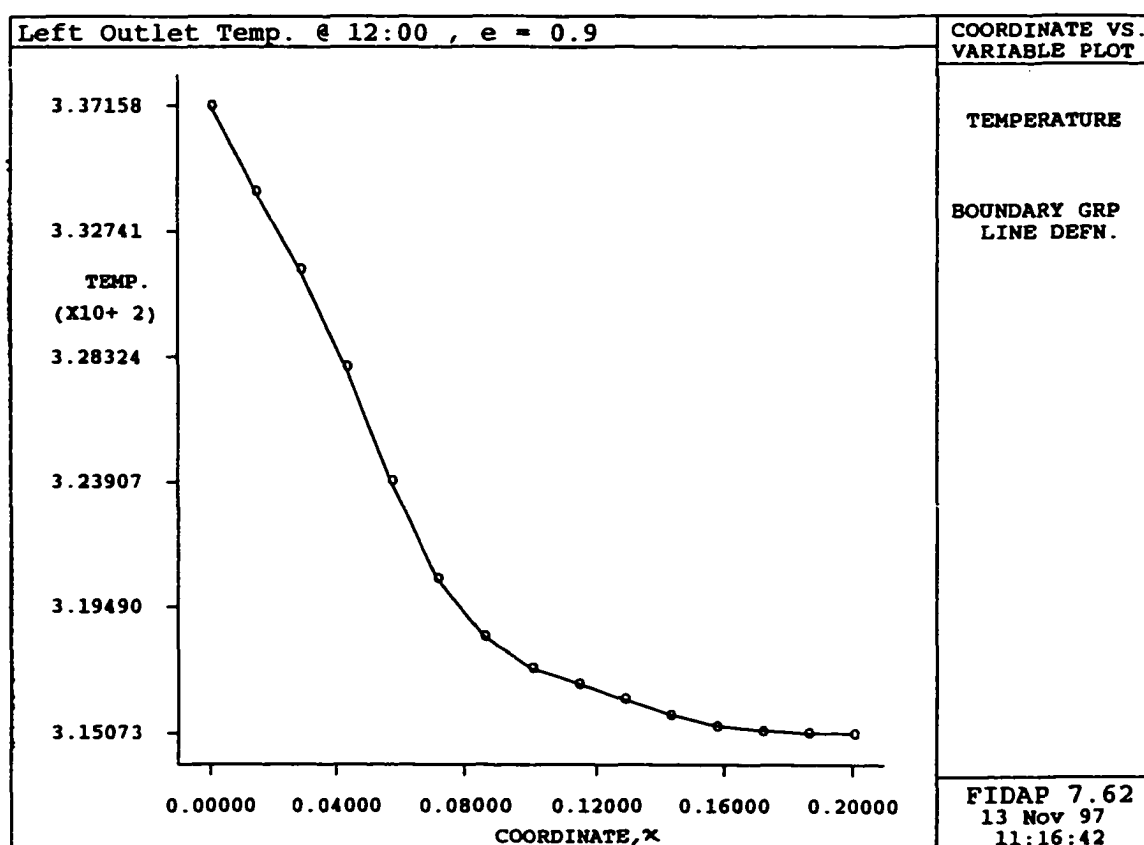
The solution, presented in Figure 3-11, showed that with convection and radiation, there is some variation in the air temperature along the inclined surface of the attic. The figure shows a temperature contour plot for the entire solution and indicates that the temperature variation is small in the core region and is around 315K. A case where there is a variation of the temperature in the core of the attic, at 10:00 am, is due to the difference of the heat flux imposed on either inclined surface, the left side has a value of 189.90 W/m<sup>2</sup> and the right side has a value 273.90 W/m<sup>2</sup>. Figure 3-12 shows the temperature at the boundary of the outlet which varies between 315 K to 337 K. The maximum temperature occurred near the inclined surface and then dropped gradually to its minimum; this phenomenon can be explained by using the theory of thermal boundary layers<sup>9</sup>. Figure 3-13 shows temperature distribution within the thermal boundary layer ( $\delta_t$ ) having a gradient which is infinite at the leading edge and becomes smaller as the boundary develops downstream.

The temperature at the middle section of the top of bottom surface (top of insulation) varies between 310K to 319K as shown in Figure 3-14. Notice that the lower temperature occurs at and near the air entrance (i.e inner inlet) then starts to rise gradually until reaches its maximum at the mid point of the center surface. Since there are no recirculation zones in this region, the temperature remain steady at 318K. The same phenomena also occur at the left and the right side of the bottom surface, where the temperature drops near the at 308 K air inlet and then rises to 319K on the area away from the inlet where there is no recirculation zones. Then it drops to 313.5 K as it approaches the inlet from the other side as shown in Figure 3-15. Hence near the relatively cooler inlet areas of the slots, the temperatures of the surfaces drop. Also, the drop in the temperature in some of these regions can be explained

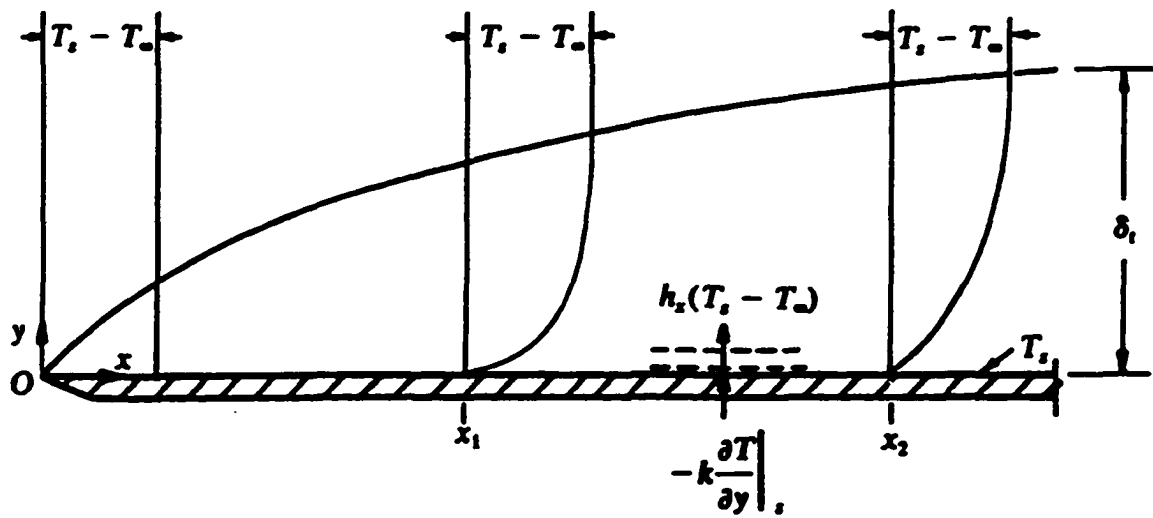
by the recirculation zones present as in the case with the inner inlets.



**Figure 3-11** Temperature contour plot for the attic at 12:00 PM with Emissivity = 0.9.

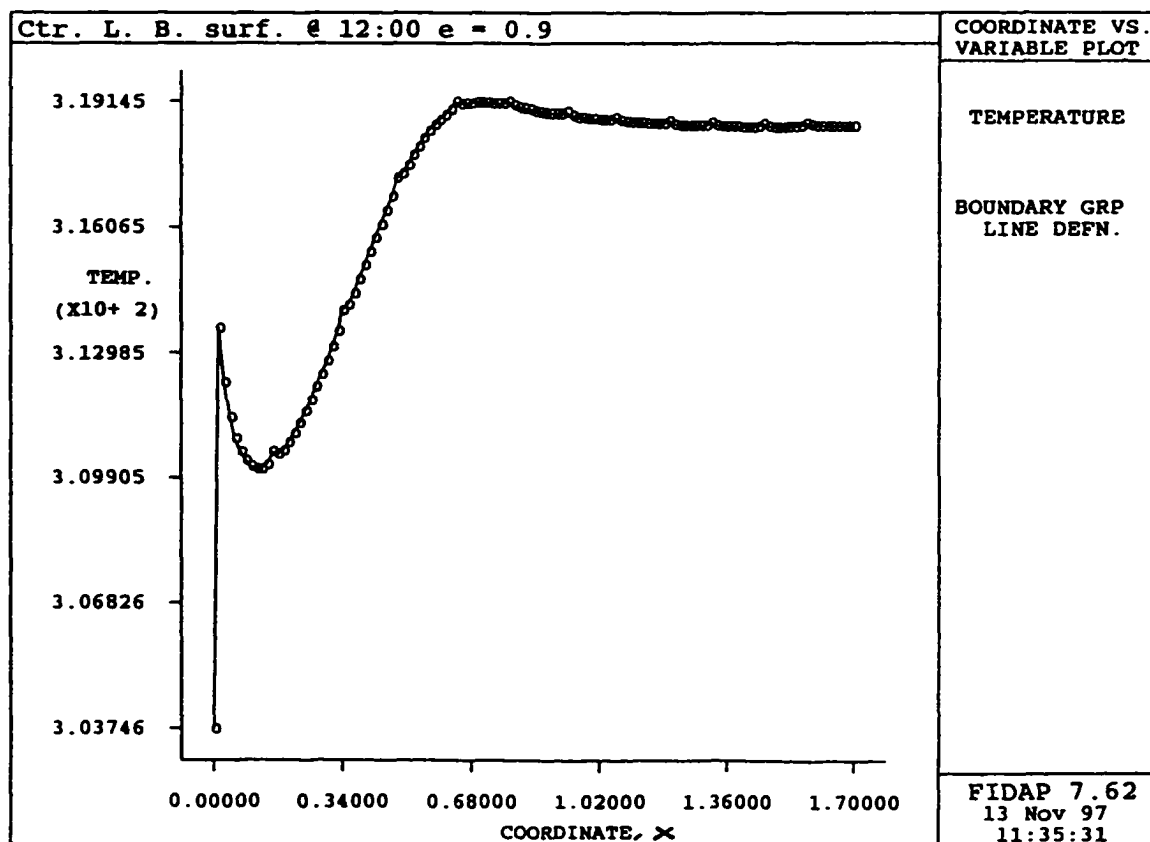


**Figure 3-12 Air Temperature Profile at the Top of the Attic (L. Outlet)  
at 12:00 PM with Emissivity = 0.9.**

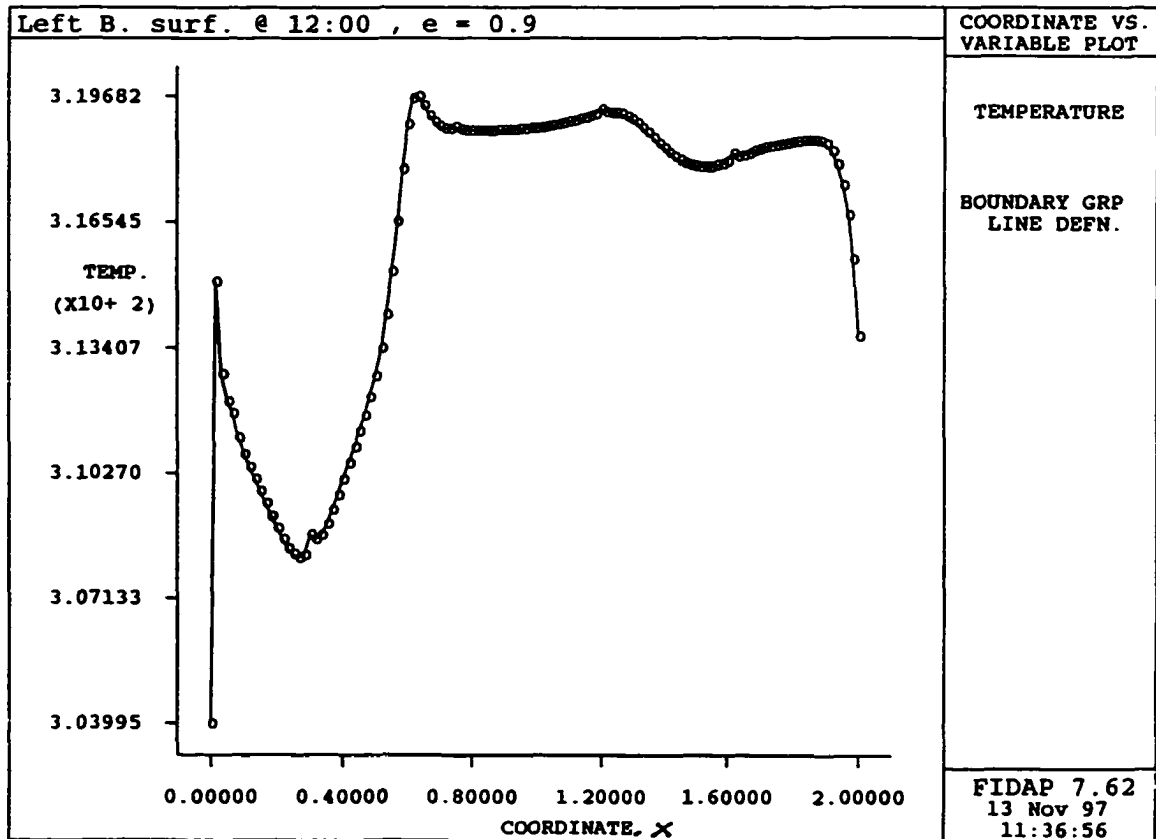


**Figure 3-13 Temperature Distribution Layout within the Thermal B.L.**





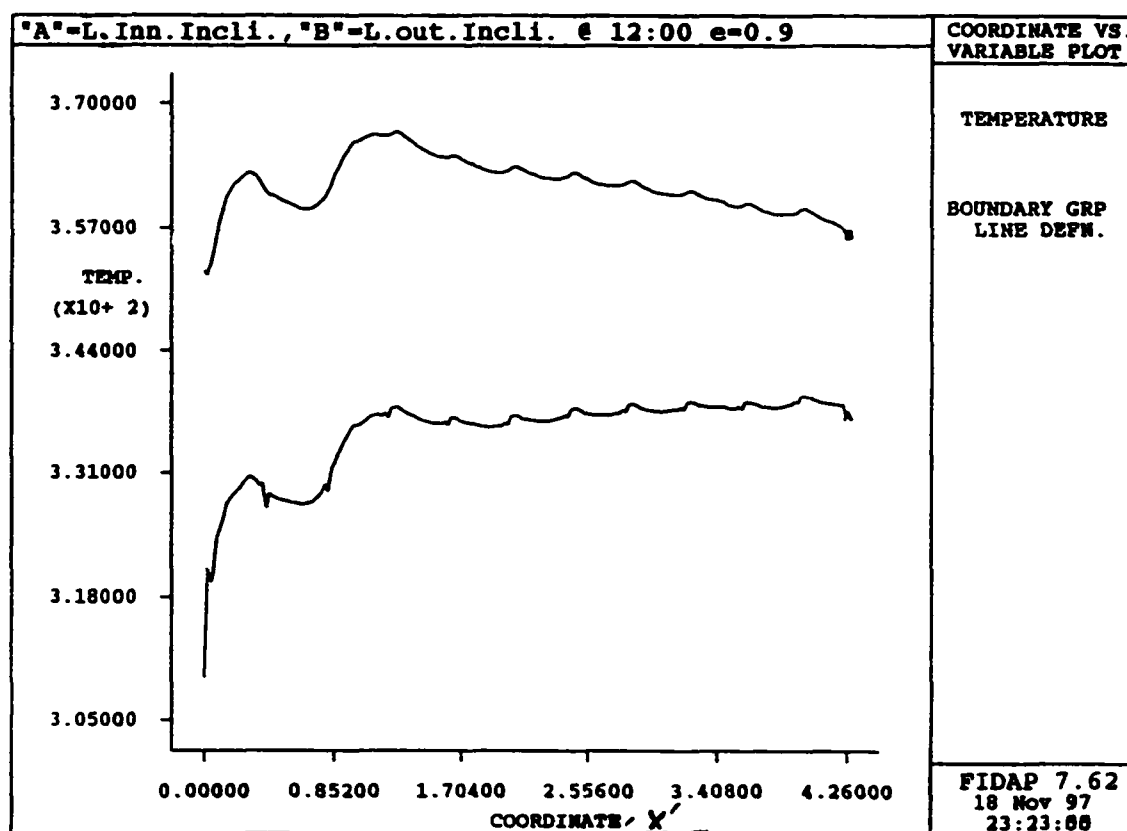
**Figure 3-14 Temperature Profile at the Center Bottom Inner Surface  
at 12:00 PM with Emissivity = 0.9.**



**Figure 3-15 Temperature Profile at the Left Bottom Inner Surface  
at 12:00 PM with Emissivity = 0.9.**

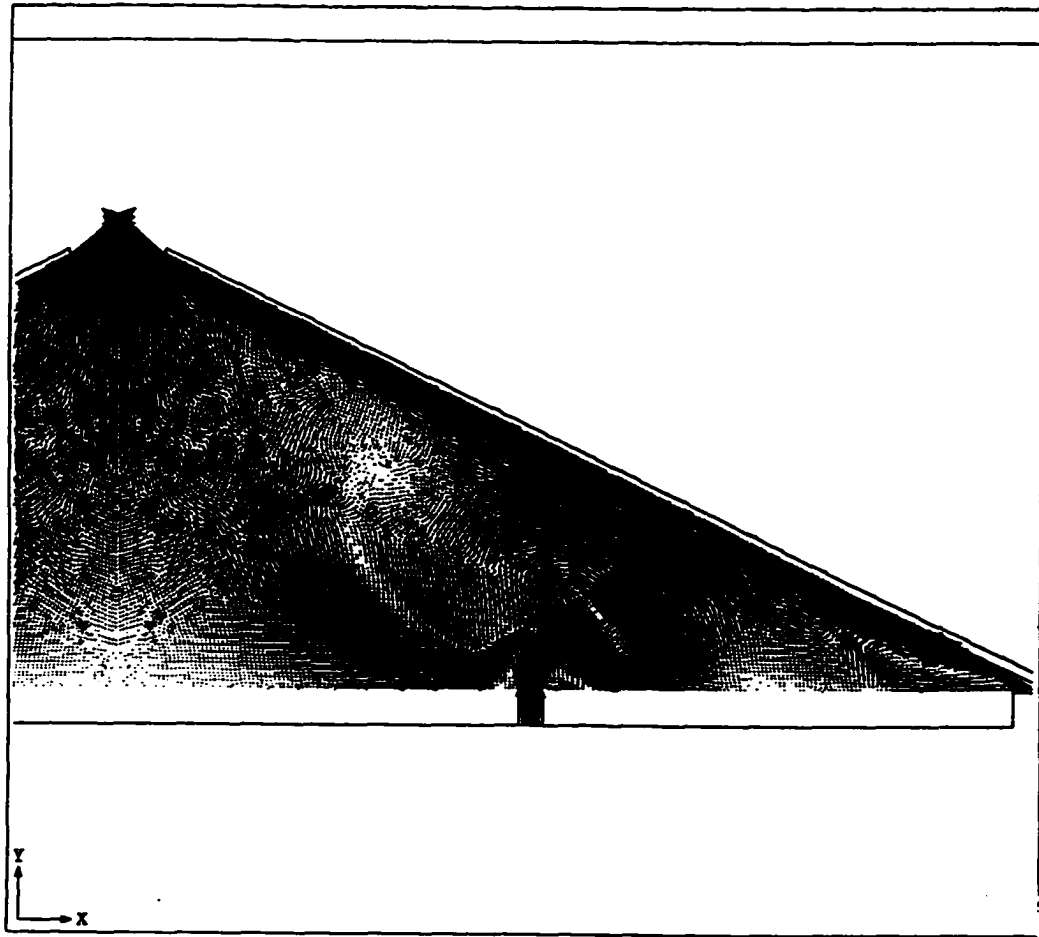
### 3.3 Temperature Profile Along the Inclined Surfaces:

Figure 3-16 shows the temperature profile of the two inclined plywood surfaces (Inner and Outer). At 12:00 PM with a 0.9 emissivity and a solar flux of  $213 \text{ W/m}^2$ , the temperature on the outer surface varies between 350 K to 367 K and at the inner surface the temperature varies between 310 K to 340 K. The variation of temperature along the lower surface can be explained by the existence of lower air temperature coming into the attic from outside which explains the initially low temperature at the inlet. The decrease in the temperature difference between the two surfaces along the air flow can be partially explained by a decrease in the local heat transfer coefficient as the boundary layer develops; this is based



**Figure 3-16 Temperature Profile for the left Inclined (Inner and Outer) Surfaces at 12:00 PM with Emissivity = 0.9.**

on the fact that the heat flux is constant along the surfaces. Figure 3-17 shows some details of the flow such as recirculation zones from a velocity contour plot of the overall model, also Figure 3-18 shows the streamlines for the air flow and indicates the location of major recirculation zones.



**Figure 3-17** Recirculation Zones at the Right Air Inlets and the Outlet of the Attic.

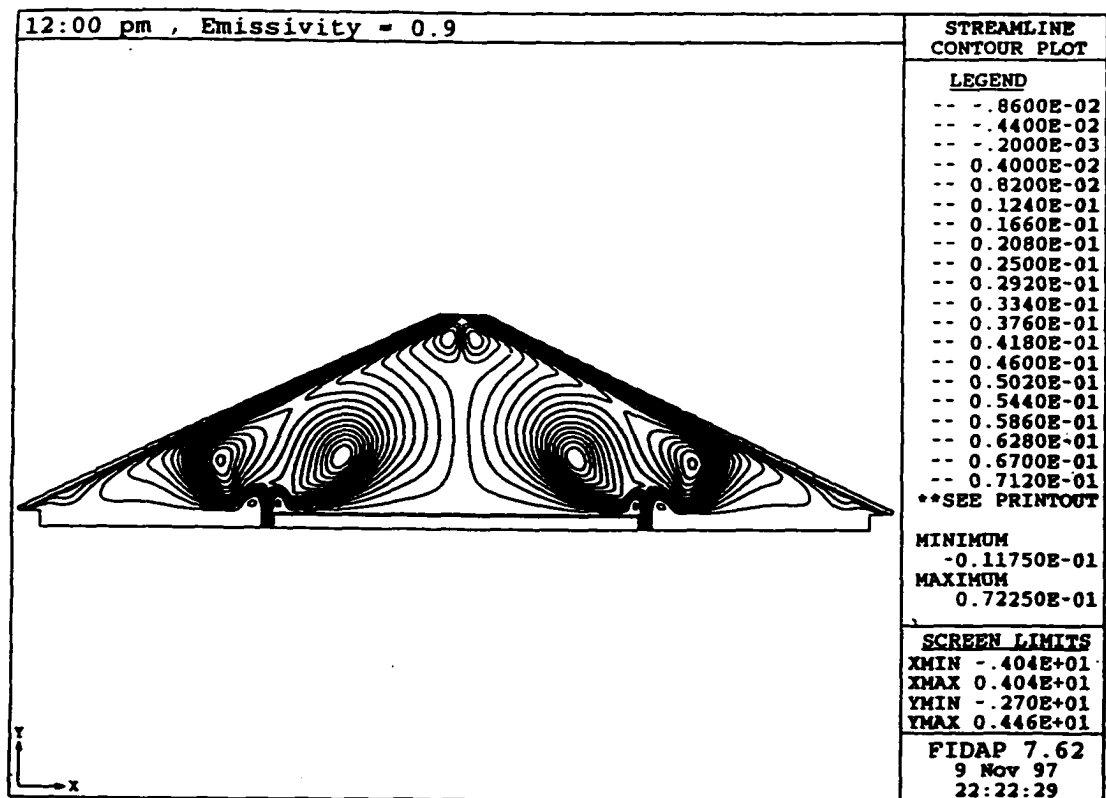


**Figure 3-18 Streamline Contour Plot Inside the Attic at 12:00 PM with Emissivity = 0.9.**

### 3.4 Velocity Profile and Velocity Contour of Air With Emissivity = 0.05

In this section, the same model is used with an emissivity of 0.05 applied on the inner inclined surfaces to investigate the effect of radiant barrier on the ceiling cooling load. The overall contour plot for the velocity in the y-direction ( $U_y$ ) at 12:00 PM is shown in Figure 3-19. It shows that the maximum velocity has a value of 0.458 m/s and it occurs at the upper region near the outlet of the enclosure. The minimum velocity in the y-direction occurs at inner inlet and has value of -0.2695 m/s. The negative sign is explained by the air entering at a velocity of 0.33 m/s, it dips down and become negative. Then it picks up speed because of the hot surfaces surrounding it and hence changes to a positive velocity.

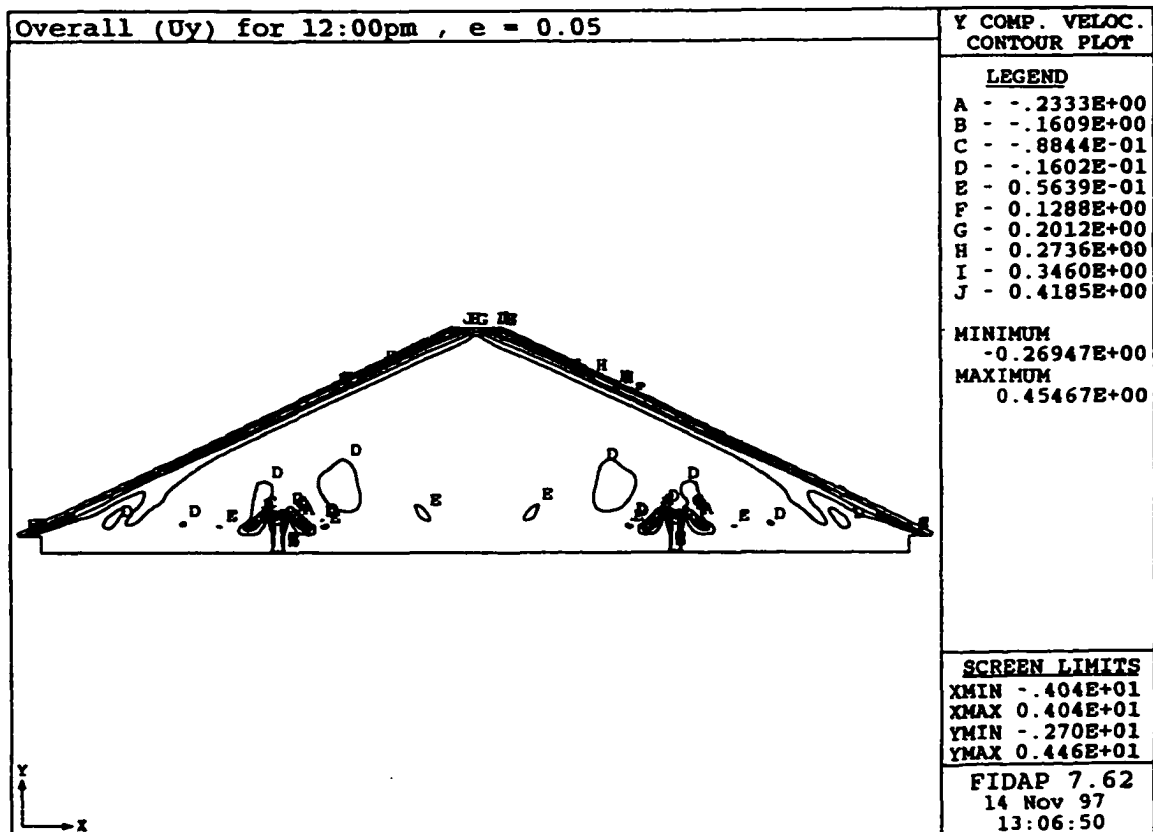
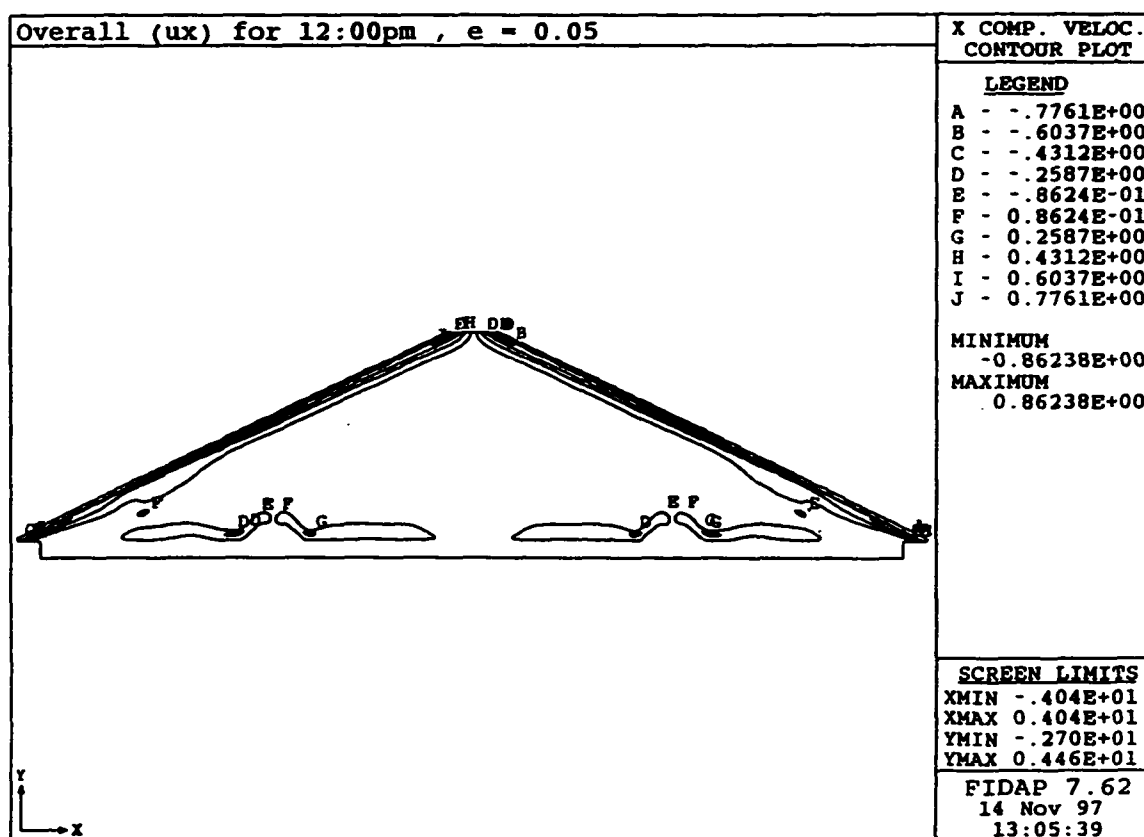
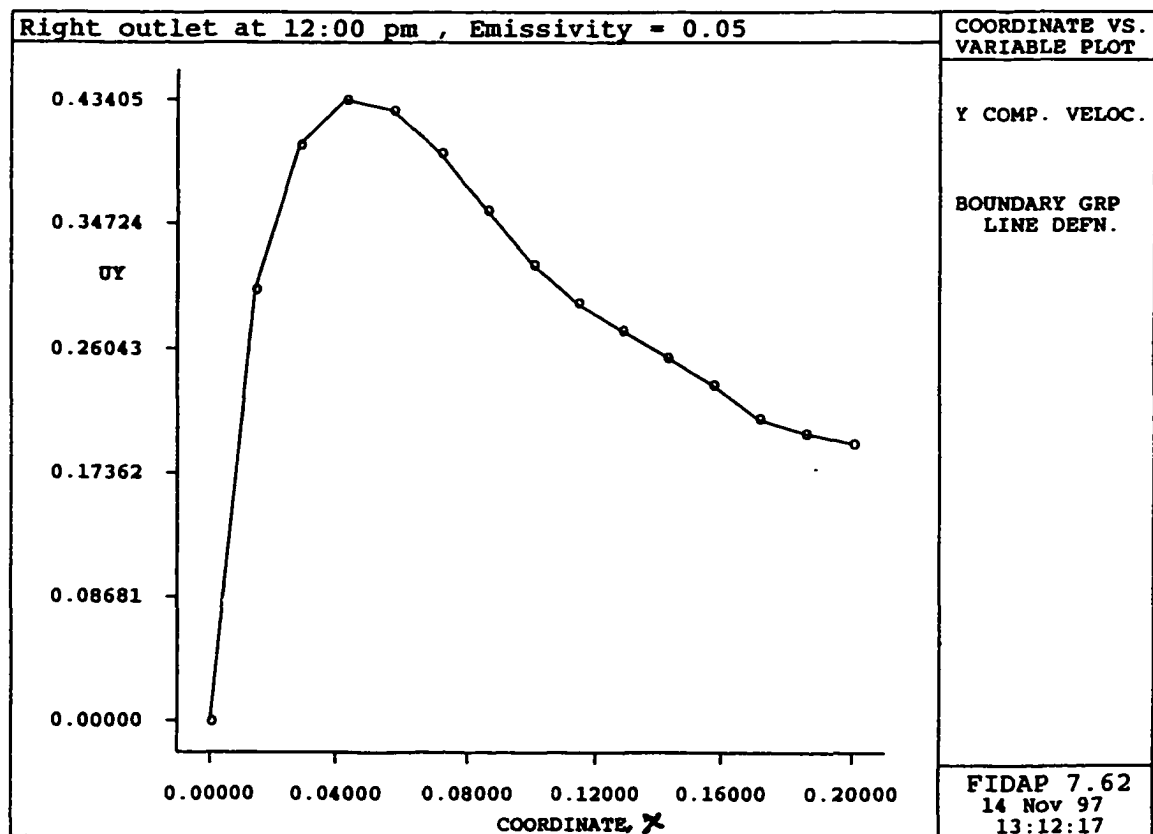


Figure 3-19 Velocity Contour Plot in Y- Direction at 12:00 PM with Emissivity = 0.05.

Observing the velocity plot in the x-direction ( $U_x$ ) in Figure 3-20, the maximum velocity of 0.776 m/s occurs at the top region of the attic. In the core region of the attic the velocity has practically no x-component since all of the air is moving vertically. At the outlet the maximum velocity in the y-direction ( $U_y$ ) has a value of 0.435 m/s as shown in Figure 3-21. The higher maximum velocity at the outlet plane for the low emissivity case is due to the fact that higher inner surface temperatures exist for the low emissivity case. The maximum velocity in the x-direction ( $U_x$ ) at the outlet is 0.6 m/s as shown in Figure 3-22.



**Figure 3-20** Velocity Contour Plot in X-Direction at 12:00 PM with Emissivity = 0.05.



**Figure 3-21 Velocity Profile in Y- Direction at the Top of the Attic  
(R. Outlet) at 12:00 PM with Emissivity = 0.05.**



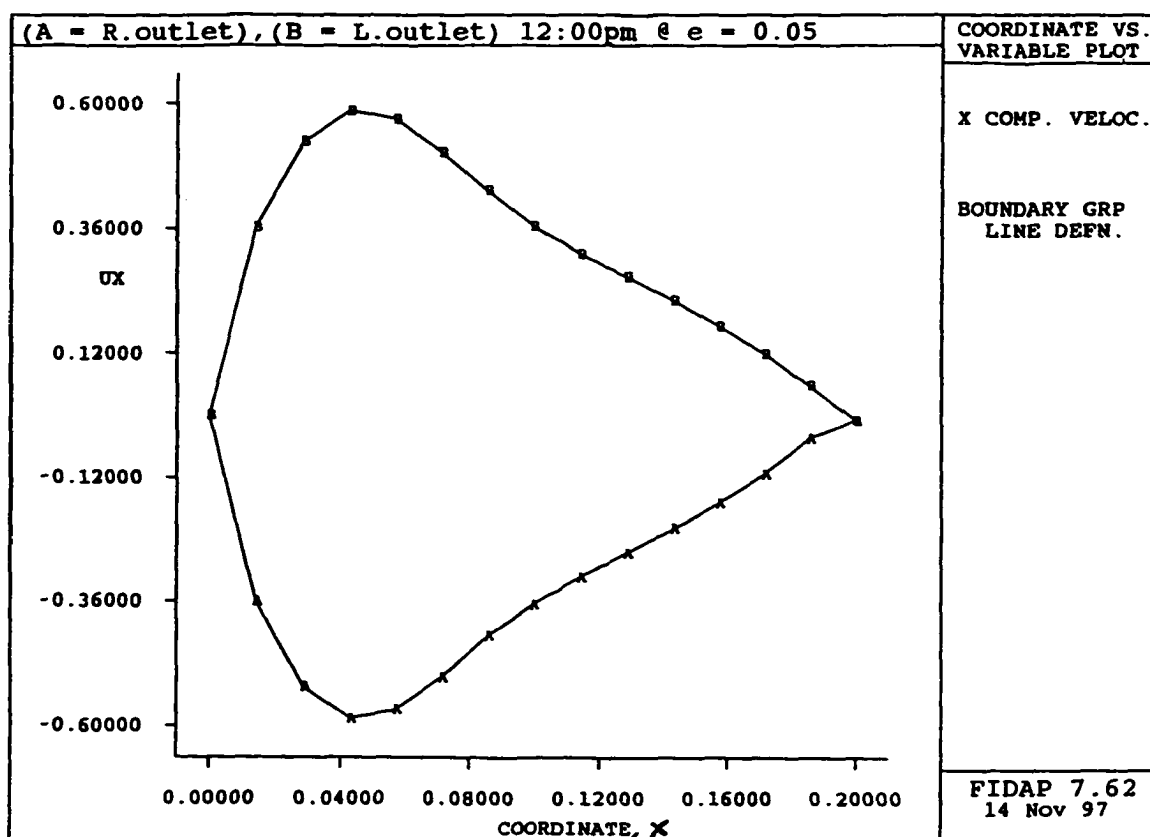


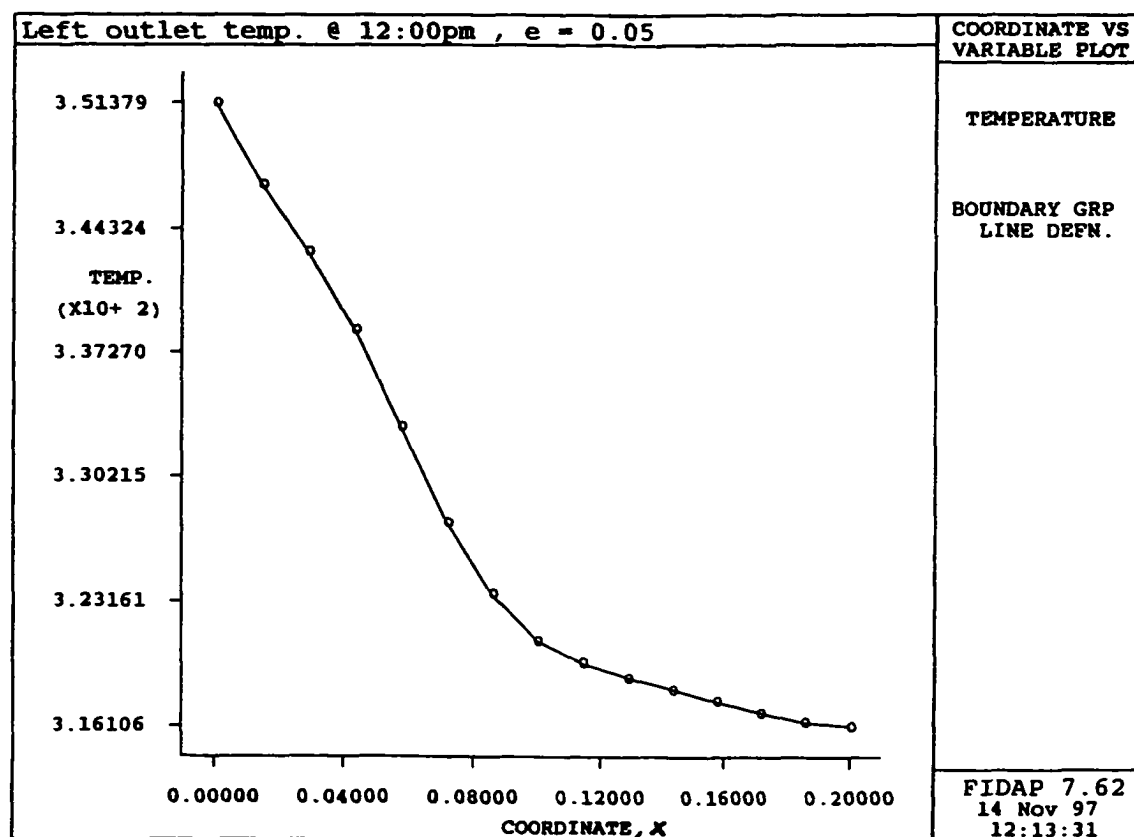
**Figure 3-22** Velocity Profile in X- Direction at the Top of the Attic  
(L.Outlet and R.Outlet) at 12:00 PM with Emissivity = 0.05.

## **NOTE TO USERS**

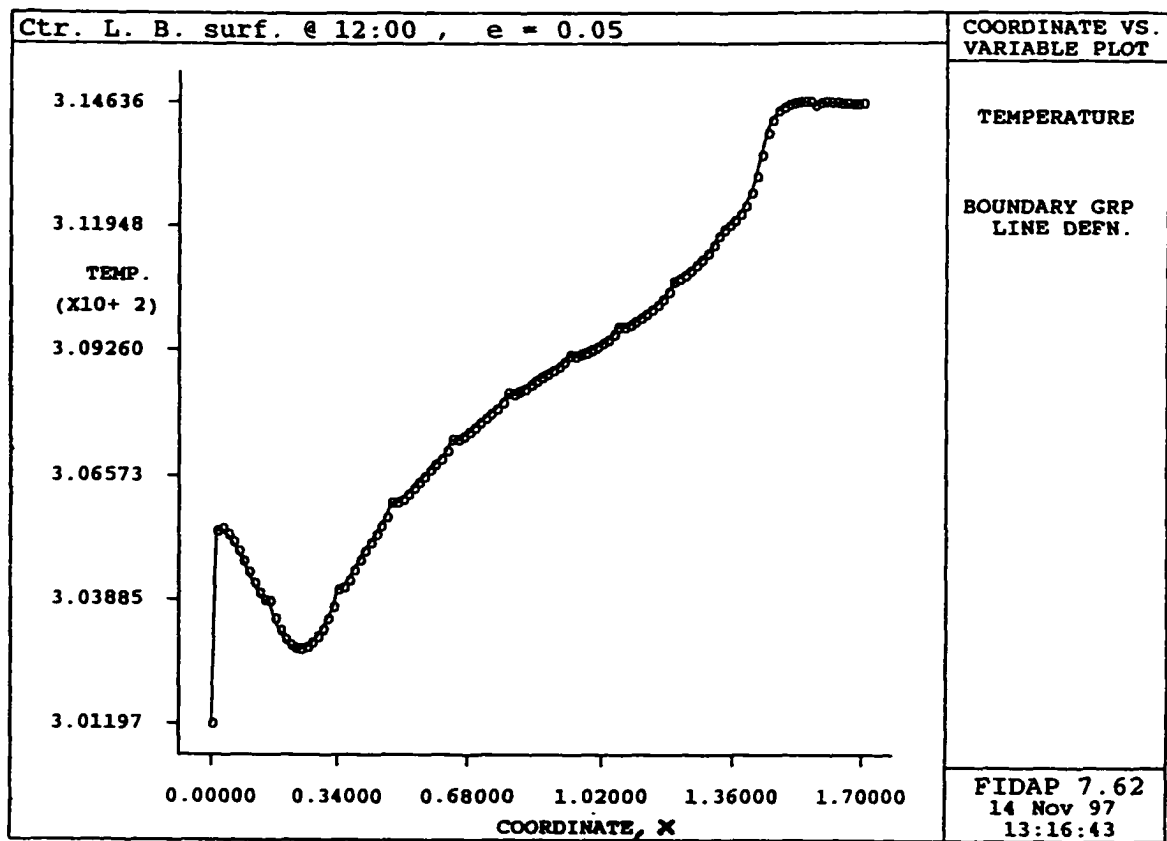
**Page(s) not included in the original manuscript are unavailable from the author or university. The manuscript was microfilmed as received.**

**UMI**

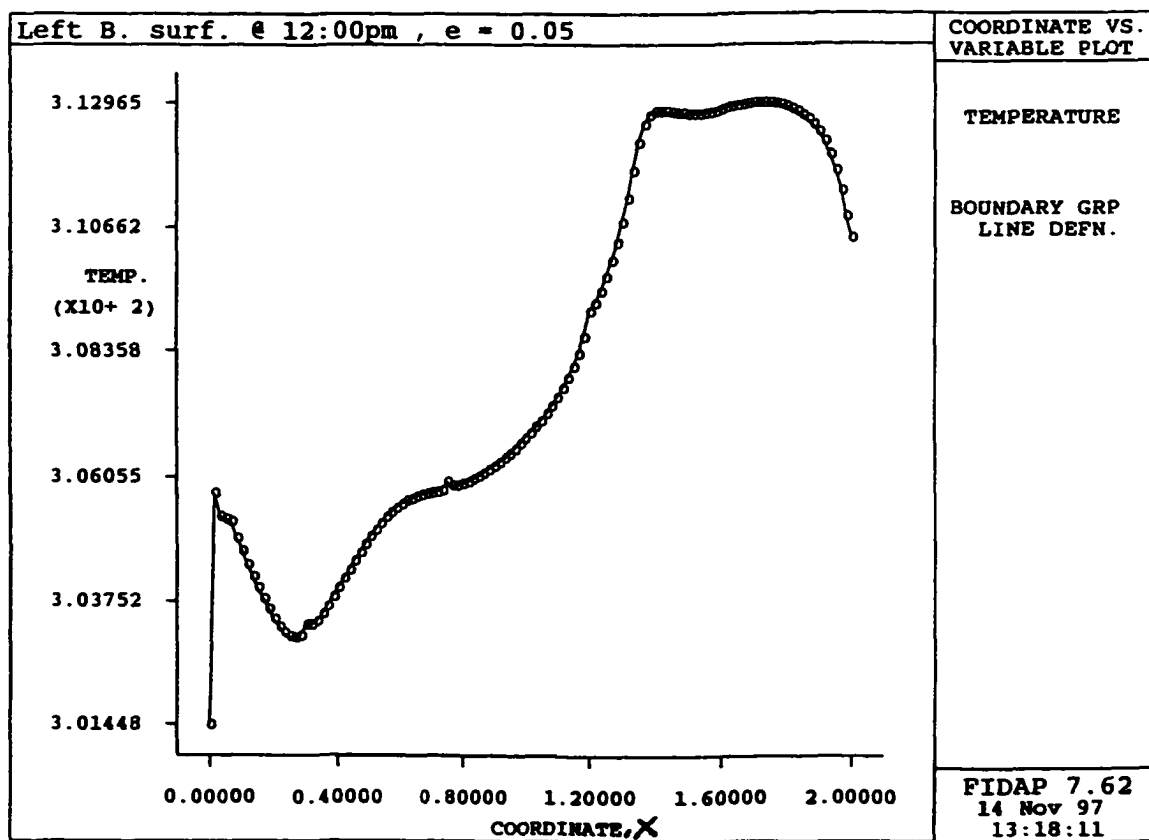
The temperature at the middle section of the bottom surface varies between 301K to 314K as shown in Figure 3-25. The lower temperature occurs at and near the air entrance (i.e. inner inlet), then starts to rise gradually until it reaches its maximum value at the mid point where it remains relatively constant at 314 K. The same phenomena also occur at the left and the right side of the bottom surface, where the temperature drops near to 302.5 K at the air inlet and then rises to 313 K on the area away from the inlet where no recirculation zones exists. Then it drops again to 310.5 K as it approaches the inlet from the other side as shown in Figure 3-26.



**Figure 3-24** Temperature Profile at the top Attic ( L.Outlet) at 12:00 PM with Emissivity = 0.05.



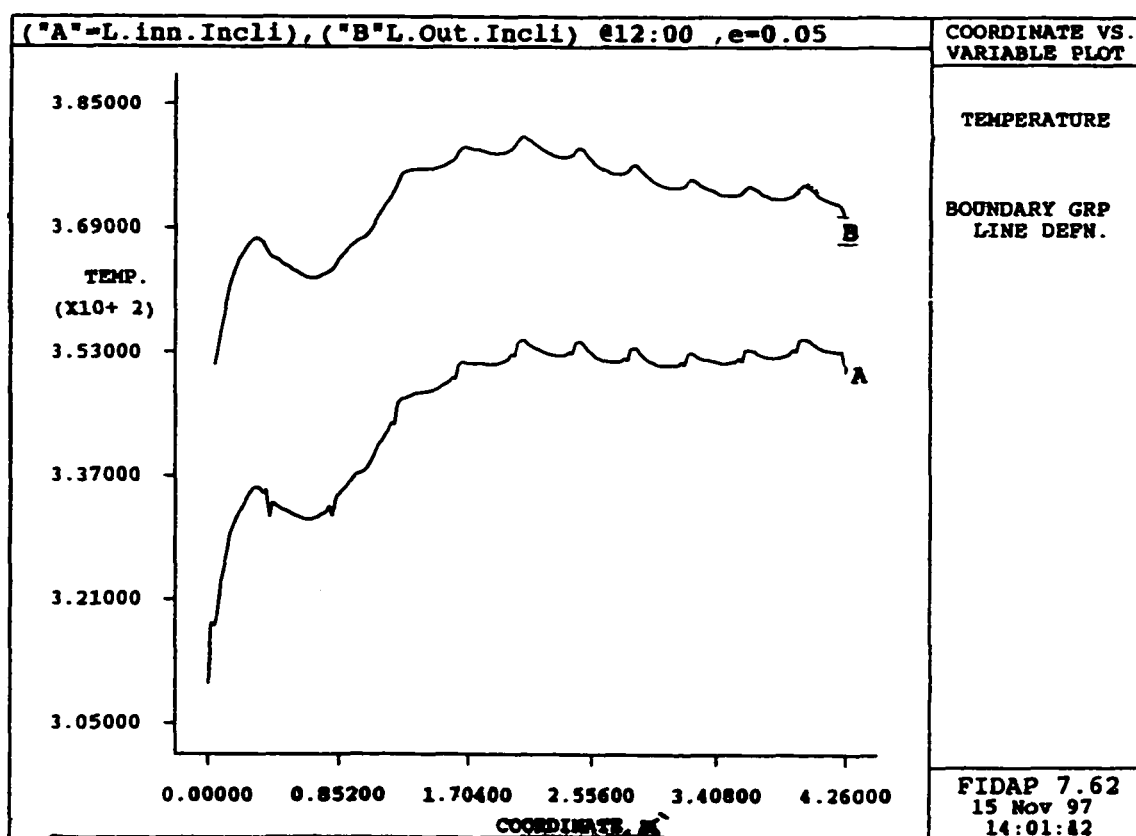
**Figure 3-25 Temperature Profile at the Center Bottom Inner Surface at 12:00 PM with Emissivity = 0.05**



**Figure 3-26** Temperature profile at the Left Bottom Inner Surface at 12:00 pm  
12:00 PM with Emissivity = 0.05

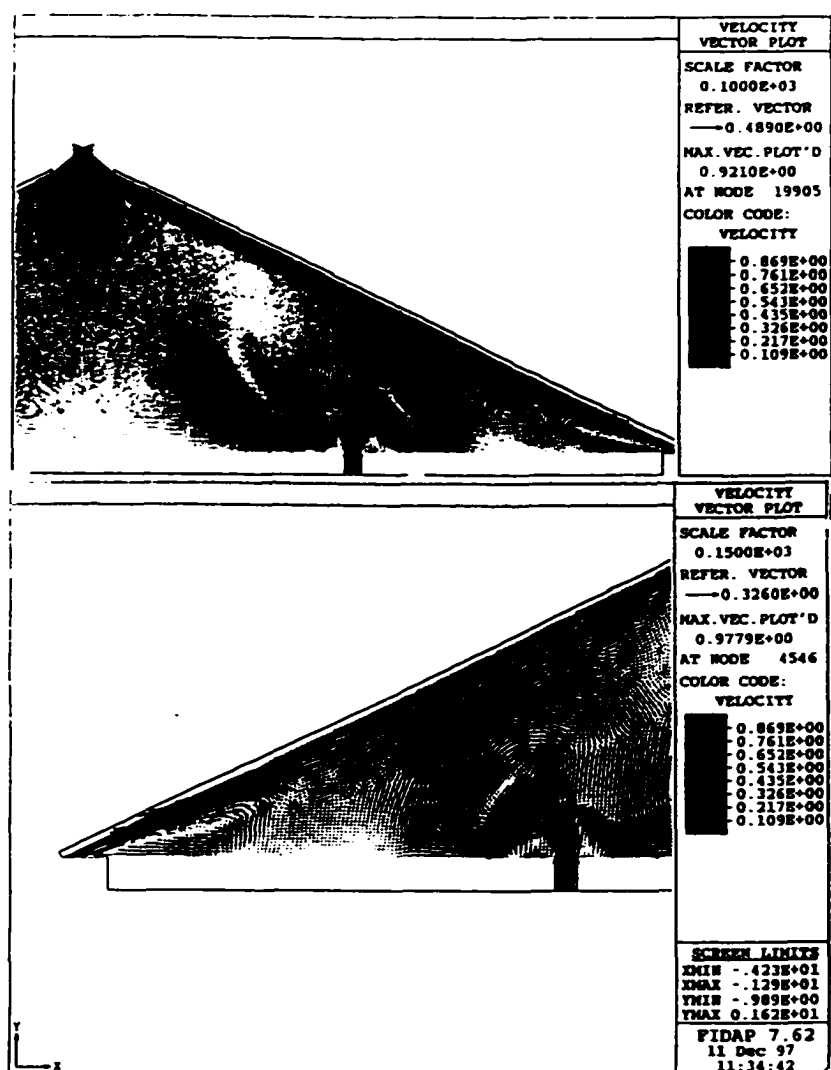
### 3.6 Temperature Profile Along the Inclined Surfaces With Emissivity = 0.05

Figure 3-27 shows the temperature profile of the two surfaces of the plywood on the inclined surfaces. At 12:00 PM with an 0.05 emissivity and a solar flux of  $213 \text{ W/m}^2$ , the temperature on the outer surface varied between 353 K to 379 K and at the inner surface temperature it varied between 310K to 350 K. The lower inlet temperature can be explained by the existence of low air temperature coming initially in to the attic.



**Figure 3-27** Temperature Profile at the Left Inclined ( Inner and Outer) Surface at 12:00 PM with Emissivity = 0.05.

A similar trend exists as in the case of the previously discussed high emissivity case. Figure 3-28 shows details of the velocity contour plot for the overall model; Figure 3-29 shows the streamline plot for the air when it enters the enclosure and again depicts recirculation zones in the air flow.



**Figure 3-28** Air Velocity Contour Plot for the Entire Attic at 12:00 with Emissivity = 0.05.

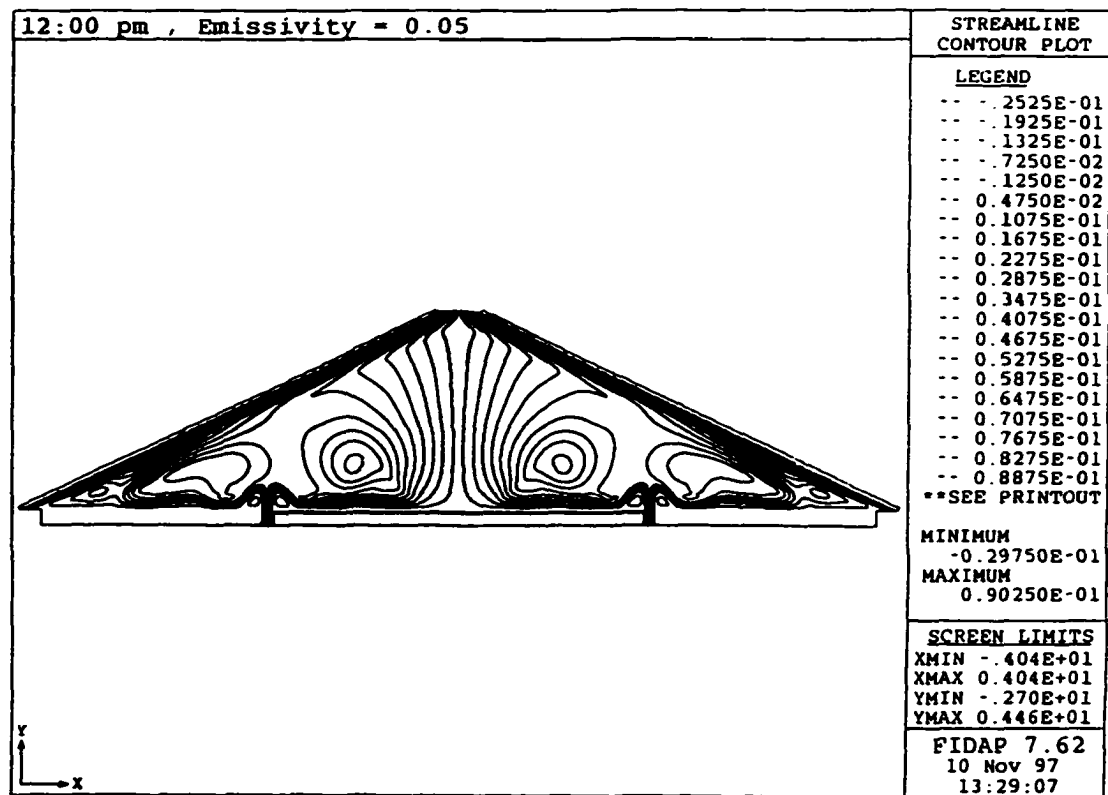


**Figure 3-29 Streamline Contour Plot Inside the Attic at 12:00 PM  
with Emissivity = 0.05**



### 3.7 Calculation of Energy Balance for the Entire Attic

A numerical check on the energy balance around the total attic is obtained by applying the first law of thermodynamics to a control volume. This is accomplished by observing that:

*Enthalpy flow of air into C.V. [A] + Heat transfer due to insolation [B] = Enthalpy flow of air out of C.V. [C] + heat flow out of insulation [D].*

$$[A] + [B] = [C] + [D]$$

$$\Delta H = [C] - [A] \quad (3-2)$$

where  $\Delta H$  is the change of air enthalpy flowing through the attic, and [A] or [C] can be described as:

$$[C] = (\Delta x) (u_y) (T) (\rho) (c_p) \quad (3-3)$$

where  $\Delta x$  - distance between each node

$u_y$  - velocity at any given node

$T$  - temperature at any given node

$\rho$  - density

$c_p$  - specific heat

The enthalpy calculation at the edge points is given by the following equation:

$$H_{edge} = \left(\frac{\Delta x}{2}\right) \left(\frac{u_y}{2}\right) \left(\frac{T_o + T_1}{2}\right) (\rho) (c_p) \quad (3-4)$$

Figure 3-30 and Figure 3-31 show the temperature and velocity distribution in the y-direction they are used to calculate the change of enthalpy for each case (i.e Emissivity = 0.9

and 0.05 respectively). Equation (3-3) is used to calculate the enthalpy for the inner nodes while equation (3-4) is used to calculate the enthalpy for the first and the last nodes (edge nodes) on the surface. Since these nodes are the points of intersection with another surface so only half of the distance is considered. The same procedure is applied for both velocity and temperature at those edge nodes.

Equation 3-2 was verified using  $A = 43363.1 \text{ J/hr}$ ,  $B = 6501 \text{ J/hr}$ ,  $C = 52916.1 \text{ J/hr}$ , and  $D = 4979.5 \text{ J/hr}$  and it was found that the difference between the left hand side and right hand side of the equation is approximately  $8031 \text{ J/hr}$  or 13.9% for the case of emissivity = 0.05. For the case of emissivity = 0.9 the difference between left hand side and right hand side is  $3589 \text{ J/hr}$  or 6.8% for  $A = 43363.5 \text{ J/hr}$ ,  $B = 6501 \text{ J/hr}$ ,  $C = 48036 \text{ J/hr}$ , and  $D = 5417.3 \text{ J/hr}$ .  $\Delta H$  at 12:00 PM with an emissivity of 0.9 was found to be  $4673 \text{ J/hr}$ ,  $\Delta H$  at 12:00 PM with an emissivity of 0.05 was found to be  $9553 \text{ J/hr}$ .

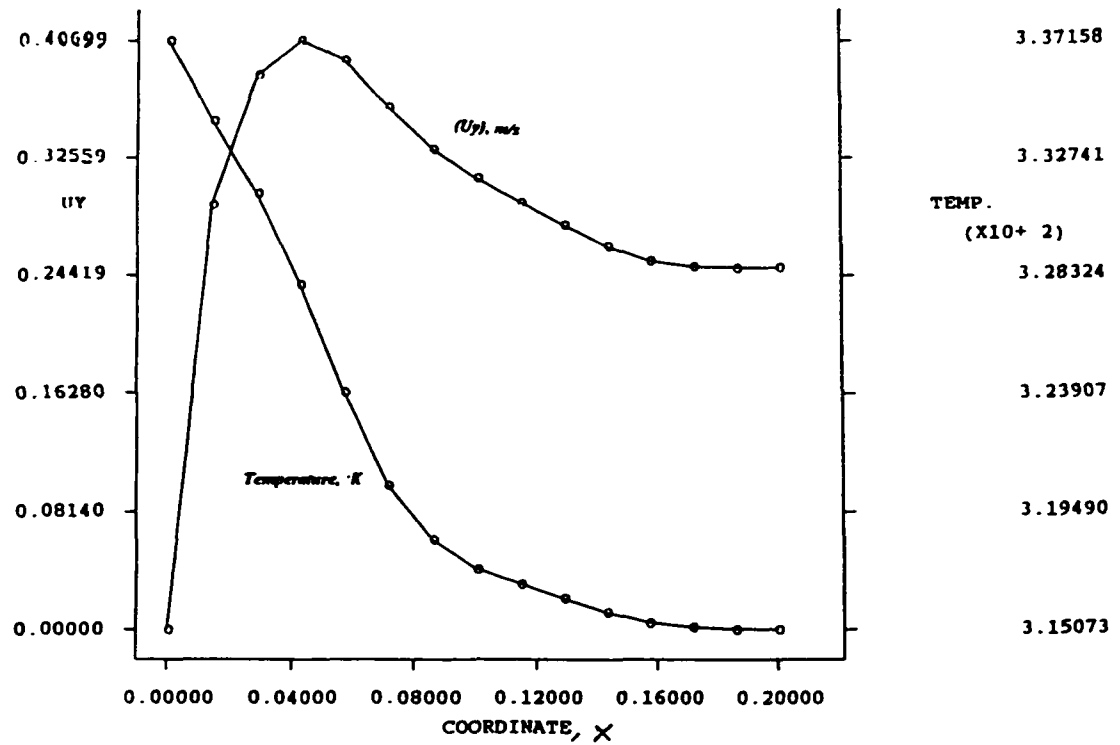


**Figure 3-30 Temperature and Velocity Distribution at 12:00 PM with Emissivity = 0.9 at the Left Outlet for Energy Balance Calculations**

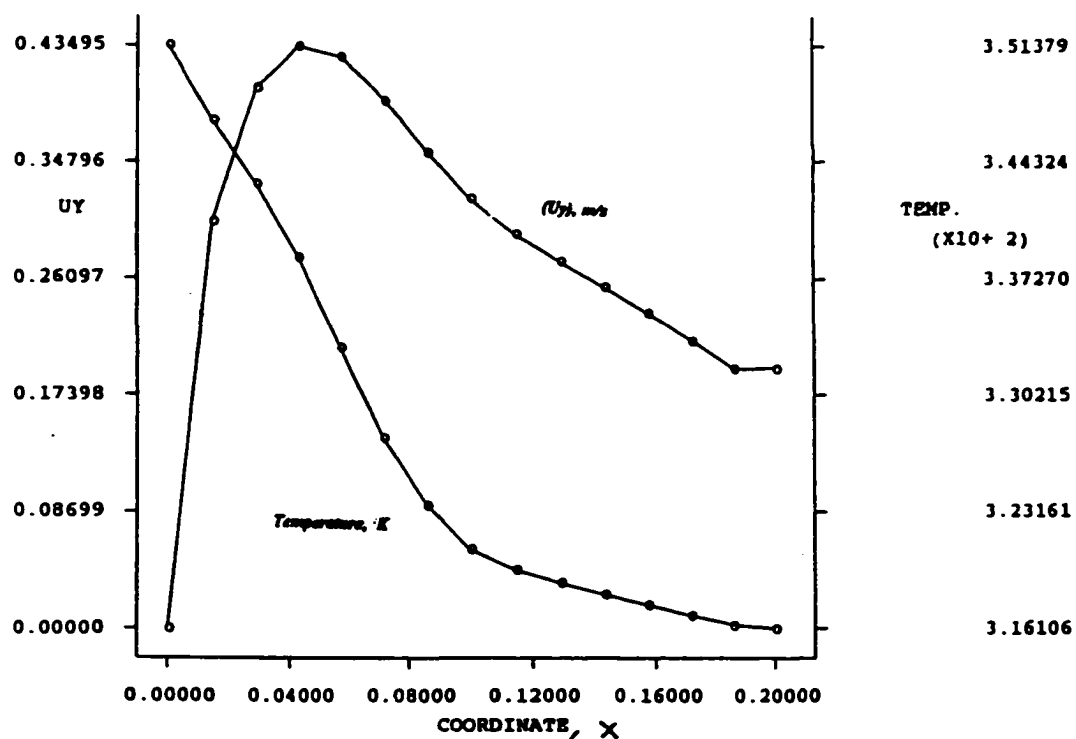


**Figure 3-31 Temperature and Velocity Distribution at 12:00 PM with Emissivity = 0.05 at the Left Outlet For Energy Balance Calculations.**

### 3.8 Calculation of Length Average Heat Transfer Coefficient.

The inclined surface is considered to be a long tilted plate with a heated surface facing downward as shown in figure 3-32

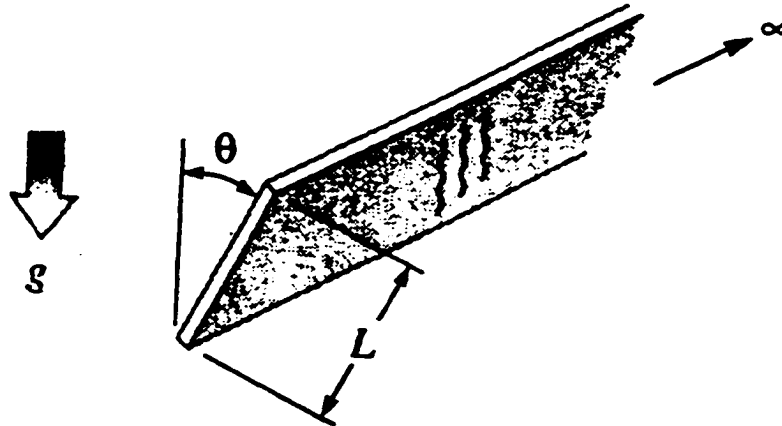


**Figure 3-32 Schematic Diagram for Long Tilted Plate.**

The Nusselt number for the above shape when subjected to a constant heat flux is given by the following empirical correlation<sup>11</sup>:

$$\overline{Nu}_L = 0.56 (Gr_L Pr \cos\theta)^{0.25} \quad (3-5)$$

in this investigation

$$Q'' = \text{constant}$$

$$10^5 < Gr_L Pr \cos \theta < 10^{11}$$

$$0 < \theta < 89^\circ$$

For  $\theta$  equal to  $65^\circ.65'$ , the Nusselt number is 132.1. Then by applying the following relation, the length average heat transfer coefficient ( $h$ ) can be calculated as:

$$\bar{h} = \frac{\overline{Nu_L} K}{L} \quad (3-6)$$

$h$  was found to be  $0.815 \text{ W/ m}^2 \text{ K}$ .

The length average heat transfer coefficient predicted by FIDAP is shown in Figure 3-33. The average value is  $0.737 \text{ W/ m}^2 \text{ K}$  at 12:00 pm for the 0.9 emissivity. The value of ( $h$ ) is slightly higher near the inlet and the outlet of the attic than in the core section of the inclined surface due to higher flow rate over these regions. Finally, an estimate of the heat flow by convection is :

$$Q''_{conv} = \bar{h} (T_s - T_\infty) \quad (3-7)$$

The values are relatively close and the differences can be partially explained by the difference in the flow conditions. As a double check to the numerical result from the relation of  $Q''_{tot} = Q''_{rad} + Q''_{conv}$ , and calculating  $Q''_{conv}$  from equation (3-7) the difference between the total heat transfer and  $Q''_{conv}$  would be the heat transfer by radiation.

For the case of emissivity = 0.05 at 12 :00 PM, the length average heat transfer coefficient ( $h$ ) was calculated by equation (3-6) and found to be  $0.76 \text{ W/ m}^2 \text{ K}$ . The predicted average value for ( $h$ ) using FIDAP was  $0.628 \text{ W/ m}^2 \text{ }^\circ\text{K}$  as shown in figure 3-34.

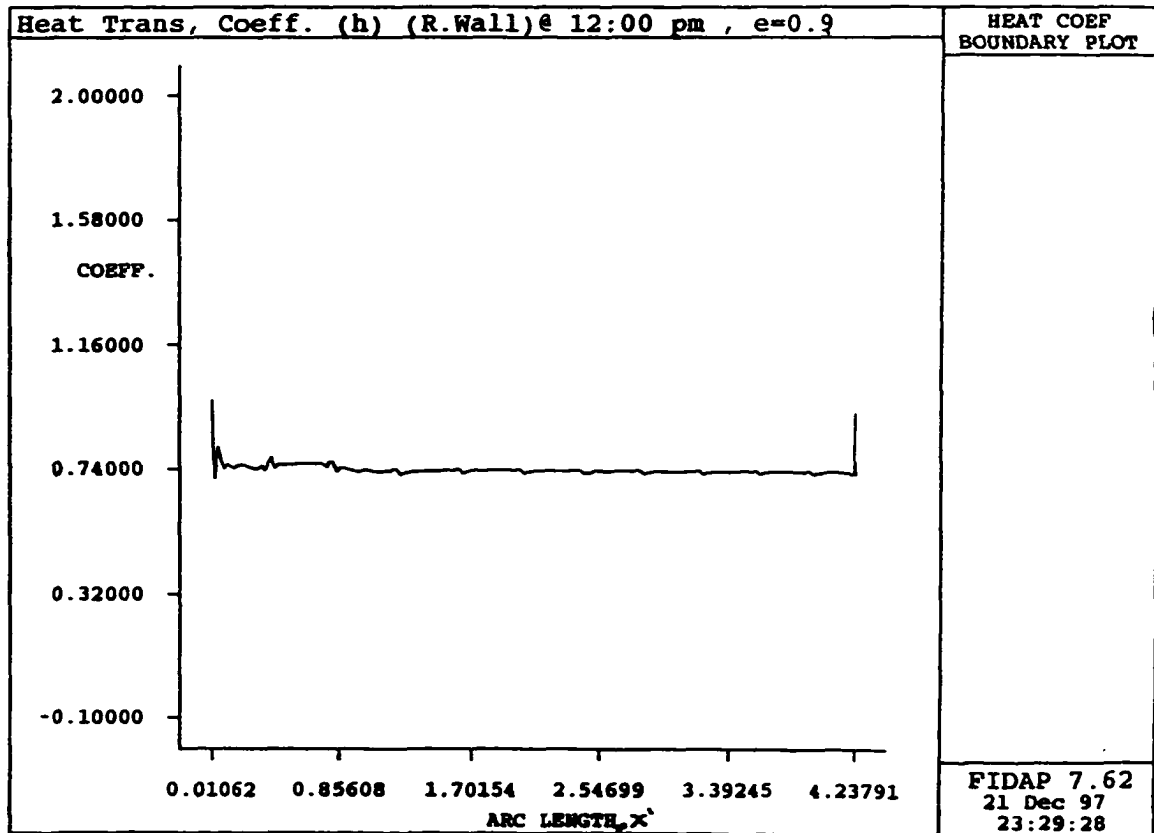


**Figure 3-33** Convective Heat Transfer Coefficient for the Inner Inclined Surface at 12:00 PM With Emissivity = 0.9.

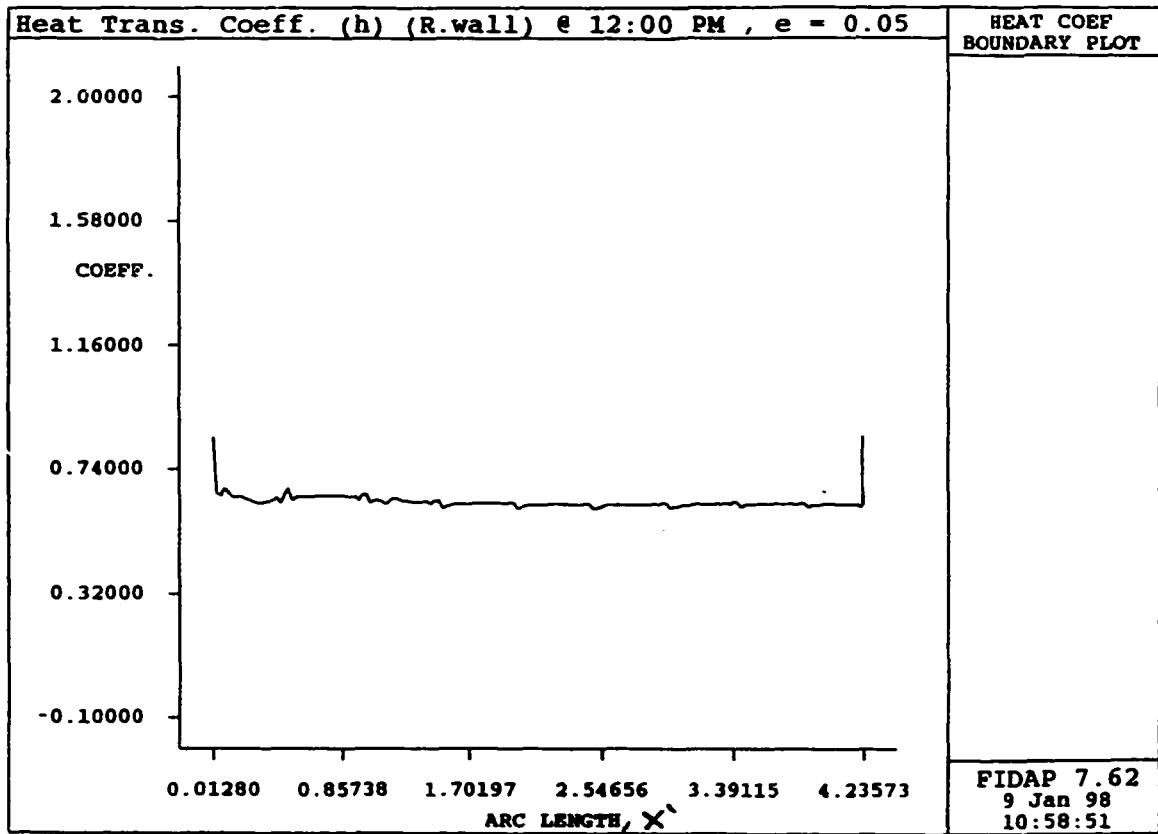


**Figure 3-34** Convective Heat Transfer Coefficient for the Inner Inclined Surface at 12:00 PM With Emissivity = 0.05.



### 3.9 Comparison for the Inclined Surface Temperatures, Outlet Air Temperature and Outlet Air Velocities for the Two Cases of Emissivity:

By Investigating the temperature profile in Figure 3-35 for the inclined inner surface and the air temperature in Figure 3-36 at the outlet, it is noticed that the higher temperature occurs with the low emissivity case (i.e.,  $\epsilon = 0.05$ ). Since a major portion of the solar heat flux is not allowed to penetrate through the attic resulting in an increase of the temperature

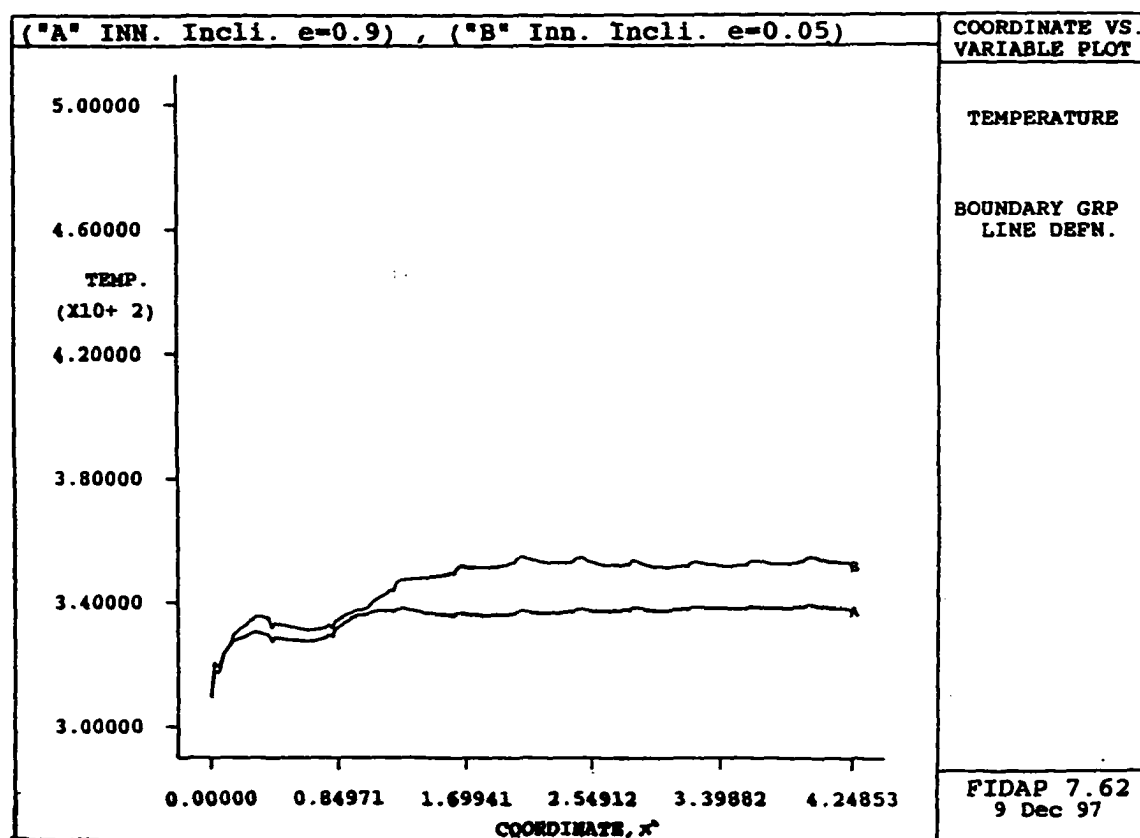


**Figure 3-35** Inclined Surface Temperature Distribution At 12:00 PM for both Emissivities ( Curve A = 0.9 and Curve B = 0.05).

on these surfaces and also an increase of temperature at the outlet of the attic and the air velocity leaving the attic as well. The inclined surface temperature at 12:00 PM with emissivity of 0.9 is between 310 K and 337 K while the surface temperature with emissivity of 0.05 ranged between 310 K and 359 K as shown in Figure 3-35. This can be explained by having a lower net radiation from the inclined surfaces while the total heat flow remains constant for the lower emissivity case.

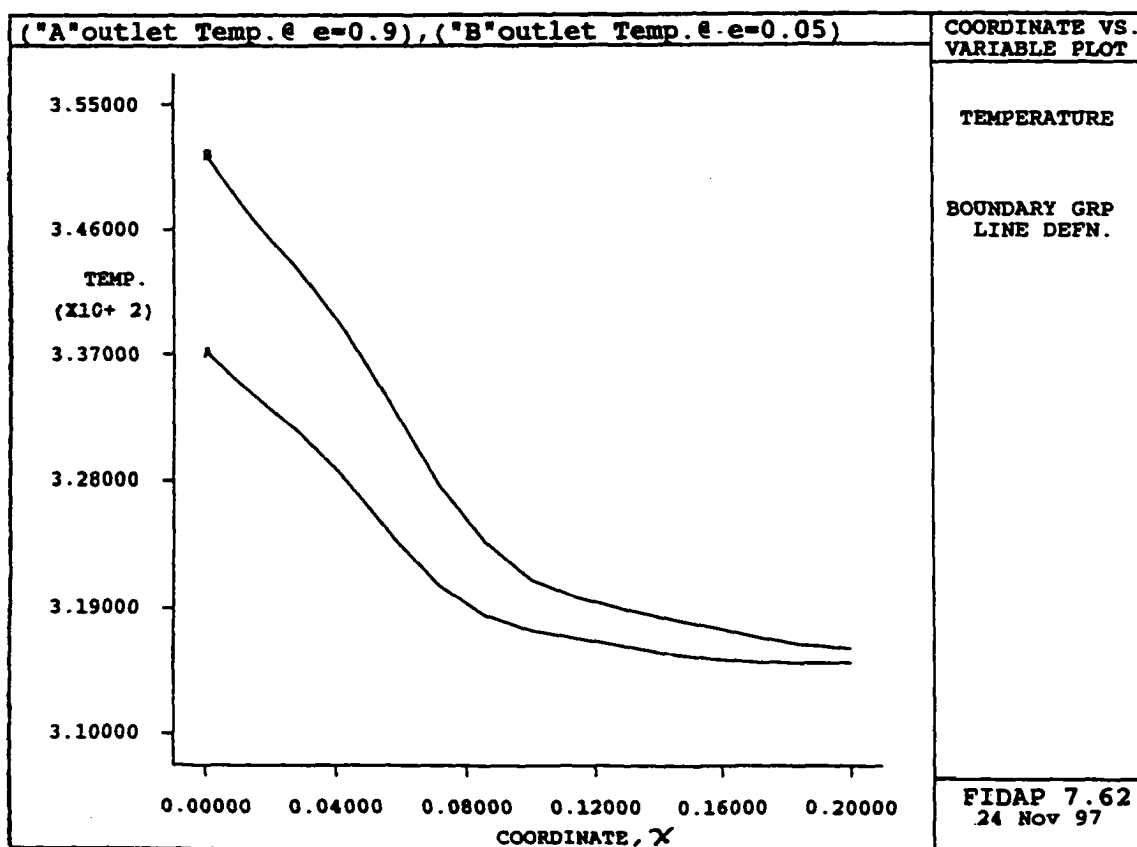


**Figure 3-36 Left Outlet Temperature Distribution at 12:00 PM for both Emissivities (Curve A = 0.9 and Curve B = 0.05).**

The velocity profile in the Y- direction ( $U_y$ ) at the left outlet also changed as shown in Figure 3-37. The higher velocity occurs in the lower emissivity case. Since hotter air has a higher velocity, it was found that when the emissivity is 0.9 the velocity ( $U_y$ ) at the outlet ranged between 0 to 0.37 m/sec while the velocity ( $U_y$ ) ranged between 0 to 0.46 m/sec when the emissivity is 0.05.

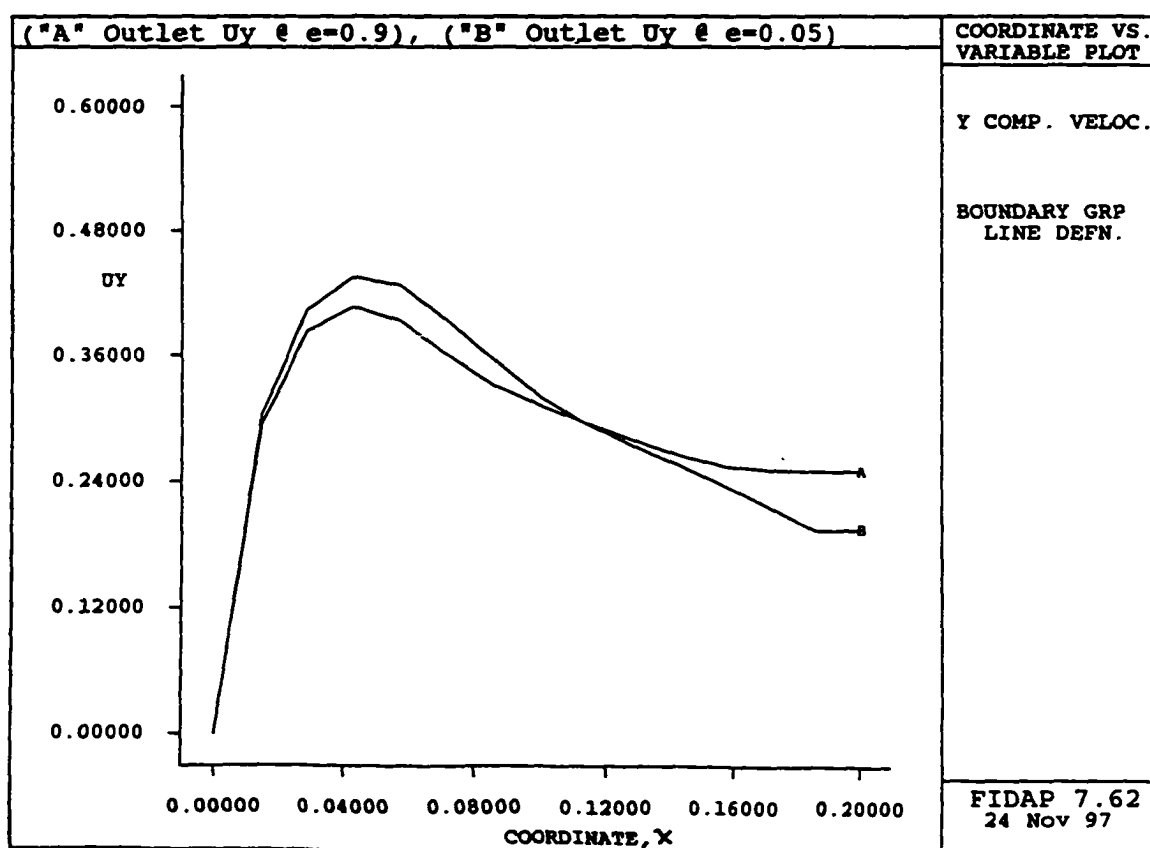


**Figure 3-37** Left Outlet Velocity Profile in Y- Direction at 12:00 PM for both Emissivities (Curve A = 0.9 and Curve B = 0.05).

## CHAPTER 4

### CONCLUSIONS AND RECOMMENDATIONS

#### 4-1 Conclusion

The velocity profile and the velocity contour of the air with both emissivities showed that there are some recirculation zones near all the inlets. Also, there are air movement and recirculation zones along the inclined surfaces of the attic. The velocity in the y-direction ( $U_y$ ) along the inclined surface has values between 0.2907 m/s to 0.4237 m/s for the 0.9 emissivity. The core region of the enclosure remained at an almost constant velocity of 0.02453 m/s. The velocity in the x-direction ( $U_x$ ) at the outlet has a maximum value of 0.5 m/s.

The air temperature profile with the surface emissivity of 0.9 shows that the emissivity has a significant effect on the air movement along the inclined surfaces. The higher the emissivity at the inner surface, the lower the air movement in the enclosure.

The low emissivity material will rise the output air temperature profile as well as the temperature of the inclined surfaces which was explained by a higher convective heat transfer from the inclined surface to offset the reduction of the radiation heat transfer from that surface. The outlet temperature indicated a peak temperature of 352 K with an emissivity of 0.05 while the temperature with an emissivity of 0.9 remained at 337 K. The heat flow out of the insulation is predicted by FIDAP for both cases, this heat flow represents the cooling load for the ceiling in the space below the attic. For the 0.05 emissivity, the conduction heat

flow has an average of 4979.5 J/hr, a reduction of 23.5% of the heat flow which had been applied originally on the inclined surfaces at 12:00 PM. For the case of the emissivity equal to 0.9, the conduction heat flow at the lower surface of the attic was reduced by 16.6% with an average value of 5417.3 J/hr.

The value of the average length heat transfer coefficient  $h$  predicted by FIDAP is compared with the empirical correlation given in equation (3-6). The discrepancy was about 9.8%; accordingly, the FIDAP predictions are interpreted to be valid. The discussions in Chapter 3 have demonstrated a scheme to model the ventilated attic using an evaporative air cooler. The fundamental structure of this modeling scheme was used in this investigation.

#### **4.2 Recommendation**

In this study a two dimensional computer model was used to simulate the heat transfer in a ventilated attic. Further studies, such as a 3-D model, are needed to simulate the air flow end effects and effects of structural members on the attic heat flow. Also, more experimental studies should be performed using different materials on the inclined surfaces to determine how accurately these mechanisms of heat transfer model and the actual condition.

# APPENDIX A

## FIDAP INPUT FILE

```

/This file contains the input for the problem which was created
and read by FIDAP Software.
/ FI-GEN INPUT FILE CREATED ON 21 Dec 97 AT 23:40:13
/
TITLE "Thermal Modeling of residential attic"

FI-GEN ()
/
/ Creating COORDINATE SYSTEMs
COORDINATE (SELECT, ID = 1)
COORDINATE (ACTIVATE)
COORDINATE (SELECT, ID = 1)
COORDINATE (MODIFY, SIZE = 0.075,
XRULER = 0, YRULER = 0, ZRULER = 0,
XLENGTH = 10, YLENGTH = 10, ZLENGTH = 10,
XSCALE = 1, YSCALE = 1, ZSCALE = 1,
XTICS = 1, YTICS = 1, ZTICS = 1,
COLOR = 2, INVISIBLE, NOSHOWNLABEL)
/
/ Creating POINTs
POINT ( ADD, COORDINATES, SYSTEM = 1, CARTESIAN,
COLOR = 2, VISIBLE, NOSHOWNLABEL )
/ [X] [Y] [Z] [Id comment]
-4 0 0 1
-0.2 1.9 0 2
0.2 1.9 0 3
4 0 0 4
3.8 0 0 5
1.8 0 0 6
1.7 0 0 7
-1.7 0 0 8
-1.8 0 0 9
-3.8 0 0 10
POINT ( ADD, COORDINATES, SYSTEM = 1, CARTESIAN,
COLOR = 1, INVISIBLE, NOSHOWNLABEL )
/ [X] [Y] [Z] [Id comment]
-0.21984203782461 1.5543204840449 0 11
-5.5511151231258e-17 1.6361268253104 0 12
0.21984203782461 1.5543204840449 0 13
POINT ( ADD, COORDINATES, SYSTEM = 1, CARTESIAN,
COLOR = 2, VISIBLE, NOSHOWNLABEL )
/ [X] [Y] [Z] [Id comment]
0 1.9 0

```

```

48
POINT ( ADD, COORDINATES, SYSTEM = 1, CARTESIAN,
COLOR = 1, INVISIBLE, NOSHOWNLABEL )
/ [X] [Y] [Z] [Id comment]
-1.9058497693684 1.0470751153158 0 49
-1.8011422578369 1.0994288710816 0 50
-0.1708429849811 0 0 51
1.9058497693684 1.0470751153158 0 52
1.8011422578369 1.0994288710816 0 53
0.1708429849811 0 0 54
4.4408920985006e-16 -0.15 0 55
POINT ( ADD, COORDINATES, SYSTEM = 1, CARTESIAN,
COLOR = 2, VISIBLE, NOSHOWNLABEL )
/ [X] [Y] [Z] [Id comment]
3.9 0 0 56
-3.9 0 0 57
POINT ( ADD, COORDINATES, SYSTEM = 1, CARTESIAN,
COLOR = 1, INVISIBLE, NOSHOWNLABEL )
/ [X] [Y] [Z] [Id comment]
3.9578362471889 0.021081876405564 0 58
3.6095238095238 0 0 59
3.6259832772344 0.050765066239968 0 0
3.642442744945 0.10153013247994 0 61
3.5722015905172 0.15230243531245 0 62
1.7595371877676 0 0 63
1.7190743755353 0 0 64
-3.9578362471889 0.021081876405563 0 65
-3.6095238095238 0 0 66
-3.6259832772344 0.050765066239968 0 67
-3.642442744945 0.10153013247994 0 68
-3.5722015905172 0.15230243531245 0 69
-1.7595371877676 0 0 70
-1.7190743755353 0 0 71
/
/ Creating CURVES
/ The following curve's id is 1
POINT ( SELECT, ID )
1 2
CURVE ( ADD, LINE,
COLOR = 8, VISIBLE, NOSHOWNLABEL, NOARROW)
/ The following curve's id is 2
POINT ( SELECT, ID )
-0.24160193008437 1.3098881541957 0 14
-5.5511151231258e-17 1.3788296359955 0 15
0.24160193008437 1.3098881541957 0 16
-0.063240107740242 0.24443232984914 0 17
3.3306690738755e-16 0.25729718931489 0 18
0.063240107740242 0.24443232984914 0 19
-0.085 0 0 20
3.3306690738755e-16 0 0 21
0.085 0 0 22
POINT ( ADD, COORDINATES, SYSTEM = 1, CARTESIAN,
COLOR = 2, VISIBLE, NOSHOWNLABEL )
/ [X] [Y] [Z] [Id comment]
3.8 -0.15 0 23
1.8 -0.15 0 24
1.7 -0.15 0 25

```

```

-1.7 -0.15 0 26
-1.8 -0.15 0 27
-3.8 -0.15 0 28
POINT ( ADD, COORDINATES, SYSTEM = 1, CARTESIAN,
COLOR = 1, INVISIBLE, NOSHOWNLABEL )
/ [X] [Y] [Z] [Id comment]
-3.777777777777778 0.111111111111111 0 29
3.777777777777778 0.111111111111111 0 30
-3.5520258316262 0.084416325183106 0 31
-0.225859990448 1.4435191606311 0 32
-1.1102230246252e-16 1.5194938532959 0 33
0.225859990448 1.4435191606311 0 34
3.5520258316262 0.084416325183106 0 35
-0.089999999999999 0 0 36
0.090000000000000 0 0 37
POINT ( ADD, COORDINATES, SYSTEM = 1, CARTESIAN,
COLOR = 2, VISIBLE, NOSHOWNLABEL )
/ [X] [Y] [Z] [Id comment]
-0.207768888888889 1.91463388888889 0 38
0.207769 1.914634 0 39
4.0153568376068 0.025250000000001 40
-4.015357 0.02525 0 41
POINT ( ADD, COORDINATES, SYSTEM = 1, CARTESIAN,
COLOR = 1, INVISIBLE, NOSHOWNLABEL )
[X] [Y] [Z] [Id comment]
-0.21084759011087 1.5098069431808 0 42
0.21084759011087 1.5098069431808 0 43
-0.063249781906372 0.27590815644875 0 44
0.063249781906373 0.27590815644875 0 45
-0.076429756438915 0 0 46
0.076429756438916 0 0 47
3 4
CURVE ( ADD, LINE,
COLOR = 8, VISIBLE, NOSHOWNLABEL, NOARROW)
/ The following curve's id is 3
POINT ( SELECT, ID )
6 7
CURVE ( ADD, LINE,
COLOR = 8, VISIBLE, NOSHOWNLABEL, NOARROW)
/ The following curve's id is 4
POINT ( SELECT, ID )
8 9
CURVE ( ADD, LINE,
COLOR = 8, VISIBLE, NOSHOWNLABEL, NOARROW)
/ The following curve's id is 5
POINT ( SELECT, ID )
5 6
CURVE ( ADD, LINE,
COLOR = 8, VISIBLE, NOSHOWNLABEL, NOARROW)
/ The following curve's id is 6
POINT ( SELECT, ID )
9 10
POINT ( SELECT, ID )
27
9
CURVE ( ADD, LINE,
COLOR = 8, VISIBLE, NOSHOWNLABEL, NOARROW)
/ The following curve's id is 16
POINT ( SELECT, ID )

```



```

CURVE ( ADD, LINE,
COLOR = 8, VISIBLE, NOSHOWNLABEL, NOARROW)
/ The following curve's id is 7
POINT ( SELECT, ID )
5 23 18
CURVE ( ADD, LINE,
COLOR = 8, VISIBLE, NOSHOWNLABEL, NOARROW)
/ The following curve's id is 8
POINT ( SELECT, ID )
23 24
CURVE ( ADD, LINE,
COLOR = 8, VISIBLE, NOSHOWNLABEL, NOARROW)
/ The following curve's id is 9
POINT ( SELECT, ID )
24
6
CURVE ( ADD, LINE,
COLOR = 8, VISIBLE, NOSHOWNLABEL, NOARROW)
/ The following curve's id is 10
POINT ( SELECT, ID )

24 25
CURVE ( ADD, LINE,
COLOR = 8, VISIBLE, NOSHOWNLABEL, NOARROW)
/ The following curve's id is 11
POINT ( SELECT, ID )
25
7
CURVE ( ADD, LINE,
COLOR = 8, VISIBLE, NOSHOWNLABEL, NOARROW)
/ The following curve's id is 12
POINT ( SELECT, ID )
25 26
CURVE ( ADD, LINE,
COLOR = 8, VISIBLE, NOSHOWNLABEL, NOARROW)
/ The following curve's id is 13
POINT ( SELECT, ID )
2 6
8
CURVE ( ADD, LINE,
COLOR = 8, VISIBLE, NOSHOWNLABEL, NOARROW)
/ The following curve's id is 14
POINT ( SELECT, ID )
26 27
CURVE (ADD, LINE,
COLOR = 8, VISIBLE, NOSHOWNLABEL, NOARROW)
/ The following curve's id is 15
27 28
CURVE ( ADD, LINE,
COLOR = 8, VISIBLE, NOSHOWNLABEL, NOARROW)
/ The following curve's id is 17
POINT ( SELECT, ID )
28
10
CURVE ( ADD, LINE,
COLOR = 8, VISIBLE, NOSHOWNLABEL, NOARROW)
/ The following curve's id is 18
POINT ( SELECT, ID )

```

```

1 41 40
CURVE ( ADD, LINE,
COLOR = 8, VISIBLE, NOSHOWNLABEL, NOARROW)
/ The following curve's id is 19
POINT ( SELECT, ID )
41
38
CURVE ( ADD, LINE,
COLOR = 8, VISIBLE, NOSHOWNLABEL, NOARROW)
/ The following curve's id is 20
POINT ( SELECT, ID )
2 38 36
CURVE ( ADD, LINE,
COLOR = 8, VISIBLE, NOSHOWNLABEL, NOARROW)
/ The following curve's id is 21
POINT ( SELECT, ID )
3 39 36
CURVE ( ADD, LINE,
COLOR = 8, VISIBLE, NOSHOWNLABEL, NOARROW)
/ The following curve's id is 22
POINT ( SELECT, ID )
39 40

CURVE ( ADD, LINE,
COLOR = 8, VISIBLE, NOSHOWNLABEL, NOARROW)
/ The following curve's id is 23
POINT ( SELECT, ID )
40
4
CURVE ( ADD, LINE,
COLOR = 8, VISIBLE, NOSHOWNLABEL, NOARROW)
/ The following curve's id is 24
POINT ( SELECT, ID )
48
21
CURVE ( ADD, LINE,
COLOR = 8, VISIBLE, NOSHOWNLABEL, NOARROW)
/ The following curve's id is 25
POINT ( SELECT, ID )
2 48 46
CURVE ( ADD, LINE,
COLOR = 8, VISIBLE, NOSHOWNLABEL, NOARROW)
/ The following curve's id is 26
POINT ( SELECT, ID )
48
3
CURVE ( ADD, LINE,
COLOR = 8, VISIBLE, NOSHOWNLABEL, NOARROW)
/ The following curve's id is 27
POINT ( SELECT, ID )
7 21 14
CURVE ( ADD, LINE,
COLOR = 8, VISIBLE, NOSHOWNLABEL, NOARROW)
/ The following curve's id is 28
POINT ( SELECT, ID )
21
8
CURVE ( ADD, LINE,

```

```

COLOR = 8, VISIBLE, NOSHOWNLABEL, NOARROW)
/ The following curve's id is 29
POINT ( SELECT, ID )
5 56 51
CURVE ( ADD, LINE,
COLOR = 8, VISIBLE, NOSHOWNLABEL, NOARROW)
/ The following curve's id is 30
POINT ( SELECT, ID )
56
4
CURVE ( ADD, LINE,
COLOR = 8, VISIBLE, NOSHOWNLABEL, NOARROW)
/ The following curve's id is 31
POINT ( SELECT, ID )
10 57 47
CURVE ( ADD, LINE,
COLOR = 8, VISIBLE, NOSHOWNLABEL, NOARROW)
/ The following curve's id is 32
POINT ( SELECT, ID )
57
1
CURVE ( ADD, LINE,
COLOR = 8, VISIBLE, NOSHOWNLABEL, NOARROW)
/
/ Creating SURFACES
/ The following surface's id is 1
POINT ( SELECT, ID )
6
5 24 19
23
SURFACE ( ADD, POINTS, UGRID = 2, VGRID = 2,

NOADDCURVES, UORDER=1, VORDER=1, ROWWIDTH=2,
CONTROL, UKNOTS=4, VKNOTS=4, WEIGHTED=0,
COLOR = 12, VISIBLE, NOSHOWNLABEL)
/ U[1..UKNOTS]
0 0 1 1
/ V[1..VKNOTS]
0 0 1 1
/ The following surface's id is 2
POINT ( SELECT, ID )
6 7
24 25
SURFACE ( ADD, POINTS, UGRID = 2, VGRID = 2,
NOADDCURVES, UORDER=1, VORDER=1, ROWWIDTH=2,
CONTROL, UKNOTS=4, VKNOTS=4, WEIGHTED=0,
COLOR = 12, VISIBLE, NOSHOWNLABEL)
/ U[1..UKNOTS]
0 0 1 1
/ V[1..VKNOTS]
0 0 1 1
/ The following surface's id is 3
POINT ( SELECT, ID )
8 9
26 27
SURFACE ( ADD, POINTS, UGRID = 2, VGRID = 2,
NOADDCURVES, UORDER=1, VORDER=1, ROWWIDTH=2,
CONTROL, UKNOTS=4, VKNOTS=4, WEIGHTED=0,

```

```

COLOR = 12, VISIBLE, NOSHOWNLABEL)
/ U[1..UKNOTS]
0 0 1 1
/ V[1..VKNOTS]
0 0 1 1
/ The following surface's id is 4
POINT ( SELECT, ID )
9 10
27 28
SURFACE ( ADD, POINTS, UGRID = 2, VGRID = 2,
NOADDCURVES, UORDER=1, VORDER=1, ROWWIDTH=2,
CONTROL, UKNOTS=4, VKNOTS=4, WEIGHTED=0,
COLOR = 12, VISIBLE, NOSHOWNLABEL)
/ U[1..UKNOTS]
0 0 1 1
/ V[1..VKNOTS]
0 0 1 1
/ The following surface's id is 5
POINT ( SELECT, ID )
1 41 40
2 38 36
SURFACE ( ADD, POINTS, UGRID = 2, VGRID = 2,
NOADDCURVES, UORDER=1, VORDER=1, ROWWIDTH=2,
CONTROL, UKNOTS=4, VKNOTS=4, WEIGHTED=0,
COLOR = 12, VISIBLE, NOSHOWNLABEL)
/ U[1..UKNOTS]
0 0 1 1
/ V[1..VKNOTS]
0 0 1 1
/ The following surface's id is 6
POINT ( SELECT, ID )
3 39 36
4 40 36
SURFACE ( ADD, POINTS, UGRID = 2, VGRID = 2,
NOADDCURVES, UORDER=1, VORDER=1, ROWWIDTH=2,
CONTROL, UKNOTS=4, VKNOTS=4, WEIGHTED=0,
COLOR = 12, VISIBLE, NOSHOWNLABEL)
/ U[1..UKNOTS]
0 0 1 1
/ V[1..VKNOTS]

0 0 1 1
/ The following surface's id is 7
POINT ( SELECT, ID )
25 55 30
26
7 21 14
8
SURFACE ( ADD, POINTS, UGRID = 2, VGRID = 2,
NOADDCURVES, UORDER=1, VORDER=1, ROWWIDTH=3,
CONTROL, UKNOTS=5, VKNOTS=4, WEIGHTED=0,
COLOR = 12, VISIBLE, NOSHOWNLABEL)
/ U[1..UKNOTS]
0 0 0.5 1
1
/ V[1..VKNOTS]
0 0 1 1
/ The following surface's id is 8

```

```

POINT ( SELECT, ID )
5 56 51
4 58 54
3 59 56
60 62
48
6 63 57
64
7 21 14
SURFACE ( ADD, POINTS, UGRID = 2, VGRID = 2,
NOADDCURVES, UORDER=1, VORDER=1, ROWWIDTH=5,
CONTROL, UKNOTS=7, VKNOTS=5, WEIGHTED=0,
COLOR = 12, VISIBLE, NOSHOWNLABEL)
/ U[1..UKNOTS]
0 0 0.022479340129093 0.044958680258186
0.0555555555555556 1 1
/ V[1..VKNOTS]
0 0 0.095238095238095 1
1
/ The following surface's id is 9
POINT ( SELECT, ID )
10 57 47
1 65 64
2 66 64
67 69
48
9 70 61
71
8 21 13
SURFACE ( ADD, POINTS, UGRID = 2, VGRID = 2,
NOADDCURVES, UORDER=1, VORDER=1, ROWWIDTH=5,
CONTROL, UKNOTS=7, VKNOTS=5, WEIGHTED=0,
COLOR = 12, VISIBLE, NOSHOWNLABEL)
/ U[1..UKNOTS]
0 0 0.022479340129093 0.044958680258186
0.0555555555555556 1 1
/ V[1..VKNOTS]
0 0 0.095238095238095 1
1
/
/ Creating EGROUPs
/ The following egroup's id is 21
EGROUP (DATACARD, GROUP = 21, ENTITY = "R.support",
NOSHOWNLABEL)
/ [element type] [number of nodes]
0 2
/ The following egroup's id is 23
EGROUP (DATACARD, GROUP = 23, ENTITY = "R.V.S#2",
NOSHOWNLABEL)

/ [element type] [number of nodes]
0 2
/ The following egroup's id is 24
EGROUP (DATACARD, GROUP = 24, ENTITY = "R.V.S#22",
NOSHOWNLABEL)
/ [element type] [number of nodes]
0 2
/ The following egroup's id is 28

```

```

EGROUP (DATACARD, GROUP = 28, ENTITY = "L.V.S#22",
NOSHOWLABEL)
/ [element type] [number of nodes]
0 2
/ The following egroup's id is 29
EGROUP (DATACARD, GROUP = 29, ENTITY = "L.V.S#2",
NOSHOWLABEL)
/ [element type] [number of nodes]
0 2
/ The following egroup's id is 33
EGROUP (DATACARD, GROUP = 33, ENTITY = "L.support",
NOSHOWLABEL)
/ [element type] [number of nodes]
0 2
/ The following egroup's id is 37
EGROUP (DATACARD, GROUP = 37, ENTITY = "R.up.attach",
NOSHOWLABEL)
/ [element type] [number of nodes]
0 2
/ The following egroup's id is 38
EGROUP (DATACARD, GROUP = 38, ENTITY = "R.lw.attach",
NOSHOWLABEL)
/ [element type] [number of nodes]
0 2
/ The following egroup's id is 40
EGROUP (DATACARD, GROUP = 40, ENTITY = "L.lw.attach",
NOSHOWLABEL)
/ [element type] [number of nodes]
0 2
/ The following egroup's id is 41
EGROUP (DATACARD, GROUP = 41, ENTITY = "L.up.attach",
NOSHOWLABEL)
/ [element type] [number of nodes]
0 2
/ The following egroup's id is 61
EGROUP (DATACARD, GROUP = 61, ENTITY = "solid",
NOSHOWLABEL)
/ [element type] [number of nodes]
1 4
/ The following egroup's id is 63
EGROUP (DATACARD, GROUP = 63, ENTITY = "solid",
NOSHOWLABEL)
/ [element type] [number of nodes]
1 4
/ The following egroup's id is 64
EGROUP (DATACARD, GROUP = 64, ENTITY = "thksolid",
NOSHOWLABEL)
/ [element type] [number of nodes]
1 4
/ The following egroup's id is 65
EGROUP (DATACARD, GROUP = 65, ENTITY = "thksolid",
NOSHOWLABEL)
/ [element type] [number of nodes]
1 4
/ The following egroup's id is 66
EGROUP (DATACARD, GROUP = 66, ENTITY = "R.B.wall",
NOSHOWLABEL)
/ [element type] [number of nodes]

```

```

0 2
/ The following egroup's id is 67
EGROUP (DATACARD, GROUP = 67, ENTITY = "R.B.lw.wall",
NOSHOWLABEL)
/ [element type] [number of nodes]
0 2
/ The following egroup's id is 71
EGROUP (DATACARD, GROUP = 71, ENTITY = "R.wall",
NOSHOWLABEL)
/ [element type] [number of nodes]
0 2
/ The following egroup's id is 72
EGROUP (DATACARD, GROUP = 72, ENTITY = "R.thk.wall",
NOSHOWLABEL)
/ [element type] [number of nodes]
0 2
/ The following egroup's id is 73
EGROUP (DATACARD, GROUP = 73, ENTITY = "L.B.wall",
NOSHOWLABEL)
/ [element type] [number of nodes]
0 2
/ The following egroup's id is 74
EGROUP (DATACARD, GROUP = 74, ENTITY = "L.B.lw.wall",
NOSHOWLABEL)
/ [element type] [number of nodes]
0 2
/ The following egroup's id is 75
EGROUP (DATACARD, GROUP = 75, ENTITY = "L.wall",
NOSHOWLABEL)
/ [element type] [number of nodes]
0 2
/ The following egroup's id is 76
EGROUP (DATACARD, GROUP = 76, ENTITY = "L.thk.wall",
NOSHOWLABEL)
/ [element type] [number of nodes]
0 2
/ The following egroup's id is 78
EGROUP (DATACARD, GROUP = 78, ENTITY = "L.outlet",
NOSHOWLABEL)
/ [element type] [number of nodes]
0 2
/ The following egroup's id is 79
EGROUP (DATACARD, GROUP = 79, ENTITY = "R.outlet",
NOSHOWLABEL)
/ [element type] [number of nodes]
0 2
/ The following egroup's id is 80
EGROUP (DATACARD, GROUP = 80, ENTITY = "split.line",
NOSHOWLABEL)
/ [element type] [number of nodes]
0 2
/ The following egroup's id is 81
EGROUP (DATACARD, GROUP = 81, ENTITY = "fluid",
NOSHOWLABEL)
/ [element type] [number of nodes]
1 4
/ The following egroup's id is 82
EGROUP (DATACARD, GROUP = 82, ENTITY = "solid",

```

```

NOSHOWLABEL)
/ [element type] [number of nodes]
1 4
/ The following egroup's id is 83
EGROUP (DATACARD, GROUP = 83, ENTITY = "fluid",
NOSHOWLABEL)
/ [element type] [number of nodes]
1 4
/ The following egroup's id is 86
EGROUP (DATACARD, GROUP = 86, ENTITY = "L.inlet#2",
NOSHOWLABEL)
/ [element type] [number of nodes]
0 2
/ The following egroup's id is 87
EGROUP (DATACARD, GROUP = 87, ENTITY = "L.B.inlet#2",
NOSHOWLABEL)
/ [element type] [number of nodes]
0 2
/ The following egroup's id is 88
EGROUP (DATACARD, GROUP = 88, ENTITY = "Ctr.B.L.wall",
NOSHOWLABEL)
/ [element type] [number of nodes]
0 2
/ The following egroup's id is 89
EGROUP (DATACARD, GROUP = 89, ENTITY = "Ctr.B.R.wall",
NOSHOWLABEL)
/ [element type] [number of nodes]
0 2
/ The following egroup's id is 90
EGROUP (DATACARD, GROUP = 90, ENTITY = "Ctr.B.lw.wall",
NOSHOWLABEL)
/ [element type] [number of nodes]
0 2
/ The following egroup's id is 91
EGROUP (DATACARD, GROUP = 91, ENTITY = "R.inlet#2",
NOSHOWLABEL)
/ [element type] [number of nodes]
0 2
/ The following egroup's id is 92
EGROUP (DATACARD, GROUP = 92, ENTITY = "R.B.inlet#2",
NOSHOWLABEL)
/ [element type] [number of nodes]
0 2
/ The following egroup's id is 96
EGROUP (DATACARD, GROUP = 96, ENTITY = "fluid",
NOSHOWLABEL)
/ [element type] [number of nodes]
1 4
/ The following egroup's id is 97
EGROUP (DATACARD, GROUP = 97, ENTITY = "fluid",
NOSHOWLABEL)
/ [element type] [number of nodes]
1 4
/ The following egroup's id is 98
EGROUP (DATACARD, GROUP = 98, ENTITY = "R.F.corner",
NOSHOWLABEL)
/ [element type] [number of nodes]
0 2

```



```

/ The following egroup's id is 99
EGROUP (DATACARD, GROUP = 99, ENTITY = "R.corner",
NOSHOWLABEL)
/ [element type] [number of nodes]
0 2
/ The following egroup's id is 100
EGROUP (DATACARD, GROUP = 100, ENTITY = "L.corner",
NOSHOWLABEL)
/ [element type] [number of nodes]
0 2
/ The following egroup's id is 101
EGROUP (DATACARD, GROUP = 101, ENTITY = "L.F.corner",
NOSHOWLABEL)
/ [element type] [number of nodes]
0 2

/ Creating MLOOPS
/ The following mloop's id is 1
CURVE ( SELECT, ID )
9
5 7 2
8
MLOOP (ADD, MAP, EDG1=1, EDG2=1, EDG3=1, EDG4=1,
COLOR = 6, VISIBLE, NOSHOWLABEL)
/ The following mloop's id is 2
CURVE ( SELECT, ID )
17
6 15 9
16
MLOOP ( ADD, PAVE,
COLOR = 6, VISIBLE, NOSHOWLABEL)
/ The following mloop's id is 3
CURVE ( SELECT, ID )
1 18 17
19 20
MLOOP ( ADD, PAVE,
COLOR = 6, VISIBLE, NOSHOWLABEL)
/ The following mloop's id is 4
CURVE ( SELECT, ID )
2 21 19
22 23
MLOOP (ADD, MAP, EDG1=1, EDG2=1, EDG3=1, EDG4=1,
COLOR = 6, VISIBLE, NOSHOWLABEL)
/ The following mloop's id is 5
CURVE ( SELECT, ID )
15
4 13 9
14
MLOOP (ADD, MAP, EDG1=1, EDG2=1, EDG3=1, EDG4=1,
COLOR = 6, VISIBLE, NOSHOWLABEL)
/ The following mloop's id is 6
CURVE ( SELECT, ID )
13 28 15
27
11 12
MLOOP (ADD, MAP, EDG1=1, EDG2=2, EDG3=1, EDG4=1,
COLOR = 6, VISIBLE, NOSHOWLABEL)
/ The following mloop's id is 7

```

```

CURVE ( SELECT, ID )
11
3 9 6
10
MLOOP (ADD, MAP, EDG1=1, EDG2=1, EDG3=1, EDG4=1,
COLOR = 6, VISIBLE, NOSHOWNLABEL)
/ The following mloop's id is 8
CURVE ( SELECT, ID )
29 30
2 26 24
24 27 3
3 5 2
MLOOP ( ADD, PAVE,
COLOR = 6, VISIBLE, NOSHOWNLABEL)
/ The following mloop's id is 9
CURVE ( SELECT, ID )
31 32
1 25 24
24 28 4
4 6 2
MLOOP ( ADD, PAVE,
COLOR = 6, VISIBLE, NOSHOWNLABEL)
/ Creating MFACEs
/ The following mface's id is 1
SURFACE ( SELECT, ID = 1 )
MFACE (ADD, MAP, NOSPAVE, BASESPAVE = 0,
COLOR = 8, VISIBLE, NOSHOWNLABEL)
/ The following mface's id is 2
SURFACE ( SELECT, ID = 4 )
MLOOP ( SELECT, ID = 2 )
MFACE (ADD, MAP, NOSPAVE, BASESPAVE = 0,
COLOR = 8, VISIBLE, NOSHOWNLABEL)
/ The following mface's id is 3
SURFACE ( SELECT, ID = 5 )
MLOOP ( SELECT, ID = 3 )
MFACE (ADD, MAP, NOSPAVE, BASESPAVE = 0,
COLOR = 8, VISIBLE, NOSHOWNLABEL)
/ The following mface's id is 4
SURFACE ( SELECT, ID = 6 )
MLOOP ( SELECT, ID = 4 )
MFACE (ADD, MAP, NOSPAVE, BASESPAVE = 0,
COLOR = 8, VISIBLE, NOSHOWNLABEL)
/ The following mface's id is 5
SURFACE ( SELECT, ID = 3 )
MLOOP ( SELECT, ID = 5 )
MFACE (ADD, MAP, NOSPAVE, BASESPAVE = 0,
COLOR = 8, VISIBLE, NOSHOWNLABEL)
/ The following mface's id is 6
SURFACE ( SELECT, ID = 7 )
MLOOP ( SELECT, ID = 6 )
MFACE (ADD, MAP, NOSPAVE, BASESPAVE = 0,
COLOR = 8, VISIBLE, NOSHOWNLABEL)
/ The following mface's id is 7
SURFACE ( SELECT, ID = 2 )
MLOOP ( SELECT, ID = 7 )
MFACE (ADD, MAP, NOSPAVE, BASESPAVE = 0,
COLOR = 8, VISIBLE, NOSHOWNLABEL)
/ The following mface's id is 8

```

```

SURFACE ( SELECT, ID = 9 )
MLOOP ( SELECT, ID = 9 )
MFACE (ADD, PAVE, NOSPAVE, BASESPAVE = 0,
COLOR = 8, VISIBLE, NOSHOWNLABEL)
/ The following mface's id is 9
SURFACE ( SELECT, ID = 8 )
MLOOP ( SELECT, ID = 8 )
MFACE (ADD, PAVE, NOSPAVE, BASESPAVE = 0,
COLOR = 8, VISIBLE, NOSHOWNLABEL)
/ Creating MEDGES
/ The following medge's id is 1
CURVE ( SELECT, ID = 7 )
MEDGE ( ADD, SUCCESSIVE, INTERVALS = 4, RATIO = 0,
2RATIO = 0, PCENTR = 0,
COLOR = 7, VISIBLE, NOSHOWNLABEL)
/ The following medge's id is 2
CURVE ( SELECT, ID = 9 )
MEDGE ( ADD, SUCCESSIVE, INTERVALS = 4, RATIO = 0,
2RATIO = 0, PCENTR = 0,
COLOR = 7, VISIBLE, NOSHOWNLABEL)
/ The following medge's id is 3
CURVE ( SELECT, ID = 11 )
MEDGE ( ADD, SUCCESSIVE, INTERVALS = 4, RATIO = 0,
2RATIO = 0, PCENTR = 0,
COLOR = 7, VISIBLE, NOSHOWNLABEL)
/ The following medge's id is 4
CURVE ( SELECT, ID = 13 )
MEDGE ( ADD, SUCCESSIVE, INTERVALS = 4, RATIO = 0,
2RATIO = 0, PCENTR = 0,
COLOR = 7, VISIBLE, NOSHOWNLABEL)
/ The following medge's id is 5
CURVE ( SELECT, ID = 15 )
MEDGE ( ADD, SUCCESSIVE, INTERVALS = 4, RATIO = 0,
2RATIO = 0, PCENTR = 0,
COLOR = 7, VISIBLE, NOSHOWNLABEL)
/ The following medge's id is 6
CURVE ( SELECT, ID = 17 )
MEDGE ( ADD, SUCCESSIVE, INTERVALS = 4, RATIO = 0,
2RATIO = 0, PCENTR = 0,
COLOR = 7, VISIBLE, NOSHOWNLABEL)
/ The following medge's id is 7
CURVE ( SELECT, ID = 18 )
MEDGE ( ADD, SUCCESSIVE, INTERVALS = 3, RATIO = 0,
2RATIO = 0, PCENTR = 0,
COLOR = 7, VISIBLE, NOSHOWNLABEL)
/ The following medge's id is 8
CURVE ( SELECT, ID = 20 )
MEDGE ( ADD, SUCCESSIVE, INTERVALS = 3, RATIO = 0,
2RATIO = 0, PCENTR = 0,
COLOR = 7, VISIBLE, NOSHOWNLABEL)
/ The following medge's id is 9
CURVE ( SELECT, ID = 21 )
MEDGE ( ADD, SUCCESSIVE, INTERVALS = 3, RATIO = 0,
2RATIO = 0, PCENTR = 0,
COLOR = 7, VISIBLE, NOSHOWNLABEL)
/ The following medge's id is 10
CURVE ( SELECT, ID = 23 )
MEDGE ( ADD, SUCCESSIVE, INTERVALS = 3, RATIO = 0,
2RATIO = 0, PCENTR = 0,

```

```

COLOR = 7, VISIBLE, NOSHOWNLABEL)
/ The following medge's id is 11
CURVE ( SELECT, ID = 1 )
MEDGE ( ADD, SUCCESSIVE, INTERVALS = 200, RATIO = 0,
2RATIO = 0, PCENTR = 0,
COLOR = 7, VISIBLE, NOSHOWNLABEL)
/ The following medge's id is 12
CURVE ( SELECT, ID = 19 )
MEDGE ( ADD, SUCCESSIVE, INTERVALS = 200, RATIO = 0,
2RATIO = 0, PCENTR = 0,
COLOR = 7, VISIBLE, NOSHOWNLABEL)
/ The following medge's id is 13
CURVE ( SELECT, ID = 2 )
MEDGE ( ADD, SUCCESSIVE, INTERVALS = 200, RATIO = 0,
2RATIO = 0, PCENTR = 0,
COLOR = 7, VISIBLE, NOSHOWNLABEL)
/ The following medge's id is 14
CURVE ( SELECT, ID = 22 )
MEDGE ( ADD, SUCCESSIVE, INTERVALS = 200, RATIO = 0,
2RATIO = 0, PCENTR = 0,
COLOR = 7, VISIBLE, NOSHOWNLABEL)
/ The following medge's id is 15
CURVE ( SELECT, ID = 5 )
MEDGE ( ADD, SUCCESSIVE, INTERVALS = 120, RATIO = 0,
2RATIO = 0, PCENTR = 0,
COLOR = 7, VISIBLE, NOSHOWNLABEL)
/ The following medge's id is 16
CURVE ( SELECT, ID = 8 )
MEDGE ( ADD, SUCCESSIVE, INTERVALS = 120, RATIO = 0,
2RATIO = 0, PCENTR = 0,
COLOR = 7, VISIBLE, NOSHOWNLABEL)
/ The following medge's id is 17
CURVE ( SELECT, ID = 6 )
MEDGE ( ADD, SUCCESSIVE, INTERVALS = 120, RATIO = 0,
2RATIO = 0, PCENTR = 0,
COLOR = 7, VISIBLE, NOSHOWNLABEL)
/ The following medge's id is 18
CURVE ( SELECT, ID = 16 )
MEDGE ( ADD, SUCCESSIVE, INTERVALS = 120, RATIO = 0,
2RATIO = 0, PCENTR = 0,
COLOR = 7, VISIBLE, NOSHOWNLABEL)
/ The following medge's id is 19
CURVE ( SELECT, ID = 26 )
MEDGE ( ADD, SUCCESSIVE, INTERVALS = 14, RATIO = 0,
2RATIO = 0, PCENTR = 0,
COLOR = 7, VISIBLE, NOSHOWNLABEL)
/ The following medge's id is 21
CURVE ( SELECT, ID = 25 )
MEDGE ( ADD, SUCCESSIVE, INTERVALS = 14, RATIO = 0,
2RATIO = 0, PCENTR = 0,
COLOR = 7, VISIBLE, NOSHOWNLABEL)
/ The following medge's id is 22
CURVE ( SELECT, ID = 4 )
MEDGE ( ADD, SUCCESSIVE, INTERVALS = 10, RATIO = 0,
2RATIO = 0, PCENTR = 0,
COLOR = 7, VISIBLE, NOSHOWNLABEL)
/ The following medge's id is 23
CURVE ( SELECT, ID = 14 )

```

```

MEDGE ( ADD, SUCCESSIVE, INTERVALS = 10, RATIO = 0,
2RATIO = 0, PCENTR = 0,
COLOR = 7, VISIBLE, NOSHOWNLABEL)
/ The following medge's id is 24
CURVE ( SELECT, ID = 28 )
MEDGE ( ADD, SUCCESSIVE, INTERVALS = 120, RATIO = 0,
2RATIO = 0, PCENTR = 0,
COLOR = 7, VISIBLE, NOSHOWNLABEL)
/ The following medge's id is 25
CURVE ( SELECT, ID = 27 )
MEDGE ( ADD, SUCCESSIVE, INTERVALS = 120, RATIO = 0,
2RATIO = 0, PCENTR = 0,
COLOR = 7, VISIBLE, NOSHOWNLABEL)
/ The following medge's id is 26
CURVE ( SELECT, ID = 12 )
MEDGE ( ADD, SUCCESSIVE, INTERVALS = 240, RATIO = 0,
2RATIO = 0, PCENTR = 0,
COLOR = 7, VISIBLE, NOSHOWNLABEL)
/ The following medge's id is 27
CURVE ( SELECT, ID = 3 )
MEDGE ( ADD, SUCCESSIVE, INTERVALS = 10, RATIO = 0,
2RATIO = 0, PCENTR = 0,
COLOR = 7, VISIBLE, NOSHOWNLABEL)
/ The following medge's id is 28
CURVE ( SELECT, ID = 10 )
MEDGE ( ADD, SUCCESSIVE, INTERVALS = 10, RATIO = 0,
2RATIO = 0, PCENTR = 0,
COLOR = 7, VISIBLE, NOSHOWNLABEL)
/ The following medge's id is 29
CURVE ( SELECT, ID = 31 )
/ The following medge's id is 30
CURVE ( SELECT, ID = 32 )
MEDGE ( ADD, SUCCESSIVE, INTERVALS = 10, RATIO = 0,
2RATIO = 0, PCENTR = 0,
COLOR = 7, VISIBLE, NOSHOWNLABEL)
/ The following medge's id is 31
CURVE ( SELECT, ID = 30 )
MEDGE ( ADD, SUCCESSIVE, INTERVALS = 10, RATIO = 0,
2RATIO = 0, PCENTR = 0,
COLOR = 7, VISIBLE, NOSHOWNLABEL)
/ The following medge's id is 32
CURVE ( SELECT, ID = 29 )
MEDGE ( ADD, SUCCESSIVE, INTERVALS = 12, RATIO = 0,
2RATIO = 0, PCENTR = 0,
COLOR = 7, VISIBLE, NOSHOWNLABEL)
/
/ Meshing MEDGES
ELEMENT (SETDEFAULTS, EDGE, NODES=2)
MEDGE ( SELECT, ID = 1 )
MEDGE (MESH, MAP, GROUP = 21)
ELEMENT (SETDEFAULTS, EDGE, NODES=2)
MEDGE ( SELECT, ID = 2 )
MEDGE (MESH, MAP, GROUP = 23)
ELEMENT (SETDEFAULTS, EDGE, NODES=2)
MEDGE ( SELECT, ID = 3 )
MEDGE (MESH, MAP, GROUP = 24)
ELEMENT (SETDEFAULTS, EDGE, NODES=2)
MEDGE ( SELECT, ID = 4 )

```

```

MEDGE (MESH, MAP, GROUP = 28)
ELEMENT (SETDEFAULTS, EDGE, NODES=2)
MEDGE ( SELECT, ID = 5 )
MEDGE (MESH, MAP, GROUP = 29)
ELEMENT (SETDEFAULTS, EDGE, NODES=2)
MEDGE ( SELECT, ID = 6 )
MEDGE (MESH, MAP, GROUP = 33)
ELEMENT (SETDEFAULTS, EDGE, NODES=2)
MEDGE ( SELECT, ID = 7 )
MEDGE (MESH, MAP, GROUP = 40)
ELEMENT (SETDEFAULTS, EDGE, NODES=2)
MEDGE ( SELECT, ID = 8 )
MEDGE (MESH, MAP, GROUP = 41)
ELEMENT (SETDEFAULTS, EDGE, NODES=2)
MEDGE ( SELECT, ID = 9 )
MEDGE (MESH, MAP, GROUP = 37)
ELEMENT (SETDEFAULTS, EDGE, NODES=2)
MEDGE ( SELECT, ID = 10 )
MEDGE (MESH, MAP, GROUP = 38)
ELEMENT (SETDEFAULTS, EDGE, NODES=2)
MEDGE ( SELECT, ID = 11 )
MEDGE (MESH, MAP, GROUP = 75)
ELEMENT (SETDEFAULTS, EDGE, NODES=2)
MEDGE ( SELECT, ID = 12 )
MEDGE (MESH, MAP, GROUP = 76)
ELEMENT (SETDEFAULTS, EDGE, NODES=2)
MEDGE ( SELECT, ID = 13 )
MEDGE (MESH, MAP, GROUP = 71)
ELEMENT (SETDEFAULTS, EDGE, NODES=2)
MEDGE ( SELECT, ID = 14 )
MEDGE (MESH, MAP, GROUP = 72)
ELEMENT (SETDEFAULTS, EDGE, NODES=2)
MEDGE ( SELECT, ID = 15 )
MEDGE (MESH, MAP, GROUP = 66)
ELEMENT (SETDEFAULTS, EDGE, NODES=2)
MEDGE ( SELECT, ID = 16 )
MEDGE (MESH, MAP, GROUP = 67)
ELEMENT (SETDEFAULTS, EDGE, NODES=2)
MEDGE ( SELECT, ID = 17 )
MEDGE (MESH, MAP, GROUP = 73)
ELEMENT (SETDEFAULTS, EDGE, NODES=2)
MEDGE ( SELECT, ID = 18 )
MEDGE (MESH, MAP, GROUP = 74)
ELEMENT (SETDEFAULTS, EDGE, NODES=2)
MEDGE ( SELECT, ID = 19 )
MEDGE (MESH, MAP, GROUP = 79)
ELEMENT (SETDEFAULTS, EDGE, NODES=2)
MEDGE ( SELECT, ID = 20 )
MEDGE (MESH, MAP, GROUP = 80)
ELEMENT (SETDEFAULTS, EDGE, NODES=2)
MEDGE ( SELECT, ID = 21 )
MEDGE (MESH, MAP, GROUP = 78)
ELEMENT (SETDEFAULTS, EDGE, NODES=2)
MEDGE ( SELECT, ID = 22 )
MEDGE (MESH, MAP, GROUP = 86)
ELEMENT (SETDEFAULTS, EDGE, NODES=2)
MEDGE ( SELECT, ID = 23 )
MEDGE (MESH, MAP, GROUP = 87)
ELEMENT (SETDEFAULTS, EDGE, NODES=2)

```

```

MEDGE ( SELECT, ID = 24 )
MEDGE ( MESH, MAP, GROUP = 88 )
ELEMENT ( SETDEFAULTS, EDGE, NODES=2 )
MEDGE ( SELECT, ID = 25 )
MEDGE ( MESH, MAP, GROUP = 89 )
ELEMENT ( SETDEFAULTS, EDGE, NODES=2 )
MEDGE ( SELECT, ID = 26 )
MEDGE ( MESH, MAP, GROUP = 90 )
ELEMENT ( SETDEFAULTS, EDGE, NODES=2 )
MEDGE ( SELECT, ID = 27 )
MEDGE ( MESH, MAP, GROUP = 91 )
ELEMENT ( SETDEFAULTS, EDGE, NODES=2 )
MEDGE ( SELECT, ID = 28 )
MEDGE ( MESH, MAP, GROUP = 92 )
ELEMENT ( SETDEFAULTS, EDGE, NODES=2 )
MEDGE ( SELECT, ID = 29 )
MEDGE ( MESH, MAP, GROUP = 100 )
ELEMENT ( SETDEFAULTS, EDGE, NODES=2 )
MEDGE ( SELECT, ID = 30 )
MEDGE ( MESH, MAP, GROUP = 101 )
ELEMENT ( SETDEFAULTS, EDGE, NODES=2 )
MEDGE ( SELECT, ID = 31 )
MEDGE ( MESH, MAP, GROUP = 98 )
ELEMENT ( SETDEFAULTS, EDGE, NODES=2 )
MEDGE ( SELECT, ID = 32 )
MEDGE ( MESH, MAP, GROUP = 99 )
/
/ Meshing MFACEs
ELEMENT ( SETDEFAULTS, QUADRILATERAL, NODES=4 )
MFACE ( SELECT, ID = 1 )
MFACE ( MESH, MAP, GROUP = 61 )
ELEMENT ( SETDEFAULTS, QUADRILATERAL, NODES=4 )
MFACE ( SELECT, ID = 2 )
MFACE ( MESH, MAP, GROUP = 63 )
ELEMENT ( SETDEFAULTS, QUADRILATERAL, NODES=4 )
MFACE ( SELECT, ID = 3 )
MFACE ( MESH, MAP, GROUP = 64 )
ELEMENT ( SETDEFAULTS, QUADRILATERAL, NODES=4 )
MFACE ( SELECT, ID = 4 )
MFACE ( MESH, MAP, GROUP = 65 )
ELEMENT ( SETDEFAULTS, QUADRILATERAL, NODES=4 )
MFACE ( SELECT, ID = 5 )
MFACE ( MESH, MAP, GROUP = 81 )
ELEMENT ( SETDEFAULTS, QUADRILATERAL, NODES=4 )
MFACE ( SELECT, ID = 6 )
MFACE ( MESH, MAP, GROUP = 82 )
ELEMENT ( SETDEFAULTS, QUADRILATERAL, NODES=4 )
MFACE ( SELECT, ID = 7 )
MFACE ( MESH, MAP, GROUP = 83 )
ELEMENT ( SETDEFAULTS, QUADRILATERAL, NODES=4 )
MFACE ( SELECT, ID = 8 )
MFACE ( MESH, PAVE, GROUP = 96 )
ELEMENT ( SETDEFAULTS, QUADRILATERAL, NODES=4 )
MFACE ( SELECT, ID = 9 )
MFACE ( MESH, PAVE, GROUP = 97 )
/
END
/

```

```

/ FIPREP INPUT FILE CREATED ON 21 Dec 97 AT 23:40:21
/
TITLE

FIPREP
PROB (2-D, STEA, TURB, NONL, MOME, BUOY)
PRES (PENA = 0.1000000000000E-07, DISC)
EXEC (NEWJ)
SOLU (SEGR = 4000, CGS = 3000, CR = 4000,
NCGC = 0.1000000000000E-07,
SCGC = 0.1000000000000E-07, PREC = 21, ACCF = 0.8, PPRO)
DATA (CONT)
GRAV (MAGN = 9.81)
RADI (NOPA, GREY)
PRIN (ALL, BOUN)
RENU (PROF)
ENTI (NAME = "fluid", FLUI, MDEN = 1, MVIS = 1,
MSPH = 1, MCON = 1, MEXP = 1)
ENTI (NAME = "solid", SOLI, MDEN = 2, MCON = 2)
ENTI (NAME = "L.wall", RADI, MEMS = 2, GREY,
ATTA = "fluid")
ENTI (NAME = "R.wall", RADI, MEMS = 2, GREY,
ATTA = "fluid")
ENTI (NAME = "R.corner", PLOT, ATTA = "fluid")
ENTI (NAME = "L.corner", PLOT, ATTA = "fluid")
ENTI (NAME = "R.B.inlet#2", VENT, INLE, OFFC)
ENTI (NAME = "L.B.inlet#2", VENT, INLE, OFFC)
ENTI (NAME = "R.inlet#2", GAP = 1.0, ATTA = "fluid")
ENTI (NAME = "L.inlet#2", GAP = 1.0, ATTA = "fluid")
ENTI (NAME = "R.B.wall", RADI, MEMS = 1, GREY,
ATTA = "fluid")
ENTI (NAME = "L.B.wall", RADI, MEMS = 1, GREY,
ATTA = "fluid")
ENTI (NAME = "R.support", PLOT, COND, ATTA = "solid")
ENTI (NAME = "L.support", PLOT, COND, ATTA = "solid")
ENTI (NAME = "R.B.lw.wall", PLOT, COND, ATTA = "solid")
ENTI (NAME = "L.B.lw.wall", PLOT, COND, ATTA = "solid")
ENTI (NAME = "R.V.S#2", PLOT, ATTA = "solid")
ENTI (NAME = "R.V.S#22", PLOT, ATTA = "solid")
ENTI (NAME = "L.V.S#22", PLOT, ATTA = "solid")
ENTI (NAME = "L.V.S#2", PLOT, ATTA = "solid")
ENTI (NAME = "Ctr.B.lw.wall", PLOT, COND,
ATTA = "solid")
ENTI (NAME = "R.thk.wall", PLOT, COND,
ATTA = "thksolid")
ENTI (NAME = "L.thk.wall", PLOT, COND,
ATTA = "thksolid")
ENTI (NAME = "R.up.attach", PLOT)
ENTI (NAME = "R.lw.attach", PLOT)
ENTI (NAME = "L.lw.attach", PLOT)
ENTI (NAME = "L.up.attach", PLOT)
ENTI (NAME = "thksolid", SOLI, MDEN = 3,
MSPH = 3, MCON = 3)
ENTI (NAME = "L.outlet", VENT, OUTL, OFFC)
ENTI (NAME = "R.outlet", VENT, OUTL, OFFC)
ENTI (NAME = "Ctr.B.R.wall", RADI, MEMS = 1, GREY,
ATTA = "fluid")
ENTI (NAME = "Ctr.B.L.wall", RADI, MEMS = 1, GREY,

```



```

ATTA = "fluid")
ENTI (NAME = "split.line", GAP = 1.0, ATTA = "fluid")
ENTI (NAME = "R.F.corner", VENT, INLE, OFFC)
ENTI (NAME = "L.F.corner", VENT, INLE, OFFC)
DENS (SET = 1, CONS = 1.174, TYP1, TEMP = 315.0)
DENS (SET = 2, CONS = 220.0)
DENS (SET = 3, CONS = 700.0)
VISC (SET = 1, CONS = 0.1983000000000E-04, TWO-)
SPEC (SET = 1, CONS = 1000.0)
SPEC (SET = 3, CONS = 2390.0)
COND (SET = 1, CONS = 0.2620000000000E-01)
COND (SET = 2, CONS = 0.3500000000000E-01)
COND (SET = 3, CONS = 0.19)
VOLU (SET = 1, CONS = 0.3332000000000E-02, REFT = 315.0)
EMIS (SET = 1, CONS = 0.9, STEF = 0.5667000000000E-07)
EMIS (SET = 2, CONS = 0.9, STEF = 0.5670000000000E-07)
BCNO (VELO, ENTI = "L.wall", ZERO)
BCNO (VELO, ENTI = "R.wall", ZERO)
BCNO (VELO, ENTI = "R.B.wall", ZERO)
BCNO (VELO, ENTI = "L.B.wall", ZERO)
BCNO (VELO, ENTI = "Ctr.B.L.wall", ZERO)
BCNO (TEMP, ENTI = "R.B.lw.wall", CONS = 304.0)
BCNO (TEMP, ENTI = "L.B.lw.wall", CONS = 304.0)
BCNO (TEMP, ENTI = "Ctr.B.lw.wall", CONS = 304.0)
BCNO (TEMP, ENTI = "R.F.corner", CONS = 309.6)
BCNO (TEMP, ENTI = "L.F.corner", CONS = 309.6)
BCNO (TEMP, ENTI = "L.B.inlet#2", CONS = 300.0)
BCNO (UY, ENTI = "R.B.inlet#2", CONS = 0.33)
BCNO (UY, ENTI = "L.B.inlet#2", CONS = 0.33)
BCNO (KINE, ENTI = "L.B.inlet#2", CONS =
0.1000000000000E-02)
BCNO (KINE, ENTI = "R.B.inlet#2", CONS =
0.1000000000000E-02)
BCNO (KINE, ENTI = "L.F.corner", CONS =
0.1000000000000E-02)
BCNO (KINE, ENTI = "R.F.corner", CONS =
0.1000000000000E-02)
BCNO (DISS, ENTI = "R.F.corner", CONS =
0.4500000000000E-03)
BCNO (DISS, ENTI = "L.F.corner", CONS =
0.4500000000000E-03)
BCNO (DISS, ENTI = "R.B.inlet#2", CONS =
0.4500000000000E-03)
BCNO (DISS, ENTI = "L.B.inlet#2", CONS =
0.4500000000000E-03)
BCNO (VELO, ENTI = "Ctr.B.R.wall", ZERO)
BCNO (VELO, ENTI = "R.corner", ZERO)
BCNO (VELO, ENTI = "L.corner", ZERO)
BCNO (TEMP, ENTI = "R.B.inlet#2", CONS = 300.0)
BCNO (UY, NODE = 1981, CONS = 0.3)
BCNO (UY, NODE = 1982, CONS = 0.3)
BCNO (UY, NODE = 1983, CONS = 0.3)
BCNO (UY, NODE = 1984, CONS = 0.3)
BCNO (UY, NODE = 1985, CONS = 0.3)
BCNO (UY, NODE = 1986, CONS = 0.3)
BCNO (UY, NODE = 1987, CONS = 0.3)
BCNO (UY, NODE = 1988, CONS = 0.3)
BCNO (UY, NODE = 1971, CONS = 0.3)

```

```

BCNO (UY, NODE = 1972, CONS = 0.3)
BCNO (UY, NODE = 1973, CONS = 0.3)
BCNO (UY, NODE = 1974, CONS = 0.3)
BCNO (UY, NODE = 1975, CONS = 0.3)
BCNO (UY, NODE = 1976, CONS = 0.3)
BCNO (UY, NODE = 1977, CONS = 0.3)
BCNO (UY, NODE = 1978, CONS = 0.3)
BCNO (UY, NODE = 1979, CONS = 0.3)
BCNO (UY, NODE = 1989, CONS = 0.3)
BCNO (PRES, NODE = 1319, CONS = 100000.0)
BCNO (PRES, NODE = 1320, CONS = 100000.0)
BCNO (PRES, NODE = 1321, CONS = 100000.0)
BCNO (PRES, NODE = 1322, CONS = 100000.0)
BCNO (PRES, NODE = 1323, CONS = 100000.0)
BCNO (PRES, NODE = 1324, CONS = 100000.0)
BCNO (PRES, NODE = 1325, CONS = 100000.0)
BCNO (PRES, NODE = 1326, CONS = 100000.0)
BCNO (PRES, NODE = 1327, CONS = 100000.0)
BCNO (PRES, NODE = 1328, CONS = 100000.0)
BCNO (PRES, NODE = 1329, CONS = 100000.0)
BCNO (PRES, NODE = 1330, CONS = 100000.0)
BCNO (PRES, NODE = 1331, CONS = 100000.0)
BCNO (PRES, NODE = 1332, CONS = 100000.0)
BCNO (PRES, NODE = 1433, CONS = 100000.0)
BCNO (PRES, NODE = 1434, CONS = 100000.0)
BCNO (PRES, NODE = 1435, CONS = 100000.0)
BCNO (PRES, NODE = 1436, CONS = 100000.0)
BCNO (PRES, NODE = 1437, CONS = 100000.0)
BCNO (PRES, NODE = 1438, CONS = 100000.0)
BCNO (PRES, NODE = 1439, CONS = 100000.0)
BCNO (PRES, NODE = 1440, CONS = 100000.0)
BCNO (PRES, NODE = 1441, CONS = 100000.0)
BCNO (PRES, NODE = 1442, CONS = 100000.0)
BCNO (PRES, NODE = 1443, CONS = 100000.0)
BCNO (PRES, NODE = 1444, CONS = 100000.0)
BCNO (PRES, NODE = 1445, CONS = 100000.0)
BCFL (HEAT, ENTI = "R.support", CONS =
0.000000000000E+00)
BCFL (HEAT, ENTI = "L.support", CONS =
0.000000000000E+00)
BCFL (HEAT, ENTI = "R.thk.wall", CONS = 216.22)
BCFL (HEAT, ENTI = "L.thk.wall", CONS = 216.22)
BCFL (HEAT, ENTI = "R.lw.attach", CONS = 0.000000000000E+00)
BCFL (HEAT, ENTI = "L.lw.attach", CONS = 0.000000000000E+00)
ICNO (VELO, ZERO, ALL)
ICNO (DISS, CONS = 0.400000000000E-02, ALL)
ICNO (KINE, CONS = 0.300000000000E-02, ALL)
ICNO (TEMP, CONS = 315.0, ALL)
ICNO (PRES, CONS = 10000.0, ALL)
VIEW (COMP, SMOO, XZON = 8.0, YZON = 8.0)
RADS (ENTI = "L.wall")
RADS (ENTI = "R.wall")
RADS (ENTI = "R.B.wall")
RADS (ENTI = "L.B.wall")
RADS (ENTI = "Ctr.B.R.wall")
RADS (ENTI = "Ctr.B.L.wall")
OBST (NONE)
END

```

## APPENDIX B

### PROCEDURES AND COMMANDS FOR OPERATING FIDAP

With FIDAP correctly installed on the computer, the first thing to do in order to retrieve the FIDAP screen is to type the following statement:

**fidap -id *filename* -gui**

The file name can be any name with seven characters.

**press Enter**

Once the above command is entered, a startup screen will be initialized, this screen is called the FIDAP work sheet, shown in Figure App. B-1. It contains all the commands that are needed to write a successful input file for any problem.

To start creating an input file for a problem, the following procedures must be observed:

**A.** Click on **FI-GEN** module button in order to start drawing the mesh. To draw the mesh, the following items are on the screen colored with navy blue must be used:

1. Points
2. Curves
3. Surfaces
4. Mesh edges
5. Mesh loops

## 6. Mesh face

for **3-D** problem Mesh shell and Mesh solid command must be used (refer to FIDAP Tutorial manual for more details ).

**B.** Click on **FI-BC** module button in order to call each boundary group an entity, this can be done by clicking on the boundary group then by clicking on each edge that needs to be given a name. Then after the name is given for each edge click on the **ACCEPT** button.

**C.** Click on **FI-PREP** module button in order to give the program the values for the constants and the values for the boundary conditions, the initial conditions for the problem and all other assumptions for the problem.

**D.** Click on **CREATE** module button ( module selection menu, far right), then click on the create command button (navy blue with white letters), finally click on the form **ACCEPT** button. FIDAP lets the user know if the problem statement is given in proper order by writing a message to the Command History Window in the lower right part of the screen. The message says, "FISOLV INPUT DATA SUCCESSFULLY CREATED" otherwise FIDAP gives a message "THIS SESSION IS ABORTED DUE TO ERRORS.". Errors can be anywhere in FI-GEN or FI-PREP. FIDAP will give the user the error number and by clicking on the Help button and then click on the area of the screen where the question is about. The GUI will pop up and help window that contains the text manual section pertaining to the area of the screen that the user clicked on.

**E.** Click on the **RUN** button ( Module Selection Menu, toward the left).

Click on the **FORE/BACKGROUND** field button ( **FOREGROUND** appears).

Click on the **ACCEPT** button. The **FOREGROUND** option should be used for small runs only. In the foreground a window with the label "FOREGROUND TASK IS

RUNNING”appears showing the approximate wall clock time the job has run and giving the user some option to follow the convergence of the run.

Click on the FDSTAT Monitor START button.

Click on the HISTORY BIG button. Now the convergence of the problem can be monitored.

Using the STOP button will stop the run in a graceful manner.

F. Once the run is finished the “FOREGROUND TASK IS RUNNING” window will disappear. To reestablish connection to the files ( including the results database FDPOST):

#### **Reconnect to files-IDENT**

Click on the IDENT button (Module Selection Menu, far left).

Click on the form ACCEPT button, Messages will appear in the Command History window listing the files and the message “UNCOMPRESSING DATABASE.”

G. Click on FIPOST module button ( Module Selection Menu) to post-process the results.

Click on the FIPOST COMMAND Form ACCEPT button.

To recap the sub-modules of FIDAP that are used as follows:

- **FI-GEN**
- **FI-BC**
- **FIPREP**
- **CREATE**
- **RUN**
- **Reconnect to files- IDENT**
- **FIPOST**

In order to make hard copies for the results the following statements should be followed:

**FIPOST**

DEVICE (POSTSCRIPT)

MESH( )

END

END

This should create a file called (*filename.FILOT*).

Next is the procedure to use the **fdp2ps** utility file.

**atom% \$FIDAPROOT/bin/fdp2ps *filename.FILOT***

**press Enter**

FIDAP postscript conversion program will activate.

The program will print the following statements.

Enter file name of plot file (default=FILOT):[write here *filename.FILOT*]

**Press Enter**

Enter file name of a postscript file ( default=PSFILE):[write here *filename.PSFILE*]

**Press Enter**

(M)onochrome, (G)rayscale, or (C)olor (default= m):

**Press Enter**

(A)ll plots, (S)kip plot, (B)reak or (P)lot (default=P):

**Press Enter**

1 plot(s) finished

A file called *filename.PSFILE* is created, it can be seen by using a software

called GOSTSCRIPT or any software which can read a postscript files. Giving the command

(**gs *filename.PSFILE***) will let the user to see the file.

In order to print the file the following command should be used:

**lpr -P(*printer name*) *filename*.PSFILE**

In order to see an example which is given in FIDAP examples manual the following command must be given:

**atom% cd \$FIDAPROOT/examples**

**press Enter**

**atom% ls**

**press Enter**

Using the above command will give the user a list of all the examples in which they are stored in FIDAP examples directory. To retrieve (example 1) the following command should be given:

**atom% cp \$FIDAPROOT/examples/ex1.FDREAD .**

Now the user can check to see if **ex1.FDREAD** is the main directory by going back to the main directory and again giving the following command:

**atom% ls**

When the file is in the main directory the user can give the command to initialize FIDAP screen, once the screen is up the user must click on the READFILE module button and by writing the file name in the yellow field of READFILE command, then by clicking on the ACCEPT button the file will be read automatically by FIDAP then by observing the above procedures C through G the user will be able to see the results of that example file.

## **NOTE TO USERS**

**Page(s) not included in the original manuscript are unavailable from the author or university. The manuscript was microfilmed as received.**

**UMI**



## REFERENCES

1. H. R. Al-Asmar, B. W. Jones, D. K. Matteson, "Experimental Evaluation of Attic Radiant Barriers", ASHRAE Transactions, vol 102, (1996), pp 297-306.
2. McQuiston, F. C. Der, Sun Li, S. B. Sandoval, "Thermal Simulation of Attic and Ceiling Spaces" ASHRAE Transactions Technical papers, vol 90, (1984), pp 139-163.
3. P. Cleary, M. Sherman, "Seasonal Storage of Moisture in Roof Sheathing" Measurement and Control in Science and Industry, Proceedings of the international Symposium Association, (1985), pp 313-323.
4. S. Katipamula, D. O'Neal, W. D. Turner, W. E. Murphy, "Experimental Study of Heat Transfer in Attics With a Small-Scale Simulator", ASHRAE Transactions Technical and Symposium Papers vol 93, (1987), pp 122-134.
5. D. W. Yarbrough, R. S. Graves, D.L. McElroy, "Effectiveness of Thermal Insulation in The Attic Spaces of Manufactured Homes", ASME Heat Transfer Division vol 1, (1988), pp 71-79.
6. A. J. Baker, R. M. Kelso, E. B. Gordon, S. Roy, E.G. Schaub, "Computational Fluid Dynamics: A Two-Edged Sword", ASHRAE Journal, (August 1997), pp 51-62.
7. M. A. Medina, D. L. O'Neal, W. D. Turner, "Development of Transient Heat Transfer Model of Residential Attics Used to Simulate Radiant Barrier Retrofits", ASME-JSES-JSME International Solar Energy Conference vol 1, (1995), pp 253-263.
8. S. Moujaes, "Use of Passive Radiation in Ventilated Attics" ASHRAE Transactions vol 102, (1996), pp 307-314.
9. D. R. Pitts, L. E. Sissom, Heat Transfer, SCHAUM'S Outlines, McGraw-Hill Inc. ISBN 0-07-050203-X. (1992).
10. G. K. Batchleor, An Introduction to Fluid Dynamics, Cambridge University Press, ISBN 0-335-1109043-X. (1967).

11. F. Kreith, M. S. Bohn, Principles of Heat Transfer, 5th ed., West Publishing Company ISBN 0-314-01360-1. (1993).

12. A. J. Chapman, Fundamentals of Heat Transfer, 1st ed., Macmillan Publishing Company, ISBN 0-02-321600-X. (1984).

**VITA**

**Graduate College  
University of Nevada, Las Vegas**

**Neezar Taher Alsaiegh**

**Home Address:**

**1600 East University Avenue  
Apt # 229  
Las Vegas, Nevada 89119**

**Degrees:**

**Associate in Applied Science, Aeronautical Engineering Technology, 1978  
Wentworth Institute of Technology**

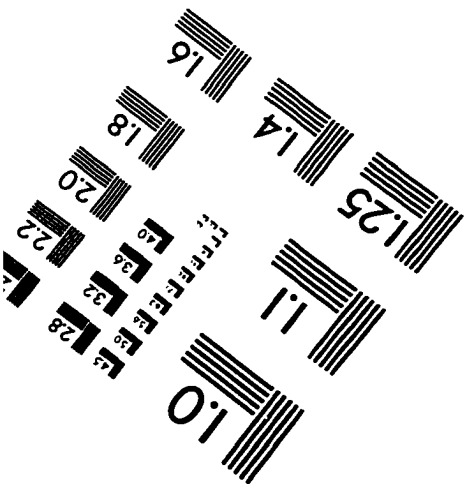
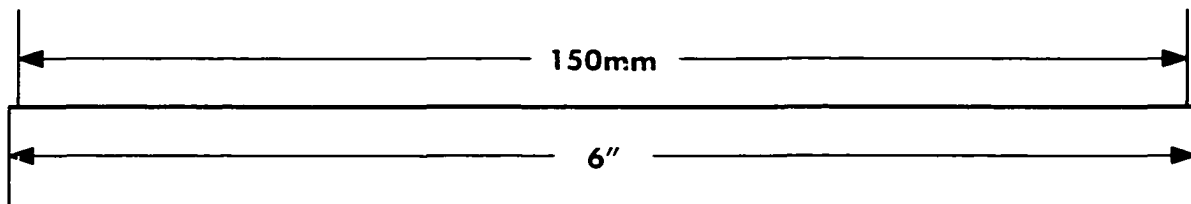
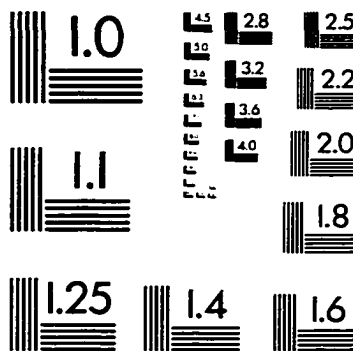
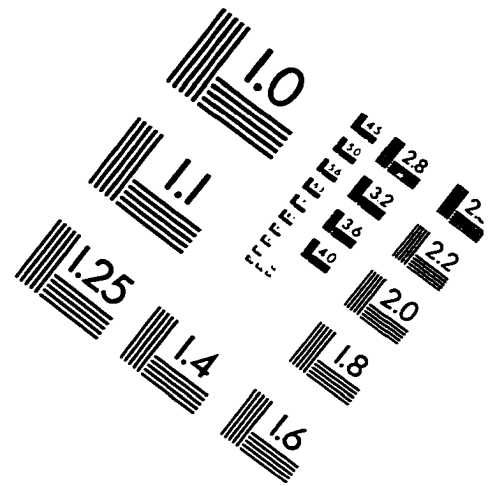
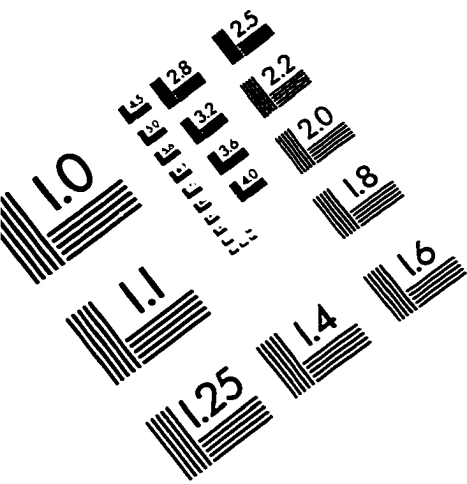
**Bachelor of Science, Mechanical Engineering, 1980  
Northeastern University**

**Thesis Title: 2-D Finite Element Model for Heat Transfer in Residential Attic Using an Attic  
Barrier System.**

**Thesis Examination Committee:**

**Chairperson, Dr. Samir F. Moujeas, Ph.D., P.E.  
Committee Member, Dr. Darrell W. Pepper, Ph.D.  
Committee Member, Dr. Robert F. Boehm, Ph.D., P.E.  
Graduate Faculty Representative, Dr. Gerald R. Frederick, Ph.D., P.E.**

# IMAGE EVALUATION TEST TARGET (QA-3)



APPLIED IMAGE, Inc  
1653 East Main Street  
Rochester, NY 14609 USA  
Phone: 716/482-0300  
Fax: 716/288-5989

© 1993, Applied Image, Inc., All Rights Reserved

